Deutsches Zentrum
DLR für Luft- und Raumfahrt

Institutsbericht
DLR-IB-FT-BS-2024-106

Development of a toolchain for the conceptual design of fixed-wing VTOL UAVs

Ivo Poelma

Institut für Flugsystemtechnik
Braunschweig

120	Seiten
046	Abbildungen
011	Tabellen
023	Referenzen

Braunschweig, den 06.09.2024

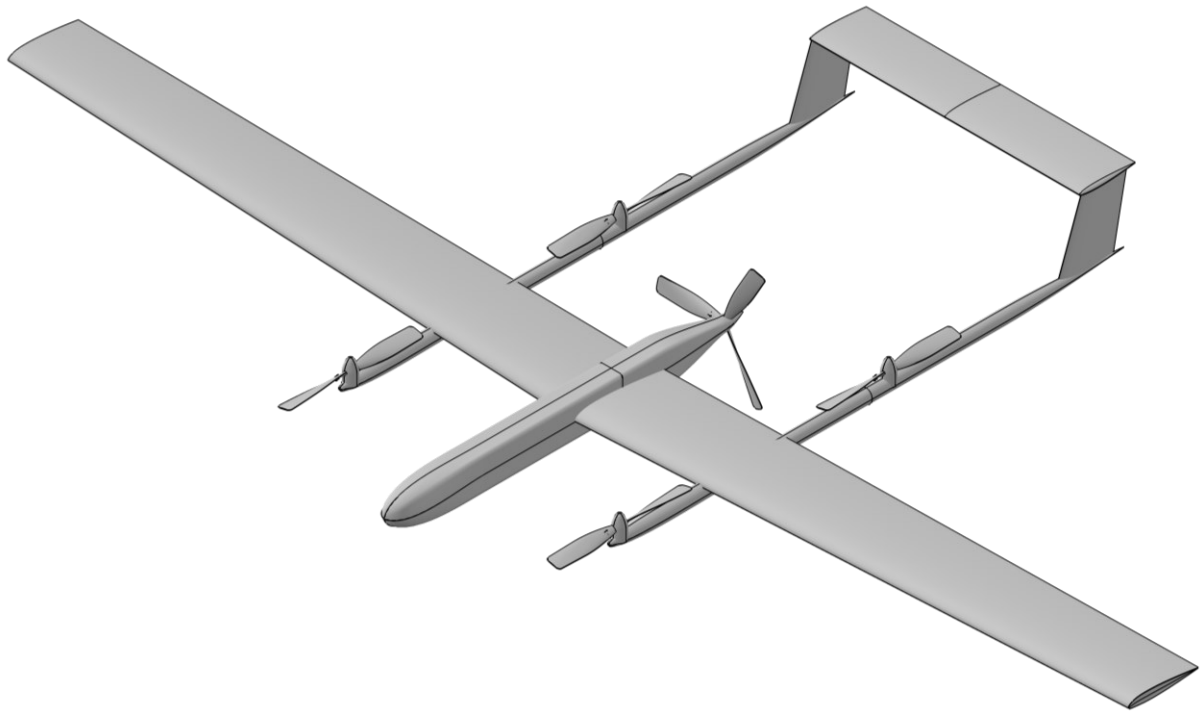|	
Institutsleitung:	Prof. Dr.-Ing. S. Levedag
Abteilungsleitung:	Johann Dauer
Betreuer:in:	Lennart Kracke
Verfasser:in:	Ivo Poelma

Development of a toolchain for the conceptual design of fixed-wing VTOL UAVs

Thesis report

"How can the conceptual design phase for a fixed-wing, VTOL-capable UAV be automated based on a given set of requirements?"

**Deutsches Zentrum
für Luft- und Raumfahrt**
German Aerospace Center

inholland
hogeschool

Bachelor graduation intern
Ivo Martijn Poelma,▮▮▮▮▮▮
Aeronautical Engineering

Thesis project supervisor
L. Kracke, DLR

[This page has been intentionally left blank]

Development of a toolchain for the conceptual design of fixed-wing UAVs

Thesis report

By

Ivo Martijn Poelma

"How can the conceptual design phase for a fixed-wing, VTOL-capable UAV be automated based on a given set of requirements?"
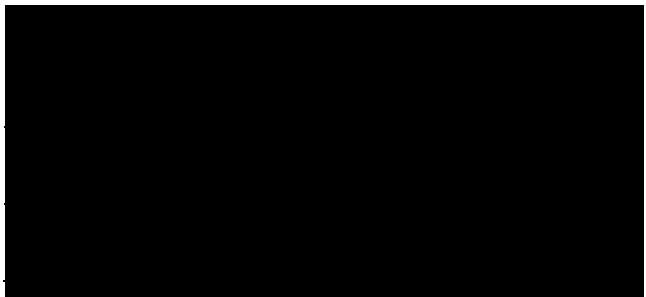
Abstract

This report presents the techniques and methods used to set up an toolchain for the automation of the conceptual design phase for a small, fixed-wing UAV with VTOL capabilities. The conceptual design is a phase in the design process of a UAV that heavily influences both the preliminary and detailed design that follows. The main challenge for the development of a conceptual design for a small, VTOL-capable UAV is the number of circular dependencies between the different components of the aircraft. A literature review is conducted to find existing methods to determine the required size and weight of the systems. A conceptual design toolchain using the Python programming language has been developed to determine the size and weight of the systems for a set of requirements, in the form of a toolchain in Python. Lastly, a verification process is conducted to ensure that the methods employed result in a realistically sized UAV.

Keywords

Toolchain, UAV, VTOL, Open class, concept, design, Python

[Non-confidential]

[This page has been intentionally left blank]

I.   Preface

This thesis report is presented for the completion of the Bachelor's degree in Aeronautical Engineering, with the minor in Light Weight Structures at Inholland University of Applied Sciences in Delft, Netherlands. The project, on which the thesis is based started on the 12th of February 2024 and this report will be delivered on the 9th of June.

The target audience for this report are the examinators of the Inholland University of Applied Sciences, and the engineers who will either continue with this project, engineers who will implement the toolchain developed with the methods described in this report, or engineers who want to develop their own, similar, program in the same field of automated conceptual design for small UAVs.

I would like to thank everyone who has helped directly, and indirectly, in creating and completing this project and setting up this report. In particular, I would like to thank the following people:

Lennart Krake

As the official project supervisor, you helped me a lot during the project, and would like to thank you for the guidance, advice, and feedback. Without this, the project would have not been possible to complete.

Marcel Riedel

As unofficial project supervisor you helped me any time I needed some advise or guidance on how to solve a problem during the project and I would like to thank you for the guidance, elaborate explanations, advise, and feedback during the project.

Marcel Bruin

As the university project supervisor, you guided me on how to successfully complete my Bachelor's thesis and I would like to thank you for this.

II. Summary

This report presents techniques and methods for the conceptual design phase of a small UAV with VTOL capabilities. These design techniques have been selected and/or modified to generate a conceptual design for a UAV with a specific configuration. This configuration consists of conventional wing, pusher propeller, and twin-boom tail configuration with an inverted U-tail, which is also shown on the cover page. The methods to achieve this are gathered from the books and papers of the authors Gudmundsson [1], Gundlach [2], Jae-Hun & Co. [3], Nicolai [4], Raymer [5], Roskam [6], Sadraey [7], Tyan & Co. [8], and Yi & Heping [9]. For each of the methods presented in this report, a summary is given on how the methods works and when it might be applied. Next, a selection is made of the method presented in order to set up a toolchain design program in Python which can automatically estimate the size and weights of all major systems that contribute to the performance of a UAV. This is done by implementing equations which are either determined empirically, based on design guidelines, based on energy conservation, based on a database, or simple drag models. This results in a toolchain program capable of determining the parameters required to initiate a preliminary design for the desired UAV. These parameters are, for example, the maximum take-off weight, wing weight and sizing, empennage weight and sizing, fuselage weight and sizing, propulsion weight and sizing, and the landing gear weight, location, and sizing. The parameters are calculated based on the following requirements for the aircraft; the payload capacity, range, rate-of-climb, flight speeds, loiter duration, preliminary data on the airfoils desired, and the main material that wants to be used. When the UAV must be capable of vertical flight (VTOL), the requirements on the hover duration, ascent rate-of-climb, and ascent altitude must be given.

In order to verify that the methods employed in the toolchain result in a viable conceptual design, a verification process is performed by comparing the outputs of the toolchain to an actual existing UAV, while being given the requirements that the UAV also complies with. This verification process gave insight that particular employed methods do not represent certain aspects of the conceptual design very well. An example of which is, the propeller sizing method employed for the forward flight propeller gives a larger propeller than that the reference UAV has. In itself, this isn't a significant issue, but it can result in other modules also giving results different from the reference UAV. This is due to (circular-) dependencies throughout the modules in the toolchain. These characteristics must be kept in mind when implementing, and/or modifying the toolchain

Overall the project was a success with the toolchain being able to automate the conceptual design process of a UAV with a conventional wing, pusher propeller, twin-boom tail configuration with an inverted U-tail, and VTOL capabilities. In order to increase the accuracy of the toolchain and allow it to analyze multiple configurations of small UAVs more research must be done on this topic.

III. Nomenclature

Don't forget any abbreviations AND variables + units!

Abbreviations

Centre of Gravity	CG
Defense Advanced Research Projects Agency	DARPA
Deutsche Zentrum für Luft- und Raumfahrt	DLR
Electric Speed Controller	ESC
Federal Aviation Regulation	FAR
Finite Element Method	FEM
General Aviation	GA
High Altitude, Long Endurance	HALE
Medium-Altitude Long Endurance	MALE
Micro Air Vehicles	MAV
Off-The-Shelf	OTS
Short Take-Off and Land	STOL
Small Tactical Unmanned Aerial Vehicles	STUAV
Small Unmanned Aerial Vehicles	SUAV
Stanford University Aerospace Vehicle Environment	SUAVE
Tactical Unmanned Aerial Vehicles	TUAV
United States AirForce	USAF
Unmanned Aerial Vehicle	UAV
Vertical Take-Off and Land	VTOL
Vortex Latice Method	VLM

Variables

Aspect Ratio	AR	[-]
Bank Angle	ϕ	[°]
Density	ρ	[kg/m³] or {slug/ft³}
Diameter	D	[m] or {ft}
Disk Loading	DL	[N/m²] or {lbf/ft²}
Distance	s	[m] or {ft}
Drag	D	[N] or {lbf}
Dynamic pressure	q	[kg/m²] or {lbs/ft²}
Efficiency	η	[-]
Figure of Merit	FoM	[-]
Gravitational Acceleration	g	[m/s²]
Length	l	[m] or {ft}
Lift Coefficient (2D)	C_l	[-]
Lift Coefficient (3D)	C_L	[-]
Lift to Drag ratio	L/D	[-]
Load Factor	n	[-]
Local Chord	c	[m] or {ft}
Maximum Take-Off Mass	MTOM	[kg] or {lbs}
Maximum Take-Off Weight	MTOW	[N] or {lbf}
Mean Aerodynamic Chord	C	[m] or {ft}
Moment	m	[Nm] or {lbf*ft}
Oswald Efficiency Factor	e	[-]
Angle (of Attack)	α	[°]
Power	P	[W]
Power-to-Weight ratio	P/W	[W/N]
Pressure	P	[Pa] or {psi}
Propeller efficiency	η_{prop}	[-]
Radius	R	[m] or {ft}
Rate of Climb	RoC	[m/s] or {ft/s}
Rolling Resistance	μ	
Safety Factor	SF	[-]
Span	b	[m] or {ft}
Surface aera	S	[m²] or {ft²}
Sweep	Λ	[°]
Take-off drag coefficient	$C_{D_{To}}$	[-]
Take-off lift coefficient	$C_{L_{To}}$	[-]
Taper ratio	λ	[-]
Thickness	t	[m] or {ft}
Thrust	T	[N]
Thrust-to-Weight ratio	T/W	[-]
Time duration	t	[sec]
Velocity	V	[m/s] or {knots}
Voltage	U	[Volt]
Volume	V	[m³] or {ft³}
Volume Fraction	$\bar{V}$	[-]
Weight	W	[N] or {lbf}
Weight fraction	W_f	[-]
Wing Efficiency Factor	k	[-]
Wing loading	W/S	[N/m²] or {lbf/ft²}
Yield Strength	σ	[Pa] or {psi}
Zero-lift drag coefficient	C_{D_0}	[-]

Subscripts

Battery	bat
Climb Flight Phase	$climb$
Cruise Flight Phase	$cruise$
Density Factor	ρ
Electric Speed Controller	ESC
Elevator	e
Fraction	f
Fuselage	$fuse$
Horizontal Stabilizer	ht
Hover	h
Inflow	i
Landing	L
Landing Gear	LG
Landing Gear Main	$main$
Landing Gear Nose	$nose$
Leading Edge	LE
Main Wing	$wing$
Material	mat
Maximum	max
Minimum	min
Payload	$payload$
Propeller	$prop$
Quarter Chord	$\frac{c}{4}$
Required	req
Service Ceiling	$ceiling$
Specific (per unit of mass)	$spec$
Take-Off	To
Total	tot
Ultimate	ult
Vertical Stabilizer	vt
Take-off distance	g

Superscript

Forward Flight	FF
Vertical Flight	VTOL

IV. List of Figures

Contents

1. Introduction

Unmanned aviation has grown to be an important part of the aviation industry, as well as in the defence, healthcare, and agricultural industries. Each of these industries has different requirements which the UAVs (Unmanned Arial Vehicles) must comply with. For this reason, the DLR Institute of Flight Systems in Braunschweig, Germany is conducting research in the following areas for the implementation of UAVs [10]:

- Robust flight control and mission control solutions for systems operating under high uncertainty
- Sensor fusion and environmental perception
- Optical navigation
- Machine Learning
- UAV integration into the existing airspace
- Detect and avoid
- Airworthiness
- Drone defence

To conduct and prove the research the DLR undertakes, mission-appropriate UAVs are required. This thesis will focus on the development process for these UAVs.

1.1 Aim of Research

The goal of automating the conceptual design process for small VTOL-capable UAVs is to decrease the amount of time it takes to create the conceptual design. This is desired due to the fact that the process that must be gone through to get a viable conceptual design contains several iterative processes that take, when done manually, a significant amount of time. To make this process faster and more efficient, research will be conducted to automate this process to a point where requirements must be setup and the automated conceptual design analysis programs, i.e. a toolchain, outputs a list of parameters that can be used as a starting point for a preliminary design.

1.2 Research Questions

Main Research Question

"How can the conceptual design phase for a fixed-wing UAV be automated based on a given set of requirements?"

Sub-research Questions

1. What types of automated conceptual design analysis programs exist and what is the primary use case of these programs within the aviation industry? {chapter 2.3}
2. How do flight performance requirements affect the sizing, and geometry of a UAV? {chapter 3.4.3}
3. How is the design of a UAV influenced by a set of requirements on the weight and balance of the UAV? {chapter 3.4.11}
4. Which requirements are necessary, and how will these be processed to result in a realistic and desired conceptual UAV design? {chapter 3.4.14}
5. How can the conceptual designs generated by an automated conceptual design analysis program be verified? {chapter 3.5}

1.3 Thesis Scope

The scope of this thesis is limited to the conceptual design of a small UAV that must be able to take-off conventionally, as well as vertically. Within this scope, the initial mass, thrust requirements, component sizing, component weights, and mass and balance of the desired UAV are determined.

The component sizing is entailing the sizing of major components, like, the wing, empennage, fuselage, propulsion system, energy source, and landing gear. The weights will be determined for the same major components listed previously.

The scope of the thesis does not include a detailed structural nor aerodynamic analysis, and will be limited to one UAV configuration, a Conventional Wing – Pusher – Single propulsion system – Twin-boom – Inverted U-tail. This configuration is depicted on the cover page.

1.4 Thesis Structure

This thesis, including this introduction, contains the chapters Literature , Methodology, Verification, Conclusion, and Future Work. The Literature in chapter 2 analyses research that has been done by other sources regarding the topics of small UAV – VTOL design and gives an overview of possible methods that can be employed to answer the research questions stated previously. The Methodology in chapter 3 presents the methods and techniques selected to be used to answer the research questions. Next to this, it gives a more detailed description on the selected methods on how they work, and why these are chosen. The Verification in chapter 4 will implement the methods presented in the Methodology in order to verify the methods and analyze where in the process improvements must be made. The Conclusion in chapter 5 will answer the main question and present, in short, the results of the Verification. Lastly, the Future Work in chapter 6 will summarize the assumptions made during the Methodology, present the limitations of the methods used, and give an overview of how future endeavours should proceed with this research and similar research.

2. Literature Review

This chapter will present the literature review conducted within the project, this review will encompass the classification of several manned and unmanned aircraft, how to design an aircraft (specifically in the conceptual design phase), and methods to determine the size, weight, and location of the components in an aircraft. This last topic will be broken down into literature review on;

- existing automatic conceptual design programs,
- how to determine the (preliminary) weight of an aircraft based on limited requirements,
- how to determine the weight of the components within an aircraft,
- how to determine the power requirements during the different phases of a flight mission,
- how to size the control surfaces of an aircraft,
- how to size and locate the landing gear of an aircraft,

The majority of the topics reviewed are based on methods for manned aviation, this is to be able to know which methods are used in similar use cases and how these could be modified/justified for use in unmanned aviation.

2.1 Aircraft Categories

This chapter will present a general description of the aircraft types which will be mentioned in this report and give a classification of a small subset of the unmanned aircraft regarding size and function.

2.1.1 General Aircraft Categories

The more general aircraft categories are classified by the Federal Aviation Administration (FAA), two of these categories will be discussed in this sub-section.

General Aviation

General Aviation is the aviation class aircraft with a MTOW of less than 19000 lbs, or 8600 kg and have a relatively small occupancy capacity of 19 passengers. The general aviation category is further defined by the Federal Aviation Regulation (FAR) Part 23 regulations.

Cargo/Transport Aircraft

The Cargo/Transport Aircraft are, aircraft with a MTOW of more than 19000 lbs, or 8600 kg, and have an occupancy capacity of more than 19 passengers but can also be specialized in cargo transport which results in a smaller occupancy capacity. The Cargo/Transport category is further defined by the FAR Part 23 regulations.

2.1.2 UAV Classification

The Unmanned Aerial Vehicle (UAV) classification will be based on the one presented by Gundlach [2]. A selection of which that are in a similar mission and/or configuration class that this report targets will be presented below:

Micro Air Vehicles

Micro Air Vehicles, or MAV, is an unmanned aircraft with a maximum length of 6 inch (15.4 cm), this is according to the Defense Advanced Research Projects Agency (DARPA) MAV program. However other sources, like drone manufacturers claim that the MAV class has a maximum wingspan of 2.5 ft (76.2 cm). A MAV generally weighs no more than 0.5 lb (0.227 kg). An example of a MAV is the AeroVironment Wasp III.

Small Unmanned Aerial Vehicles

Small Unmanned Aerial Vehicles, or SUAVs, are defined by Gundlach as having a mass range of 1 – 55 lbs (0.454 – 24.95 kg). The upper limit of the SUAV is defined by the Academy of Model Aeronautics (AMA). This class of UAVs have a typical endurance of 0.5 – 2 hrs of flight time when electrically-powered. An example of a SUAV is the AeroVironment Raven RQ-11B.

Small Tactical Unmanned Aerial Vehicles

Small Tactical Unmanned Aerial Vehicles, or STUAVs, is a class between the SUAV class and the Tactical Unmanned Aerial Vehicles class. Which means that the typical weight of this class is between 55 and 200 lbs (24.95 - 90.72 kg). Due to the increased size of the aircraft within this class allows for higher performance, long endurance aircraft which are capable of flight times of upwards of 24 hrs, for example the Integrator STUAV.

Tactical Unmanned Aerial Vehicles

Tactical Unmanned Aerial Vehicles, or TUAVs, is a class of UAV which has most commonly a mass range of between 200 and 1000 lbs (90.72 - 453.59 kg). The aircraft within the TUAV class most typically have a flight performance of between 5 – 12 hrs with a maximum service altitude of 20000 ft (6096 m). An example of a TUAV is the AAI Shadow 200 (RQ-9B).

Medium-Altitude Long Endurance Unmanned Aerial Vehicles

Medium-Altitude Long Endurance Unmanned Aerial Vehicles, or MALE UAVs, usually weight between 1000 and 10000 lbs (453.59 – 4535.9 kg) with a usual payload weight capacity of 200 – 1000 lbs (90.72 - 453.59 kg), and an endurance of 12 – 40 hrs. The typical maximum service altitudes are determined by the type of engine of a MALE UAV, the maximum service altitude for a reciprocating engine lies between 15000 and 30000 ft (4572 - 9144 m) and between 30000 and 50000 ft (9144 – 15240 m) for turbo-prop engines. An example of a MALE UAV is the MQ-9 Reaper.

High-Altitude Long Endurance Unmanned Aerial Vehicles

High-Altitude Long Endurance Unmanned Aerial Vehicles, or HALE UAVs, usually weight is above 5000 lbs (2268 kg) and an endurance of greater than 24 hrs. The typical maximum service altitude is most commonly above 50000 ft (15240 m). An example of a HALE UAV is the RQ-4A Global Hawk.

2.2 Design Process

In order to design an aircraft, certain steps must be followed to do this in the most effective way possible. This chapter will provide insight on how to do this based on the methodology presented by Gudmundsson and Sadraey. These two sources both give clear overviews/steps that can be followed in order to successfully develop a conceptual design of an aircraft. Another sources, like Gundlach, don't give a (clear) review of these steps, or are not applicable for the use for the design of a UAV. The methodology presented by Gudmundsson and Sadraey are however applicable to be used for UAVs while they are intended for manned aircraft due to their process/steps describing general methods and parameters that must be determined. These are both required for manned and unmanned aviation.

2.2.1 Gudmundsson

Gudmundsson [1] presents a book that describes the designing process for General Aviation (GA) from the early conceptual design phase to the early preliminary design phase. Here Gudmundsson gives insight into the methods used to develop a GA aircraft and provides guidelines on parameters that are required in the conceptual design phase.

Gudmundsson presents an "Aircraft Design Algorithm" which gives a guide on the steps required in the conceptual design phase. This algorithm is presented below:

1. Setup the desired requirements, mission profiles, and list the regulatory requirements which the aircraft must comply with.
2. Review aircraft which fall in the same class of aircraft as the one to be designed. This can provide insight on methods that can be used in the design of the aircraft, but also systems and philosophies that can be implemented.
   Determine the desired configuration of the aircraft and the type of propulsion system, based on the requirements and what previously developed aircraft have implemented.
3. If cost and revenue are significant factors in the design of the aircraft, conduct research on similar aircraft which materials and systems they use and determine how much this will cost and if the market supports this market plan.
4. Setup a size-matching diagram to determine the penalties for each of the performance requirements determined previously on the required thrust-to-weight ratios, and the associated wing loading.
5. Select the desired/optimal wing loading from the size-matching diagram and the thrust-to-weight ratios for each of the performance requirements and considering the wing loading at which an airfoil will stall.
6. Estimate initial weight utilizing weight fraction, and/or historical relations.
7. Utilizing the initial weight determined previously, and the chosen wing loading (from step 5), determine the wing surface area.
8. Estimate the surface area of the vertical and horizontal stabilizers utilizing volume fractions.
9. Determine an initial appropriate aspect ratio, taper ratio, airfoils, planform, dihedral, washout, etc for the main wing. These parameters might/probably will change during the design process.
10. Sketch the configuration for the desired aircraft, this entails the planform of the wing, placement of the fuselage, tail, landing gear, and wing.
11. Determine the engine layout desired for the aircraft, meaning the location, number of and the properties of the engine(s)/motor(s).
12. Determine the, estimate empty, gross, and fuel weight using a combination of statistical, direct, and/or known weights methods.
13. From the previously determined weight determinations, determine the Centre of Gravity (CG) location for the empty weight, loaded weight, and the range that the CG shifts due to fuel burn.
14. Determine the mass moments of inertia for the aircraft based on its weight and weight distribution.
15. Determine a candidate CG envelope based on the outputs of steps 13 and 14. This envelope might/probably will change when more parameters are known.

16. Determine how the fuselage will be loaded, i.e. where are the occupants located, where does the baggage go, where does the cargo go, and where is the fuel stored.
17. Conduct a static and dynamic stability analysis on the aircraft to determine if the CG range is viable, as well as are the stabilizers correctly sized.
18. Modify the size of the stabilizers according to the stability analysis, when significant changes in the size/layout of the stabilizers have occurred, revert to step 13.
19. Analyse the following design modifications as needed, based on the previous analyses:
    a. Structural load paths (wing, horizontal- and vertical stabilizer, fuselage, etc.)
    b. Control system functionality (manual, hydraulic, fly-by-wire/light)
    c. Flight control functionality (geometry, aerodynamic balancing, trim tabs)
    d. High-lift systems (flaps, slats)
    e. Landing Gear configurations (tricycle, tail-dragger, (non)retractable)
20. Analyse stall characteristics and modify systems as required
21. Perform a detailed drag analysis
22. Perform a detailed performance analysis (take-off, climb, cruise, loiter, descent, and landing) and create a payload weight-to-range analysis.
23. Optimize systems as required and update previously done analyses for more accurate results.
24. Check if the developed aircraft complies with all applicable regulatory- and performance requirements setup in step 1
25. Setup a V-n diagram to publish the flight envelope of the aircraft.
26. Conduct a detailed structural analysis.
27. Output the characteristic parameters of the aircraft to be implemented in a preliminary design.

2.2.2 Sadreay

Sadreay [7] presents a book that describes the designing process for a wide range of aircraft from the early conceptual design phase to the detailed design phase. Here Sadreay presents methods, guidelines, and philosophies that can be used throughout the designing process. During the presentation of (nearly) each designing method/phase Sadreay also presents a series of steps, or a flowchart to follow. For the conceptual design phase, Sadraey presents the flowchart shown in Figure 1. This flowchart gives a great overview of the steps that must be taken during the conceptual design phase when conducting this (mostly) manually, meaning that decisions are made based on judgment throughout the process.
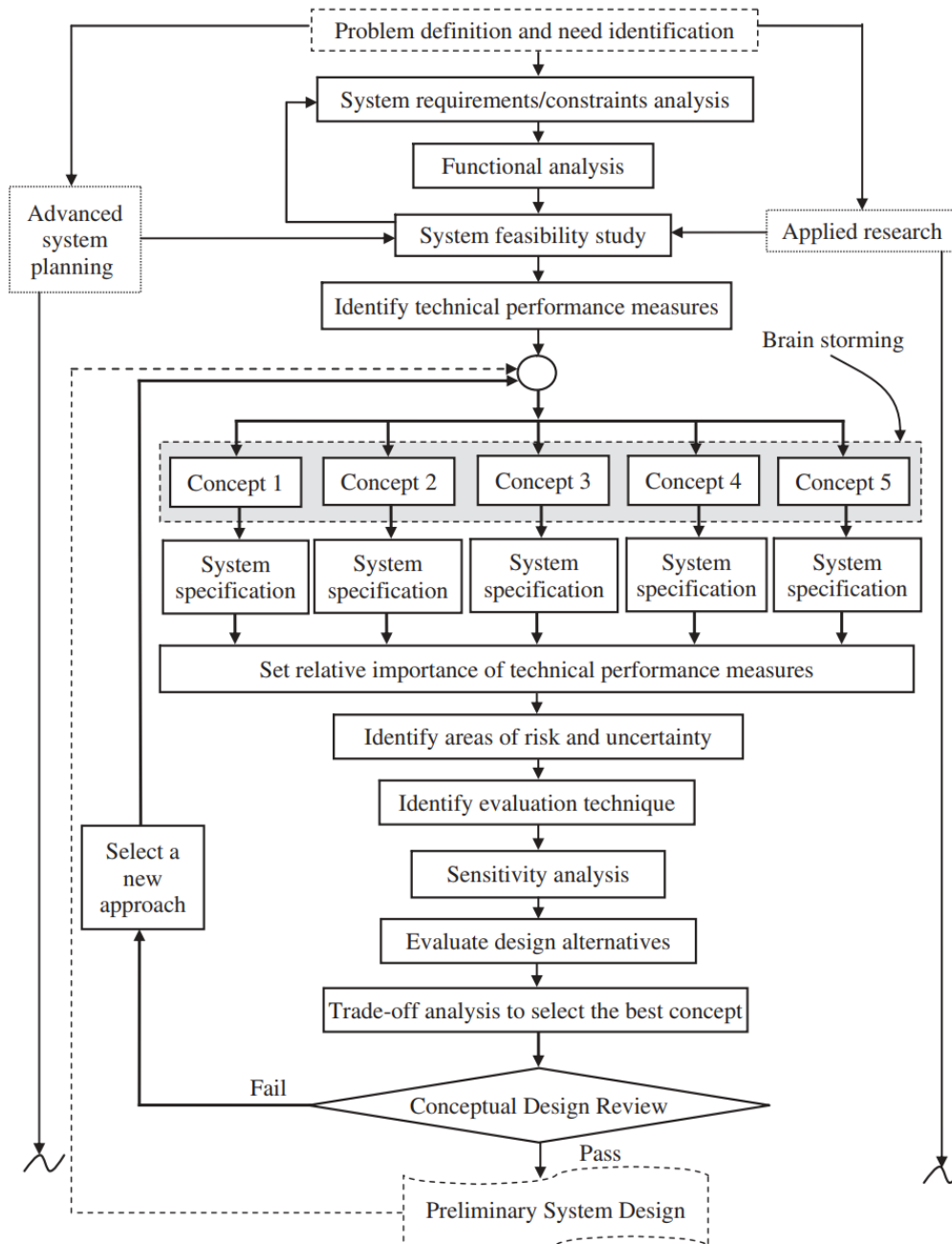
Figure 1 - conceptual design flowchart Sadraey [7]

2.3 Existing Automated Conceptual Design Analysis Programs

As the nearly all aircraft must go through the conceptual design phase, this means that there has been an interest in making this process easier/more efficient/faster. A solution to this is to make a program which does this automatically, in this chapter one such program will be discussed, SUAVE, and why this project will create a custom design program to do this.

2.3.1 SUAVE

SUAVE (Stanford University Aerospace Vehicle Environment) [10] is a Python-based program which has been developed by the University of Stanford for the development of conceptual designs for a wide range of aircraft configurations, these are for example, conventional aircraft, blended-wing-body e-VTOLs, solar-powered aircraft, airliners, multi-copters, supersonic aircraft, and more. The main difference between SUAVE and other methods/programs are that other programs rely more on empirically derived techniques and other design guidelines discovered/developed during the design of previous aircraft. [10] This is achieved by implementing advanced techniques and physics-based models in order to determine the weight and sizing of the systems within an aircraft.

SUAVE has the capability of determining the size and weight of the following aircraft components; the lifting surfaces, fuselage, empennage, nacelles, propulsion systems, energy systems, and payload. This is done by following the flowchart shown in Figure 2. After these systems are modelled, SUAVE can perform both structural, and aerodynamic analyses in the systems to optimize the layout of the aircraft together with the sizing of the lifting/stabilizing surfaces. It does this with the use of the Vortex Latice Method (VLM) for the aerodynamic analysis.

An analysis of the prespecified mission is conducted in order to optimize the aircraft for this. The analysis is performed by determining the amount of stored energy is required for the mission, determines the impact this has on the design of the aircraft, and optimizes the overall design for the most effective configuration.

2.3.2 Confidential Software

Most major aircraft manufacturers have developed their own techniques in order to determine the preliminary size and weight of their aircraft's conceptual designs. However, these techniques are rarely/never published due to the proprietary nature of this topic.
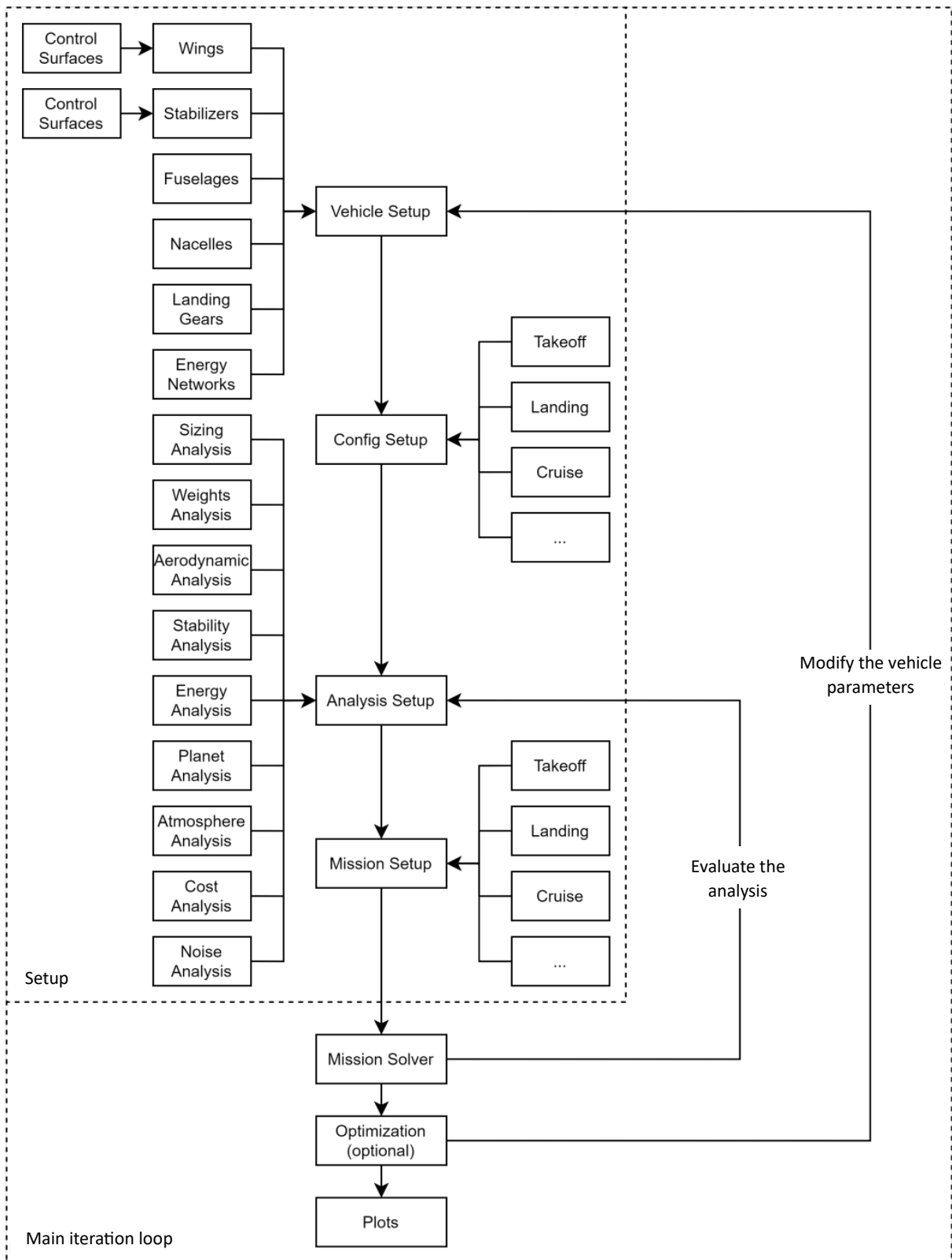
Figure 2 - functional flowchart SUAVE [11]

2.4 Initial Weight Estimation

In order to determine the take-off weight of an aircraft an initial weight estimation must be performed to give a starting point for the conceptual weight analysis to initiate from. This chapter will describe two methods of determining the initial take-off weight of an aircraft based on the payload weight of the desired aircraft.

2.4.1 Mass Fractions

A well-known method of estimating the mass of an aircraft early on in the design process is using Mass Fractions. These are factors that are determined by utilizing statistical data from existing aircraft in the same class as the aircraft that will be developed. The factors are most commonly dependent on the fraction of the payload- and fuel mass with respect to the total take-off mass of the aircraft. The payload mass being the most common given requirement for an aircraft provides a good starting point for the determination of the take-off mass of the desired aircraft.

2.4.1.1 Sadraey

Sadraey [7] presents a general technique to estimate the Maximum Take-Off Weight (MTOW) for a manned aircraft as follows; the aircraft is divided into several sections, some section weights are determined based on statistics, some are based on performance equations, and some section weights are given as requirements. The payload weight (W_{PL}) and the crew's weight (W_C) are given as requirements, the fuel weight fraction (W_f) is based on performance equations, and the empty weight (W_E) is determined by statistical data on existing manned aircraft. Formula (2-1) combines all these terms in order to estimate the take-off weight of the aircraft.

$$W_{To} = \frac{W_{PL} + W_C}{1 - \left(\frac{W_f}{W_{To}}\right) - \left(\frac{W_E}{W_{To}}\right)}$$

(2-1)

Sadraey provides a formula to calculate the empty weight fraction for the following types of aircraft; Hang Gliders, Man-powered aircraft, Glider/sailplanes, Motor-gliders, Microlight, Home-built, Agricultural, General Aviation-single engines, General Aviation-twin engines, Twin turboprop, Jet trainer, Jet Transport, Business Jet, Fighter, and Long-range/Long-endurance.

2.4.2 Database Regression

As Sadraey does not provide an empty mass fraction formula for unmanned aircraft, another method to determine the take-off weight of an aircraft is to utilize a database with data on the specific class of aircraft that is desired. The data collected in the database can in turn be regressed into a formula that returns the MTOW dependent on specified variables. These variables can, for example, be the payload weight, range, and/or endurance, or a combination of these variables. The regressed formula can look like the formulas (2-2) until (2-5) [12].

$$z = \beta_0 + \beta x$$

(2-2)

$$z = \beta_0 + \beta_1 x + \beta_2 y$$

(2-3)

$$z = \beta_0 + \beta_1 x + \beta_2 x^2$$

(2-4)

$$z = \beta_0 + \beta_1 x + \beta_2 y + \beta_3 x^2 + \beta_4 y^2 + \beta_5 xy$$

(2-5)

This technique is based on the one presented by Sadraey but can be more flexible with the desired dependencies of the mass fraction formulas and, when this is available, on the data utilized that determine the mass fraction formulas. Both the data that is used to create the regressed formula and the regressed formula itself must be reviewed for validity and applicability, as this must also be done for the data used to determine the mass fraction formulas provided by Sadraey.

2.5 Weight Determination

After the initial weight of the desired aircraft is determined, the component weights can be calculated, from which the total weight of the entire conceptual design of the UAV can be calculated, as visualized in Figure 3. This can be done by the two methods that are presented in this sub-chapter.
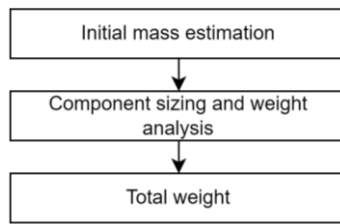
Figure 3 - weight determination flowchart

2.5.1 Analytical Weight Determination

The analytical weight determination method is based on calculating the weight of the structure of an aircraft by means of physics-based models. The weight is calculated by determining the type and amount of material required within a structure. This is based on the aerodynamic and structural loads acting on the geometry of the aircraft. This method is mainly used within the preliminary and detailed design due to the fact that the geometry of the aircraft must be known to implement this method. (Text based on [11]) A limitation of this method is that it is only able to calculate the weight of the structure of the aircraft, and unable to determine the weight of the systems within the aircraft.

2.5.1.1 Boom-and-Web Method

A method of analytical weight determination is the use of the Boom-and-Web method. This method assumes that the structure of the aircraft is a hollow structure composed of rods, only taking axial loads, and webs, only taking shear loads. This method simplifies the geometry, as seen in Figure 4, of the aircraft in order to solve the calculations to determine the stresses within the structure with minimal computing power. The Boom-and-Web method calculates the minimum skin thickness of the structure for the loads it experiences.
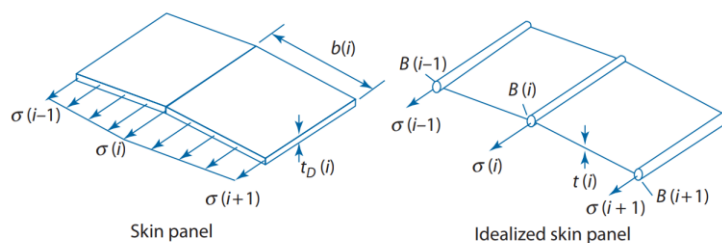
Figure 4 – Boom-and-Web method idealized geometry.

Because a geometry is required to be analyzed, this method is best suited to be used within the preliminary design phase. [2]

2.5.1.2   Finite Element Method Analysis

Much like the Boom-and-Web method, the Finite Element Method (FEM) Analysis, simplifies the geometry of interest. The simplification is part of the discretization of the geometry, which converts the solid structure into a mesh, this is shown in Figure 6. This is done to enable a computer to analyze the structure, and the simplification of the mesh is to reduce the amount of processing required to solve the structural analysis. A mesh is able to be much more detailed than the simplified geometry of the Boom-and-Web method and will also give a more accurate result on the stresses present within the aircraft structure. Solving the matrices of the mesh that describe the structure and loads takes significantly more processing time than solving the calculation for the Boom-and-Web method. However, this does result in a more accurate representation of the actual stresses within the structure. Due to this, the FEM analysis is best suited for the analysis of the detailed design of the aircraft. [2] An example of a structure that has been analyzed by the Finite Element Method is shown in Figure 5.
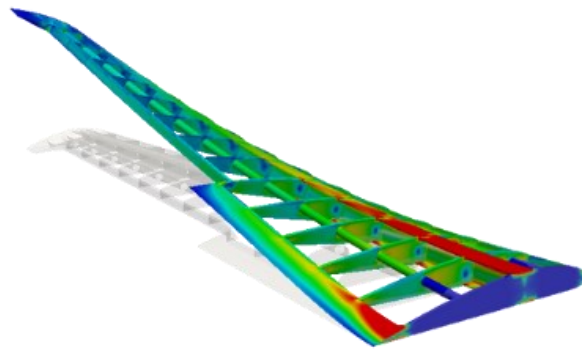
Figure 5 - example of a wing structure analyzed by the Finite Element Method [13]
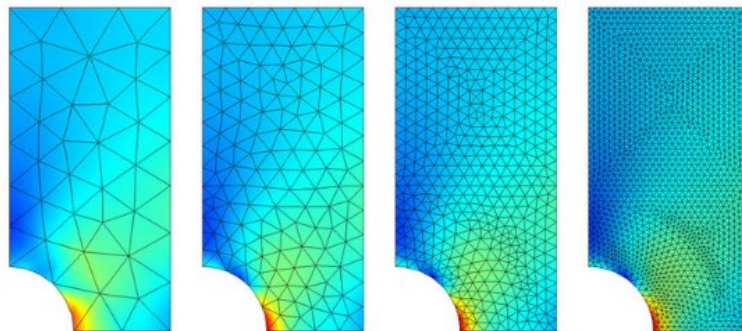
Figure 6 - example of mesh simplification [13]

2.5.2 Empirical Weight Determination

The empirical weight determination method is based on calculating the weight of an aircraft by means of statistics-based models. Meaning that, the weight of the desired aircraft will be calculated by using data from previously developed aircraft in the same aircraft class. This data is most commonly in the form of determining the influence which a certain characteristic, or parameter, has on the weight of the overall component/system. The weight is calculated for each component and system separately and later all weights are added up to give the MTOW of the desired aircraft. Several sources have created formulas to calculate the weight of the components within an aircraft.

2.5.2.1 Nicolai

The methods presented by Nicolai [4] apply to several types of aircraft, these are; 'Conventional Metal Aircraft-Moderate Subsonic to Supersonic Performance Aircraft' and 'Conventional Metal Aircraft-Light Utility Aircraft'. The Light Utility Aircraft is the most applicable out of these for the use case of small UAVs. This class of aircraft has a low-to-moderate performance level (maximum airspeed up to about 300 kt).

The method Nicolai presents is based on formulas that consider the geometry features that influence the overall weight of the components of the aircraft. Multiple regression analyses were used to determine the amount of influence each feature has. This is expressed as a parameter (a type of measurement of the feature) combined with a factor (the amount of influence the feature has) in the formulas. This method contains the following formulas:

$$W_{wing} = 96.948 \left[\left(\frac{S_{wing}}{100}\right)^{0.61} \cdot \left(\frac{AR_{wing}}{cos\,\Lambda_{\frac{c}{4}}}\right)^{0.57} \cdot \left(1 + \frac{V_e}{500}\right)^{0.5} \cdot \left(\frac{1+\lambda}{2\frac{t}{c}}\right)^{0.36} \cdot \left(\frac{n_{ult} \cdot W_{To}}{10^5}\right)^{0.65} \right]^{0.993} \qquad (2\text{-}6)$$

$$W_{ht} = 127 \left[\left(\frac{l_{tail}}{10}\right)^{0.483} \cdot \left(\frac{S_{ht}}{100}\right)^{1.2} \cdot \left(\frac{b_{ht}}{t_{ht}}\right)^{0.5} \cdot \left(\frac{n_{ult} \cdot W_{To}}{10^5}\right)^{0.286} \right]^{0.87} \qquad (2\text{-}7)$$

$$W_{vt} = 98.5 \left[\left(\frac{S_{vt}}{100}\right)^{1.2} \cdot \left(\frac{b_{vt}}{t_{ht}}\right)^{0.5} \cdot \left(\frac{n_{ult} \cdot W_{To}}{10^5}\right)^{0.87} \right] \qquad (2\text{-}8)$$

$$W_{fuse} = 200 \left[\left(\frac{l_{fuse}}{10}\right)^{0.857} \cdot \left(\frac{4R_{fuse}}{10}\right) \left(\frac{V_e}{100}\right)^{0.338} \cdot \left(\frac{n_{ult} \cdot W_{To}}{10^5}\right)^{0.286} \right]^{1.1} \qquad (2\text{-}9)$$

$$W_{LG} = 0.054 \left[(l_{LG})^{0.501} \cdot \left(n_{ult_L} \cdot W_L\right)^{0.684} \right] \qquad (2\text{-}10)$$

The previously stated formulas can only be used in Imperial units. Thus, the weights (W) is in lbs, surface areas (S) in ft², velocity (V) in knots, load factors (n) in g, lengths (l) in ft, thicknesses (t) in inch, spans (b) in ft, fuselage radius (R_{fuse}) in ft, and landing gear lengths (l_{LG}) in inch.

2.5.2.2 Raymer

The methods presented by Raymer [5] apply to several types of aircraft, these are; General Aviation Aircraft, Cargo/Transport Aircraft, and Fighter/Attack Aircraft. The most applicable out of these for the use case of small UAVs is the General Aviation Aircraft. Revert to chapter 2.1 for more information about aircraft classification. Applying the methods for the General Aviation Aircraft class results in the following formulas that can represent the contribution of each characteristic of a component to the weight of the component. This method contains the following formulas:

$$W_{wing} = 0.036 \left[(S_{wing})^{0.758} \cdot \left(\frac{AR_{wing}}{\cos^2 \Lambda} \right)^{0.6} \cdot (q)^{0.006} \cdot (\lambda)^{0.04} \cdot \left(\frac{100 \cdot t/c}{\cos \Lambda_{ht}} \right)^{-0.3} \cdot (n_{ult} \cdot W_{To})^{0.49} \right] \qquad (2\text{-}11)$$

$$W_{ht} = 0.016 \left[(S_{ht})^{0.896} \cdot \left(\frac{AR_{wing}}{\cos^2 \Lambda_{ht}} \right)^{0.043} \cdot (q)^{0.168} \cdot (\lambda_{ht})^{-0.02} \cdot \left(\frac{100 \cdot t/c}{\cos \Lambda_{ht}} \right)^{-0.12} \cdot (n_{ult} \cdot W_{To})^{0.414} \right] \qquad (2\text{-}12)$$

$$W_{vt} = 0.073 \left[(S_{vt})^{0.873} \cdot \left(\frac{AR_{wing}}{\cos^2 \Lambda_{vt}} \right)^{0.357} \cdot (q)^{0.122} \cdot (\lambda_{vt})^{0.039} \cdot \left(\frac{100 \cdot t/c}{\cos \Lambda_{vt}} \right)^{-0.49} \cdot (n_{ult} \cdot W_{To})^{0.376} \cdot (K_{tail}) \right] \qquad (2\text{-}13)$$

$$W_{fuse} = 0.052 \left[(S_{fuse})^{1.086} \cdot (q)^{0.241} \cdot (l_{tail})^{-0.051} \cdot (L/D)^{-0.072} \cdot (n_{ult} \cdot W_{To})^{0.177} \right] + W_{press} \qquad (2\text{-}14)$$

$$W_{press} = 11.9 \left[V_{pr} \cdot P_{delta} \right]^{0.271} \qquad (2\text{-}15)$$

$$W_{LG_{main}} = 0.095 \left[\left(\frac{l_{LG_{main}}}{12} \right)^{0.409} \cdot (n_{ult_L} \cdot W_L)^{0.768} \right] \qquad (2\text{-}16)$$

$$W_{LG_{nose}} = 0.125 \left[\left(\frac{l_{LG_{nose}}}{12} \right)^{0.566} \cdot (n_{ult_L} \cdot W_L)^{0.845} \right] \qquad (2\text{-}17)$$

The previously stated formulas can only be used in Imperial units. Thus, the weights (W) is in lbs, surface areas (S) in ft², dynamic pressures (q) in lb/ft², load factors (n) in g, lengths (l) in ft, fuselage pressurized volume (V_{pr}) in ft³, fuselage-atmosphere pressure differential (P_{delta}) in psi, and landing gear lengths (l_{LG}) in inch.

K_{tail} is equal to 1.2 when the aircraft has a T-tail configuration, and K_{tail} is equal to 1.0 when the aircraft has a conventional tail configuration. If λ_{vt} is less than 0.2, use a value of 0.2. If the landing gear is non-retractable, reduce the total landing gear weight by 1.4%.

2.5.2.3 Roskam

The methods presented by Roskam [6] apply to several types of aircraft, these are; General Aviation Airplanes, Commercial Transport Airplanes, and Military Patrol, Bomb, and Transport Airplanes. The most applicable out of these for the use case of small UAVs is the General Aviation Airplanes. Within this class of aircraft, Roskam presents two methods called the Cessna Method and the USAF (United States AirForce) method. Of these, the Cessna Method is more applicable for the use case within small UAVs. This is because the Cessna Method is valid for small, relatively low-performance aircraft with a maximum airspeed below 200 knots (102.9 m/s) and the UAF Method is valid for the same class but with a maximum airspeed below 300 knots (154.3 m/s). With the chosen method Roskam presents the following empirically derived formulas:

$$W_{wing_{cantilever}} = 0.04674 \left[(W_{To})^{0.397} \cdot (S_{wing})^{0.360} \cdot (n_{ult})^{0.397} \cdot (AR_{wing})^{1.712} \right] \qquad (\text{ 2-18 })$$

$$W_{wing_{braced}} = 0.002933 \left[(S_{wing})^{1.018} \cdot (n_{ult})^{0.611} \cdot (AR_{wing})^{2.473} \right] \qquad (\text{ 2-19 })$$

$$W_{fuse_{high-wing}} = 14.86 \left[(W_{To})^{0.144} \cdot \left(\frac{l_{f-n}}{p_{max}} \right)^{0.778} \cdot (l_{f-n})^{0.383} \cdot (N_{pax})^{0.455} \right] \qquad (\text{ 2-20 })$$

$$W_{fuse_{low-wing}} = 0.04682 \left[(W_{To})^{0.692} \cdot (p_{max})^{0.374} \cdot (l_{f-n})^{0.590} \right] \qquad (\text{ 2-21 })$$

$$W_{ht} = 3.184 \left[\frac{(W_{To})^{0.887} \cdot (S_h)^{0.101} \cdot (AR_h)^{0.138}}{174.04 \left(t_{ht_{rootmax}} \right)^{0.101}} \right] \qquad (\text{ 2-22 })$$

$$W_{vt} = \frac{1.68[(W_{To})^{0.567} \cdot (S_h)^{1.249} \cdot (AR_h)^{0.482}]}{639.95 \left[\left(t_{vt_{rootmax}} \right)^{0.747} \cdot \left(\cos \left(\Lambda_{\frac{c}{4}} \right) \right)^{0.882} \right]} \qquad (\text{ 2-23 })$$

$$W_{LG_{non-retractable}} = 0.013(W_{To}) + 0.362 \left[(W_L)^{0.417} \cdot (n_{ult_{LG}})^{0.950} \cdot (l_{s_{main}})^{0.183} \right] + 6.2 + 0.0013(W_{To})$$
$$+ 0.007157 \left[(W_L)^{0.749} \cdot (n_{ult_{LG}})(l_{s_{main}})^{0.788} \right] \qquad (\text{ 2-24 })$$

$$W_{LG_{retractable}} = W_{LG_{non-retractable}} + 0.014(W_{To}) \qquad (\text{ 2-25 })$$

$$W_{nacell_{boxer}} = 0.24 \cdot P_{max} \qquad (\text{ 2-26 })$$

$$W_{engine_{NA}} = 1.1 \cdot P_{max} \qquad (\text{ 2-27 })$$

The previously stated formulas can only be used in Imperial units. Thus, the weights (W) is in lbs, surface areas (S) in ft², load factors (n) in g, lengths (l) in ft, fuselage perimeter (p_{max}) in ft, thicknesses (t) in ft, and power required (P_{max}) in hp.

The fuselage weight calculation does not account for pressurized fuselages. The $n_{ult_{LG}}$ can be set to 5.7. The l_{f-n} is the length of the fuselage, excluding the nose-mounted nacelle length.

2.5.2.4   Sadraey

Sadraey [7] *(chapter 10)* introduces the following technique to analytically determine the weight of the components of the aircraft. This technique is based on a mixture of rational analysis and statistical data on previously developed aircraft. This technique applies to several types of aircraft, these are; General Aviation (GA) aircraft, transport/cargo/airliner aircraft, supersonic fighter aircraft, and Unmanned Aerial Vehicle (UAV)/remotely controlled model aircraft. It does this by utilizing common equations between the different classes of aircraft but applying custom factors for each aircraft type within the applied formulas. For each dependency in the formulas, a relevant parameter is selected based on a curve fit approach. This results in a linear function that can represent the contribution of each dependent variable to the weight of each component. Sadraey presents the following formulas for the weight of the wing (2-28), horizontal stabilizer (2-29), vertical stabilizer (2-30), fuselage(2-31), landing gear (2-32), and motor installation (2-33):

$$W_{wing} = (S_{wing}) \cdot C \cdot (t/C_{max}) \cdot (\rho_{mat}) \cdot \left(K_{\rho_{wing}}\right) \cdot \left(\frac{AR_{wing} \cdot n_{ult}}{\cos \Lambda_{c/4}}\right)^{0.6} \cdot (\lambda)^{0.04} \cdot g \qquad (2\text{-}28)$$

$$W_{ht} = (S_{ht}) \cdot (C_{ht}) \cdot \left(t/C_{max_{ht}}\right) \cdot (\rho_{mat}) \cdot \left(K_{\rho_{ht}}\right) \cdot \left(\frac{AR_{ht} \cdot n_{ult}}{\cos \Lambda_{c/4}}\right)^{0.6} \cdot (\lambda)^{0.04} \cdot (\bar{V}_{ht})^{0.3} \cdot \left(\frac{C_e}{C_{ht}}\right)^{0.4} \cdot g \qquad (2\text{-}29)$$

$$W_{vt} = (S_{vt}) \cdot (C_{vt}) \cdot \left(t/C_{max_{vt}}\right) \cdot (\rho_{mat}) \cdot \left(K_{\rho_{vt}}\right) \cdot \left(\frac{AR_{vt} \cdot n_{ult}}{\cos \Lambda_{c/4}}\right)^{0.6} \cdot (\lambda)^{0.04} \cdot (\bar{V}_{vt})^{0.2} \cdot \left(\frac{C_e}{C_{vt}}\right)^{0.4} \cdot g \qquad (2\text{-}30)$$

$$W_{fuse} = (l_{fuse}) \cdot \left(2 \cdot R_{fuse_{max}}\right)^2 \cdot (\rho_{mat}) \cdot \left(K_{\rho_{fuse}}\right) \cdot (n_{ult})^{0.25} \cdot (K_{inlet}) \cdot g \qquad (2\text{-}31)$$

$$W_{LG} = (K_L) \cdot (K_{ret}) \cdot (K_{LG}) \cdot (W_L) \cdot \left(\frac{l_{LG}}{b}\right)(n_{LG})^{0.20} \qquad (2\text{-}32)$$

$$W_{E_{install}} = (K_E) \cdot (N_E) \cdot (W_E)^{0.9} \qquad (2\text{-}33)$$

The previously stated formulas can be used in either SI as well as in Imperial units. Thus, the weights (W) is in N, surface areas (S) in m², the Mean Aerodynamic Chord (C) in m, material density (ρ) in kg/m³, load factor (n) in g, lengths (l) in m, and fuselage radius $\left(R_{fuse}\right)$ in m.

For more information on the $\left(K_\rho\right)$ factors for the aircraft classes discussed by Sadraey, revert to Appendix D – Sadraey Empirical Weight Factors.

2.5.2.5 Yi & Heping

Yi & Heping [9] focus on the analysis of High Altitude, Long Endurance (HALE) military UAVs. These aircraft are usually configured with a high aspect ratio (about ~20-30), little to no wing sweep (~14-18%), and operate at an altitude above 18000 meters with a flight endurance of 24 hours. The wing is usually constructed from three or four main (solid carbon fibre) spars. Yi & Heping have chosen to research a V-tail configuration for the empennage of the HALE UAV.

The method Yi & Heping present is based on formulas that consider the major design parameters that influence the overall weight of the components of the HALE UAV. Linear regression is used to determine the amount of influence each parameter has. This is based on statistical data retrieved from previously developed aircraft in the same HALE UAV class.

Yi & Heping give a formula for the weight of the wing (2-34), fuselage (2-35), V-tail (2-36), and landing gear (2-37), as shown below;

$$W_{wing} = 0.0118 \frac{\left(S_{wing}\right)^{0.48} \cdot \left(AR_{wing}\right) \cdot (Ma)^{0.43} \cdot (W_{To})^{0.84} \cdot (n)^{0.84} \cdot (\lambda)^{0.14}}{(t/c)^{0.76} \cdot \cos\left(0.0175 \, \Lambda_{c/2}\right)^{1.54}} \qquad (2\text{-}34)$$

$$W_{fuse} = 0.0025 \cdot \left((K_{inlet})^{1.42} \cdot (q)^{0.283} \cdot (W_{To})^{0.95} \cdot \left(\frac{l_{fuse}}{H_{fuse}}\right)^{0.71}\right) \qquad (2\text{-}35)$$

$$W_{Vt} = 0.022 \left((W_{To})^{0.813} \cdot (n)^{0.813} \cdot (S_{Vt})^{0.584} \cdot \left(\frac{b_{Vt}}{t_{Vt}}\right)^{0.033} \cdot \left(\frac{C_{wing}}{l_{Vt}}\right)^{0.028}\right)^{0.915} \qquad (2\text{-}36)$$

$$W_{LG} = 0.165(W_{To})^{0.84} \qquad (2\text{-}37)$$

The previously stated formulas can only be used in SI units. Thus the weights (W) is in N, surface areas (S) in m², load factors (n) in g, dynamic pressures (q) in kg/m², lengths (l) in m, fuselage height $\left(H_{fuse}\right)$ in m, spans (b) in m, thicknesses (t) in m, and Mean Aerodynamic Chords (C) in m.

2.5.2.6   Jae-Hyun et al.

Jae-Hyun et al. [3] present a paper on the development of a small, fuel cell and battery-powered, VTOL UAV, containing the process of how to design and size the UAV. In this paper, a technique is presented to calculate the weight of the components associated with the propulsion system. These components are; the motor(s), Electric Speed Controller(s) (ESCs), and propellers. The techniques used by Jae-Hyun et al. are based on data from existing components and equations are setup by the use of regression models. The following equations are presented:

$$M_{motor}^{VTOL} = (0.196*10^{-5})(P_{max}^{VTOL})^2 + 0.201(P_{max}^{VTOL}) + 5.772 \qquad (2\text{-}38)$$

Formula (2-38) determining the weight of a VTOL motor (gr), M_{motor}^{VTOL}. the formula is valid for a (P) value of 0 - 7000 Watts (per motor).

$$M_{motor}^{FF} = (-0.922*10^{-5})(P_{max}^{VTOL})^2 + 0.196(P_{max}^{VTOL}) + 23.342 \qquad (2\text{-}39)$$

Formula (2-39) determining the weight of a Forward Flight motor (gr), M_{motor}^{FF}, and is valid till a (P) value of 12000 Watts (per motor).

$$M_{ESC} = (0.324*10^{-2})\left(\frac{P_{max}}{U}\right)^2 + 0.847\left(\frac{P_{max}}{U}\right) + 1.532 \qquad (2\text{-}40)$$

Formula (2-40) determining the weight of an Electric Speed Controller (gr), M_{ESC}, and is valid till a $\left(\frac{P}{U}\right)$ value of 200 Amperes (per ESC).

$$M_{prop}^{VTOL} = 7.281 \cdot exp^{3.389\cdot(D_{prop}^{VTOL})} - 3.232 \qquad (2\text{-}41)$$

Formula (2-41) determining M_{prop}^{VTOL} (gr), and valid between a D_{prop}^{VTOL} of 0.3m till 1.0m vertical flight propeller.

$$M_{prop}^{FF} = 670.644(D_{prop}^{FF})^{2.784} \qquad (2\text{-}42)$$

Formula(2-42) determining M_{prop}^{FF} (gr) has an r^2 error value of 0.93 and valid between a D_{prop}^{FF} of 0.1. till 0.7m forward flight propeller.

$$D_{prop}^{FF} = 4.735(K_v)^{-0.405} \qquad (2\text{-}43)$$

Formula (2-43) determining the D_{prop}^{FF}, and is valid for a K_v of between ~100 and 2500.

$$K_v = (-0.228*10^{-7})(P_{max}^{FF})^3 + 0.0003(P_{max}^{FF})^2 - 1.101(P_{max}^{FF}) + 1685.676 \qquad (2\text{-}44)$$

Formula (2-44) determining the K_v rating for the forward flight motor and is valid till a P value of 5000 Watts (per motor).

2.5.2.7 Tyan et al.

Tyan et al. [8] present a paper on the development of a small, battery-powered, VTOL UAV, containing the process on how to design and size the UAV. In this paper, a technique is presented to calculate the weight of the components associated with the propulsion system. These components are; the motor(s), Electric Speed Controller(s) (ESCs), propellers, and battery. The techniques used by Tyan et al. are empirically derived from data from existing components. The following equations are presented:

$$W_{motor} = (F_1(P_{max})^{E_1} \cdot (U_{max})^{E_2}) \cdot P_{max} \cdot g \cdot 1000 \tag{2-45}$$

Formula (2-45) determining W_{motor} relies on empirically found coefficients to calculate the motor weight (N) for different types of motors. Table 1 shows these coefficients for different types of motors.

$$W_{ESC} = (F_{ESC}(P_{max})^{E_{ESC}}) \cdot g \cdot 1000 \tag{2-46}$$

Formula (2-46) determines the weight (N) of an ESC this is achieved by applying empirically found coefficients to calculate the weight of an ESC, these coefficients are; $F_{ESC} = 0.7383 * 10^{\wedge} - 4$ and $E_{ESC} = 0.8854$.

$$W_{prop} = \left((6.514 * 10^{-3}) \cdot (k_{mat}) \cdot (k_{prop}) \cdot (n_{prop}) \cdot (n_{blades})^{0.391} \cdot \left(\frac{(D_{prop}) \cdot (P_{max})}{1000(n_{prop})} \right)^{0.782} \right) \cdot g \cdot 1000 \tag{2-47}$$

Formula (2-47) determines the total weight (N) of all the propellers for either the forward or vertical flight configuration. Formula (2-47) relies on empirically found coefficients to calculate the weight of the propeller(s). The k_{mat} varies with the type of material used for the propeller, a value of 1.3 can be used for a wooden propeller, 1.0 for a plastic propeller, and 0.6 for one made from composites. k_{prop} can be taken for a value of 15, this is valid for a P_{max} of less than 50 hp (37.285 kW). n_{prop} is the number of propellers for either forward or vertical flight, n_{blades} is the number of blades on the propellers, and the D_{prop} is the diameter (m) of the propellers. Lastly, P_{max} is the maximum total amount of power (W) required for either the forward or vertical flight configuration.

$$D_{prop} = k_p \sqrt[4]{(P_{max})} \tag{2-48}$$

Formula (2-62) estimated the diameter (m) of a forward flight propeller utilizing a statistical approach as function of the maximum power (W) the propeller is calculated to consume. The coefficient k_p is dependent on how many blades the forward flight propeller has. k_p has a value of 0.1072, 0.0995, and 0.0938 for two-, three-, and four-blade propellers, respectively.

$$W_{bat} = \left(\frac{t \cdot P}{(E_{spec}) \cdot (\eta_{bat}) \cdot (f_{usable})} \right) \cdot g \tag{2-49}$$

Formula (2-49) calculates the weight of the battery for each flight phase by utilizing the time (h) required by each phase (t), power (W) required during the flight phase (P), the amount of energy (Wh) that can be stored in a battery per kg (E_{spec}), the efficiency of the battery (η_{bat}) and the fraction of power that can be extracted from the battery (f_{usable}).

Table 1 – motor weight calculation coefficients. [8]

Motor class	F_1	E_1	E_2
Brushless ferrite	7.765	−0.632	0.596
Brushed rare earth	8.160	−0.961	1.166
Brushless inrunner	13.17	−0.610	0.067
Brushless outrunner	0.889	−0.288	0.1588

2.6 Forward Flight Power Requirements Determination

Determining the power requirements for an aircraft during the desired mission profile is of great importance for the sizing of the aircraft, and the sizing of the propulsion system. This is due to the sizing of the aircraft, the wing for example, has a direct and indirect effect on the power requirements during all flight segments. This power required during the segments, in turn, directly affects the size of the energy source of the aircraft. Which influences the required size of the aircraft through weight and volume. These circular dependencies are addressed during the power requirements determination.

The benefit of using empirically-based methods is that these methods are based on general energy equations, simplified drag models, and statistical parameters gathered from previously developed aircraft. This combination of dependencies for the power requirements results in relatively accurate outputs while only requiring data that can already be known in the conceptual design phase. Several sources have created formulas to calculate the power requirements for the mission profile of an aircraft.

2.6.1 Gudmundsson

Gudmundsson [1] introduces the following technique to analytically determine the optimal wing and propulsion system size for the aircraft. This technique is based on the aircraft's performance requirements and a few parameters that must be assumed in the early phase of the conceptional design. These parameters are the maximum lift coefficient, lift and drag coefficient at lift-off, minimum drag coefficient, aspect ratio, and tire-to-runway roll resistance. These parameters can be assumed empirically based on parameters of previously developed aircraft of similar class. They can be updated later in either the preliminary design phase or late-conceptual design phase to increase the accuracy of the results. The following equations calculate the Thrust-to-Weight ratios during the take-off run (2-50), climb (2-51), cruise (2-52), loiter (2-52), and decent (2-51) mission phases of the aircraft, as well as for flight at the desired service ceiling (2-53) and during a steady turn(2-54) dependent on a range of wing loading values;

$$\frac{T}{W}_{To} = q\frac{(C_{D_{To}})}{(W/S)} + \mu\left(1 + q\frac{(C_{D_{To}})}{(W/S)}\right) + \frac{V_{To}^2}{2g \cdot S_g} \tag{2-50}$$

$$\frac{T}{W}_{Climb} = \frac{RoC}{V} + q\frac{(C_{D_{min}})}{(W/S)} + \left(\frac{k}{q}\right) \cdot (W/S) = \frac{RoC}{\sqrt{\frac{2}{\rho}(W/S) \cdot \sqrt{\frac{k}{3C_{D_{min}}}}}} + q\frac{(C_{D_{min}})}{(W/S)} + \left(\frac{k}{q}\right) \cdot (W/S) \tag{2-51}$$

$$\frac{T}{W}_{cruise} = q\frac{(C_{D_{min}})}{(W/S)} + \left(\frac{k}{q}\right)(W/S) \tag{2-52}$$

$$\frac{T}{W}_{Ceiling} = \frac{RoC_{ceiling}}{\sqrt{\frac{2}{\rho}(W/S) \cdot \sqrt{\frac{k}{3C_{D_{min}}}}}} + 4 \cdot \sqrt{\frac{k \cdot C_{D_{min}}}{3}} \tag{2-53}$$

$$\frac{T}{W}_{Steady\ turn} = q\frac{(C_{D_{min}})}{(W/S)} + (n)^2 \cdot \left(\frac{k}{q}\right) \cdot (W/S) \tag{2-54}$$

$$(W/S) = (q_{stall}) \cdot (C_{L_{max}}) = \frac{1}{2}\rho V_{stall}^2 \cdot C_{L_{max}} \tag{2-55}$$

As can be seen, the equation for the climb phase of the flight is also used to determine the thrust-to-weight during descent. This can be done to the point that the Thrust-to-Weight ratio becomes negative. When the Thrust-to-Weight ratio becomes negative, the aircraft will start to accelerate which isn't the intention of the descent phase of the mission. In addition to the Thrust-to-weight ratios, Gudmundsson

also presents a formula to determine the wing loading at which the wing will stall, depending on a desired stall speed and maximum lift coefficient (2-55). This is used to limit the range of viable wing loading values that can be selected for the optimal wing loading with respect to the thrust-to-weight ratio requirements.

The previously stated formulas can be used both in SI as in Imperial units. SI units were selected over the Imperial system due to its widespread use within the company ensures consistency and compliance with organizational standards. Thus, the dynamic pressures (q) in kg/m², wing loading (W/S) in N/m², rate of climb (RoC) in m/s, velocity (V) in m/s, and take-off ground run (s_g) in m.

After the Thrust-to-Weight ratio is calculated, the required thrust is calculated. From this thrust, a power requirement can be determined.

2.6.2 Sadraey

Sadraey [7] introduces the following technique to analytically determine the optimal wing and propulsion system size for the aircraft. This technique is based on the aircraft's performance requirements and a few parameters that must be assumed in the early phase of the conceptional design. These parameters are the maximum lift coefficient, lift and drag coefficient at lift-off, minimum drag coefficient, aspect ratio, and tire-to-runway roll resistance. These parameters can be estimated empirically based on parameters of previously developed aircraft of similar class. They can be updated later in either the preliminary design phase or late-conceptual design phase to increase the accuracy of the results. The following equations calculate the Thrust-to-Weight ratios during the take-off run (2-56), climb (2-57), and decent mission phases of the aircraft (2-57), as well as for flight at the desired service ceiling (2-58) and maximum airspeed (2-59);

$$\frac{T}{W}_{To} = \frac{\mu - \left(\mu + \frac{\left(C_{D_{To}} - \mu \cdot C_{L_{To}}\right)}{C_{L_{To}}}\right)\left[\exp\left(0.6(\rho) \cdot (g) \cdot \left(C_{D_{To}} - \mu \cdot C_{L_{To}}\right) \cdot (s_g) \cdot \left(\frac{1}{(W/S)}\right)\right)\right]}{1 - \exp\left(0.6(\rho) \cdot (g) \cdot \left(C_{D_{To}} - \mu \cdot C_{L_{To}}\right) \cdot (s_g) \cdot \left(\frac{1}{(W/S)}\right)\right)} \qquad (2\text{-}56)$$

$$\frac{T}{W}_{RoC} = \frac{RoC}{\sqrt{\frac{2}{\rho\sqrt{\frac{C_{D_0}}{k}}}(W/S)}} + \frac{1}{(L/D_{max})} \qquad (2\text{-}57)$$

$$\frac{T}{W}_{Ceiling} = \frac{RoC_{ceiling}}{\sigma_{ceiling}\sqrt{\frac{2}{\rho_{ceiling}\sqrt{\frac{C_{D_0}}{k}}}(W/S)}} + \frac{1}{\sigma_{ceiling} \cdot (L/D_{max})} \qquad (2\text{-}58)$$

$$\frac{T}{W}_{V_{max}} = \frac{(\rho_0) \cdot (V_{max})^2 \cdot \left(C_{D_0}\right)}{2(W/S)} + \frac{2 \cdot k \cdot (W/S)}{(\rho) \cdot (\sigma) \cdot (V_{max})^2 \cdot \left(C_{D_0}\right)} \qquad (2\text{-}59)$$

$$(W/S)_{stall} = (q_{stall}) \cdot \left(C_{L_{max}}\right) = \frac{1}{2}\rho V_{stall}^2 \cdot C_{L_{max}} \qquad (2\text{-}60)$$

As can be seen, equation specified for the climb phase of the aircraft is also used for the descent phase of the mission profile. This can be done to the point that the Thrust-to-Weight ratio becomes negative. When the Thrust-to-Weight ratio becomes negative, the aircraft will start to accelerate which isn't the intention of the descent phase of the mission.

The previously stated formulas can be used both in SI as in Imperial units. Thus, the rate of climb (RoC) in m/s, density (ρ) in kg/m³, wing loading (W/S) in N/ m², velocity (V) in m/s, dynamic pressures (q) in kg/m², and take-off ground run (s_g) in m.

The previously stated formulas can be used both in SI as in Imperial units. To keep the report as uniform as possible it was chosen to use the SI units. Thus, the dynamic pressures (q) in kg/m², wing loading (W/S) in N/ m², rate of climb (RoC) in m/s, velocity (V) in m/s, and take-off ground run (s_g) in m.

As can be seen in the formulas (2-56) till (2-59), these are all dependent on the wing loading. In the method Sadraey presents this dependency is used to make a Size Matching Diagram. This is a diagram that graphs all the Thrust-to-Weight ratios of all the mission segments with respect to the wing loading, together with the boundary of the wing loading at the desired stall speed (2-60), as can be seen in Figure 7.

This graph can be used to either visually, or analytically determine the optimal wing loading for the aircraft. First, the graph is used to determine in which regime the requirements for all flight phases are met. This viable region is highlighted in blue in Figure 7. It can be noted that this area is above all the Thrust-to-Weight ratio lines and left of the stall speed wing loading boundary. Next, the optimal wing loading for the aircraft can be determined, this point is called the design point. The design point is located where the Thrust-to-Weight ratio required is at its minimum. This is done to minimize the amount of thrust required for the flight phases, thus minimizing the required size of the propulsion and energy systems. This again minimizes the weight of the aircraft and the production as well as the operational costs.

After the optimal wing loading is chosen the viable Thrust-to-Weight ratios are calculated for each flight segment, the required thrust can be calculated depending on the (initial estimated) weight of the aircraft. From this thrust, a power requirement can be determined for each segment.
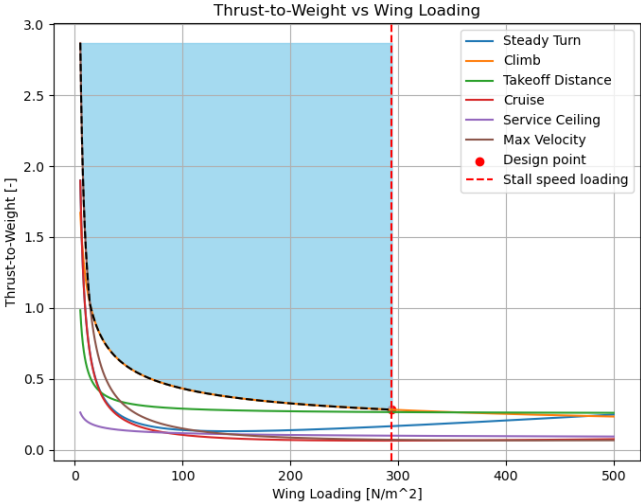

Figure 7 - Size Matching Diagram

2.7 Vertical Flight Power Requirements Determination

The Vertical Flight Power Requirements Determination process is performed in the same manner as the Forward Flight Power Requirements Determination process. Several sources have created formulas to calculate the power requirements for the mission profile of an aircraft.

2.7.1 Jae-Hyun et al.

Jae-Hyun et al. [3] present a technique to calculate the power required during vertical flight, meaning, the power requirements during the VTOL segments of the mission of the UAV. This technique is based on the aircraft's performance requirements, some parameters derived empirically by previously developed aircraft, and a few parameters that must be assumed in the early phase of the conceptional design. These parameters are the Figure of Merit (FoM), Disk Loading (DL or $\frac{W}{S_{rotor}}$), Blade Drag Coefficient ($C_{D_{blade}}$), solidity of the VTOL propeller (σ), and S_ratio ($\frac{S_{tot}}{S_{wing}}$). These parameters must be initially assumed based on statistical data and/or user experience, later in the design process these parameters will be able to be updated to increase the accuracy of the overall results. The following equations calculate the Power-to-Weight ratios during the take-off (2-61) and hover (2-62) mission phases of the aircraft during vertical flight;

$$\frac{P^{VTOL}}{W_{To}} = \frac{(RoC_{To})}{2} + \frac{1}{2}\sqrt{RoC_{To}^2 + \frac{2\left(\frac{W}{S_{rotor}}\right)}{(\rho_0)} + \frac{(\rho_0)\cdot(V_{tip}^3)\cdot(\sigma)\cdot(C_{D_{blade}})}{8\left(\frac{W}{S_{rotor}}\right)} + \frac{(\rho_0)\cdot(RoC^3)}{\left(\frac{W}{S_{rotor}}\right)}}$$
$$+ \frac{(\rho_0)\cdot(RoC^3)}{\left(\frac{S_{tot}}{S_{wing}}\right)\cdot\left(\frac{W}{S_{wing}}\right)} \qquad (\text{ 2-61 })$$

$$\frac{P^{VTOL}}{W_{To}} = \frac{\sqrt{\frac{\left(\frac{W}{S_{rotor}}\right)}{2(\rho_0)}}}{FOM} \qquad (\text{ 2-62 })$$

$$V_{tip} = \frac{\pi\cdot(rpm_{rotor})\cdot(D_{rotor})}{60} \qquad (\text{ 2-63 })$$

$$rpm_{rotor} = 2762.786\cdot D_{rotor}^{-0.932} \qquad (\text{ 2-64 })$$

The previously stated formulas shall be used in SI units. Thus, the rate of climb (RoC) in m/s, wing loading (W/S_{wing}) in N/m², disk loading (W/S_{rotor}) in N/m², density (ρ) in kg/m³, velocity (V) in m/s, surface areas S in m², and diameters (D) in m.

In the absence of further data, the following assumed/statistically determined parameters may be employed; a Blade Drag Coefficient ($C_{D_{blade}}$) of 0.01, solidity of the VTOL propeller (σ) of 0.077,

and it was assumed to be 0.077 an S_ratio ($\frac{S_{tot}}{S_{wing}}$) for a UAV of 1.3 - 1.4.

2.7.2   Tyan et al.

Tyan et al. [8] present a technique to calculate the power required during vertical flight, meaning, the power requirements during the VTOL segments of the mission of the UAV. This technique is based on the aircraft's performance requirements and a few parameters that must be estimated in the early phase of the conceptual design. These parameters are the Figure of Merit (FoM), Rotor Surface Area (S_{rotor}), Wing Loading ($\frac{W}{S_{wing}}$), and S_ratio ($\frac{S_{tot}}{S_{wing}}$). These parameters must be initially assumed based on statistical data and/or user experience, later in the design process these parameters will be able to be updated to increase the accuracy of the overall results.

The following equations calculate the Thrust-to-Weight ratios and Power requirements during the take-off/climb (2-65) and hover (2-66) mission phases of the aircraft during vertical flight;

$$\frac{T}{W}\bigg|_{climb}^{VTOL} = 1.2\left(1 + \frac{(\rho)\cdot(RoC^{VTOL})^2\cdot\left(\frac{S_{tot}}{S_{wing}}\right)}{\left(\frac{W}{S_{wing}}\right)}\right) \tag{2-65}$$

$$P_{req}^{VTOL} = \frac{T\cdot v_i}{FoM} \tag{2-66}$$

$$v_i = \sqrt{\left(\frac{1}{2}(RoC^{VTOL})\right)^2 + v_h^2} - \frac{1}{2}(RoC^{VTOL}) \tag{2-67}$$

Formula (2-67) is a helper function that determines the inflow velocity (v_i) in [m/s]. The inflow velocity is caused by the air passing through the lifting rotor due to the lift it produces and the velocity at which the entire aircraft moves through the air velocity.

$$v_h = \sqrt{\frac{T_{single\ rotor}}{2\cdot(\rho)\cdot\left(S_{rotor_{single}}\right)}} \tag{2-68}$$

Formula (2-68) is a helper function that determines the induced velocity during hover (v_h) in [m/s]. The induced velocity is caused by the air passing through the lifting rotor due to the lift it produces.

$$T_{single\ rotor} = \frac{T_{req}}{n_{rotor}} \tag{2-69}$$

$$S_{rotor_{single}} = \frac{T_{req_{max}}}{DL*n_{rotor}} \tag{2-70}$$

$$DL = \frac{W}{S_{rotor}} = 3.261(M_{To}) + 74.991 \tag{2-71}$$

Formulas (2-69) till (2-71) are helper functions that determine both the thrust each lifting rotor must produce during either take-off/climb or hover flight and the disk aera of the lifting rotor dependent on the take-off weight of the aircraft and the number of rotors (n_{rotor}).

The previously stated formulas shall be used in SI units. Thus, the density (ρ) in kg/m³, rate of climb (RoC) in m/s, wing loading $\left(W/S_{wing}\right)$ in N/m², surface areas S in m², velocity (V) in m/s, and diameters (D) in m.

In the absence of further data, the following assumed/statistically determined parameters may be employed; the Figure of Merit (FoM) of a propeller during loiter flight of 0.7 and 0.8 for during cruise, and an S_ratio ($\frac{S_{tot}}{S_{wing}}$) for a UAV of 1.3 - 1.4.

2.8 Stabilizer and Control Surface Sizing

Determining the size and the placement of the control system components is of great importance to a stability analysis and a weight and balance analysis. This is due to the significant contribution that the empennage has over the location of the Centre of Gravity (CG) of the aircraft. In order to determine the size and weight of the empennage, both empirically derived formulas and analytically based formulas can be used within the conceptual design phase of the aircraft. This chapter will describe the methods that can be used to determine the size and weight of the empennage.

2.8.1 Gudmundsson

Gudmundsson [1] presents a number of formulas that can determine the size and weight of the empennage in an empirical manner. The technique utilizes the size of the main wing together with volume fractions the size of the tail surfaces. As can be seen in formulas (2-72) and (2-74), the size of the tail surfaces are also dependent on the length of the tail. This can be analytically determined by minimizing the wetted area of the entire empennage section while assuming the tail section running to the tail surfaces is shaped like a cone, as can be seen in Figure 8, with formula (2-76). The tail length is set to be the length between the quarter chord of the main wing and the quarter chord of the stabilizers. The wetted area of an aircraft is the 'skin' of the aircraft which is exposed to the airstream which causes friction drag. By minimizing the wetted area, the amount of friction drag created by the empennage is also minimized. This method presented by Gudmundsson is specifically for a conventional tail configuration. This method can determine the surface area of the stabilizers with formulas (2-72) and (2-74), span of the stabilizers with formulas (2-73) and (2-75), and the optimal length of the tail with formula (2-76).

$$S_{HT} = \frac{V_{HT} \cdot S_{wing} \cdot C_{wing}}{l_{tail}} \qquad (\text{2-72})$$

$$b_{HT} = \sqrt{AR_{HT} \cdot S_{HT}} \qquad (\text{2-73})$$

$$S_{VT} = \frac{V_{VT} \cdot S_{wing} \cdot b_{wing}}{l_{tail}} \qquad (\text{2-74})$$

$$b_{VT} = \sqrt{AR_{VT} \cdot S_{VT}} \qquad (\text{2-75})$$

$$l_{tail} = \sqrt{\frac{2(S_{wing}) \cdot \left((V_{HT}) \cdot (C_{wing}) + (V_{VT}) \cdot (b_{wing})\right)}{\pi(R_1 + R_2)}} \qquad (\text{2-76})$$

The previously stated formulas can be used both in SI as in Imperial units. Thus, surface aera (S) in [m²], span (b) in [m], Mean Aerodynamic Chord (C) in [m], and length (l) in [m].
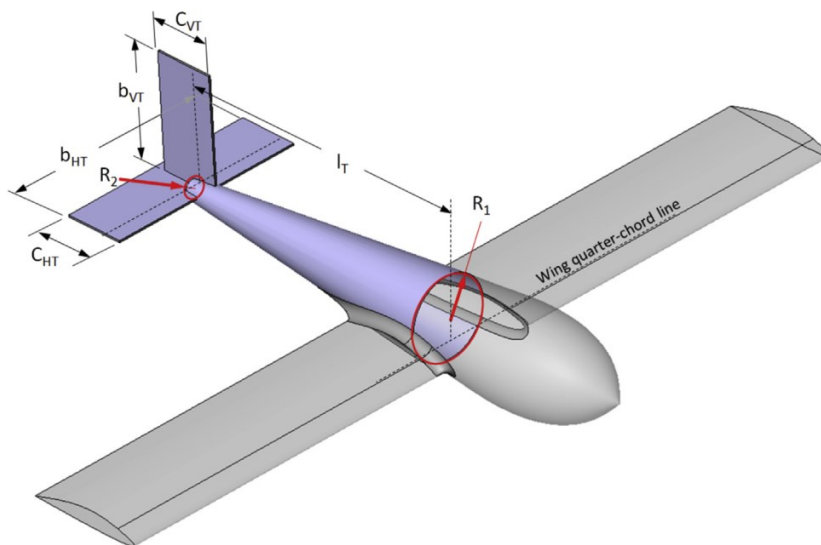

Figure 8 - Definition of dimensions for the horizontal- and vertical tail surface and tail length determination [1]

2.8.2 Sadraey

Sadraey [7] presents a number of formulas that, can estimate the size of the control surfaces of the aircraft based on empirically determined ratios between either the surface area, span, or Mean Aerodynamic Chord of a reference surface. Formulas (2-77) till (2-79) determine the surface area, formulas (2-80) till (2-82) determine the span, and (2-83) till (2-85) the chord of the control surface. Figure 10 shows the location and the method of dimensioning the control surfaces. The ratios utilized in these formulas are shown in Figure 9 and can be implemented for conventional control surfaces.

$$S_{elev} = 0.275 \cdot S_{HT} \qquad (2\text{-}77)$$
$$S_{ail} = 0.075 \cdot S_{wing} \qquad (2\text{-}78)$$
$$S_{rud} = 0.25 \cdot S_{VT} \qquad (2\text{-}79)$$
$$b_{elev} = 0.90 \cdot b_{HT} \qquad (2\text{-}80)$$
$$b_{ail} = 0.30 \cdot b_{wing} \qquad (2\text{-}81)$$
$$b_{rud} = 0.85 \cdot b_{VT} \qquad (2\text{-}82)$$
$$C_{elev} = 0.30 \cdot C_{HT} \qquad (2\text{-}83)$$
$$C_{ail} = 0.225 \cdot C_{wing} \qquad (2\text{-}84)$$
$$C_{rud} = 0.275 \cdot C_{VT} \qquad (2\text{-}85)$$

The previously stated formulas can be used both in SI as in Imperial units. To keep the report as uniform as possible it was chosen to use the SI units. Thus, surface area (S) in [m²], span (b) in [m], and Mean Aerodynamic Chord (C) in [m].

Control surface	Elevator	Aileron	Rudder
Control surface area/lifting surface area	$S_E/S_h = 0.15\text{--}0.4$	$S_A/S = 0.03\text{--}0.12$	$S_R/S_V = 0.15\text{--}0.35$
Control surface span/lifting surface span	$b_E/b_h = 0.8\text{--}1$	$b_A/b = 0.2\text{--}0.40$	$b_R/b_V = 0.7\text{--}1$
Control surface chord/lifting surface chord	$C_E/C_h = 0.2\text{--}0.4$	$C_A/C = 0.15\text{--}0.3$	$C_R/C_V = 0.15\text{--}0.4$
Control surface maximum deflection (negative)	−25 deg (up)	25 deg (up)	−30 deg (right)
Control surface maximum deflection (positive)	+20 deg (down)	20 deg (down)	+30 deg (left)

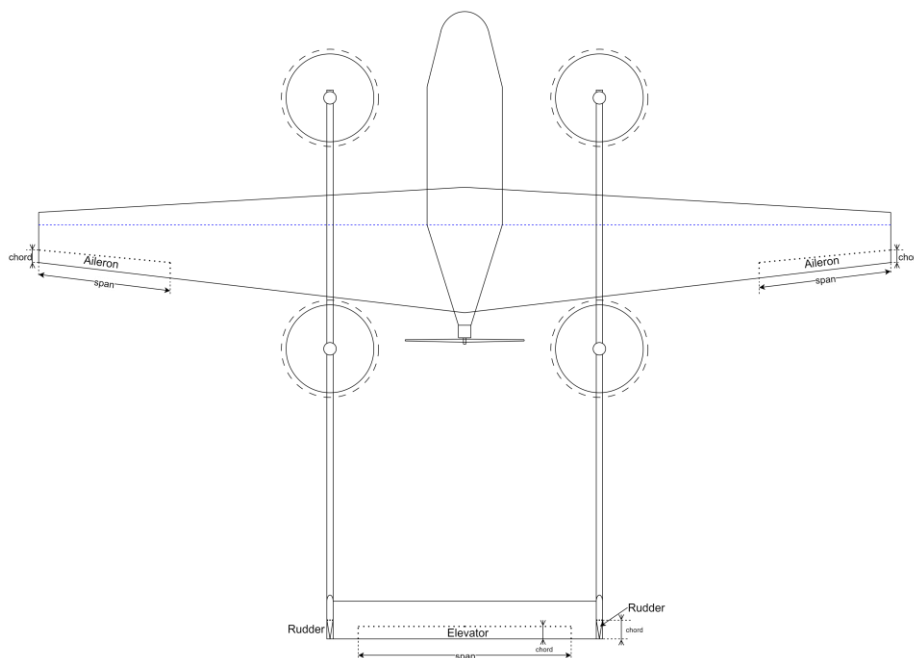*Figure 9 - Typical values for geometry of control surfaces [7]*

Figure 10 - Location and dimensions of the control surfaces, UAV top view

2.9 Landing Gear Placement

The determination of the placement of the landing gear, and the length which also is determined in this process, has a substantial effect on the overall aircraft. This is mainly due to the placement of the weight that is contributed with the landing gear, but also space must be made to mount the landing gear, especially in the case the gear is retractable. In the context of a conceptual design of a UAV a single method is presented by multiple sources to determine the placement of the landing gear. This method is described in this chapter.

2.9.1 Sadraey

Sadraey [7] states several requirements for a landing gear regarding its height and location, these are;

- The landing gear ensures clearance between the aircraft and the ground during ground operations.
- The landing gear ensures that the aircraft can rotate (increase the angle of attack during take-off) to the required angle of attack without experiencing a tail strike.
- The landing gear provides a safety margin on tipping back during ground operation (mainly loading and unloading of the payload).
- The landing gear ensures the aircraft does not "tip over" while turning on the ground, i.e. that a wing strikes the ground due to excessive rolling due to centrifugal force during turning on the ground.

To ensure that the landing gear complies with these requirements the following methods are presented for the landing gear location for a tricycle-style landing gear;

Ground clearance

The minimum length of the landing gear dependent on general ground clearance is determined by the 'lowest point' of the aircraft, this might be the fuselage, a propeller, or a different component. The length of the landing gear is in this case equal to the (vertical) distance from the mounting point of the gear to the lowest point of the aircraft with an added safety margin added to this length. This safety margin can be a multiplication factor, but also a discrete length.

Take-off rotation clearance

To ensure clearance during the take-off rotation both the length and location of the landing gear are dependent on the desired take-off attitude, i.e. the angle of attack during the take-off rotation. A visualization of this is shown in Figure 11. As in the figure, a safety margin must be added to the length of the landing gear to allow for a discrete distance between the runway and the first point of risk for a tail strike, point A in Figure 11 and Figure 12.
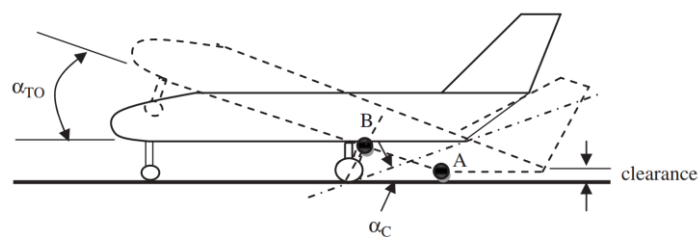

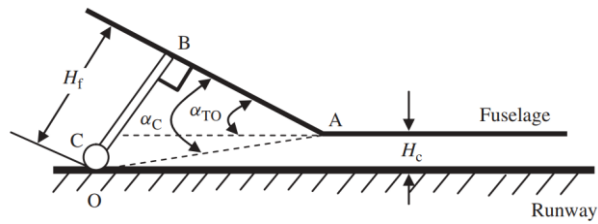*Figure 11 - Landing gear length and location for take-off clearance [7]*

Figure 12 – Landing gear clearance angle [7]

To determine the required clearance angle (α_c) of the landing gear for, the following formula is presented:

$$\alpha_c = \tan^{-1}\left(\frac{H_f}{AB}\right) \qquad\qquad (\,2\text{-}86\,)$$

With AB being the distance between the first point of risk for a tail strike and the attachment point of the landing gear. H_f being the clearance height between the fuselage and the ground.

Tip-back prevention

The tip-back prevention requirement solely effects the location of the landing gear, or in other words the wheelbase. The wheelbase is the distance between the nose gear and the main gear $((B)$ in Figure 13). Sadraey presents a method that determines the location of the landing gear with respect to the centre of gravity of the aircraft, as can be seen in Figure 13. This method is based on the minimum and maximum loads that the nose and main landing gear must/can carry, considering the centre of gravity that shifts during the loading and unloading of the aircraft. The method of dimensioning the landing gear for the shifting centre of gravity is shown in Figure 14. Sadraey recommends that the nose gear should carry a maximum of 20% of the weight of the aircraft, and a minimum of 5%. Next to this, the location of the main gear should have a minimum distance from the most aft predicted centre of gravity of 5% of the total wheelbase $((B)$ in Figure 13) of the aircraft and a maximum distance of 20%. When applying these requirements and guidelines to the formulas (2-87) - (2-92), the (approximate) location of the landing gear can be determined when only considering the tip-back requirements.
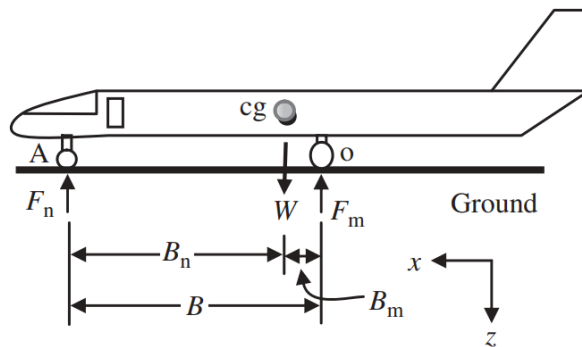

Figure 13 - landing gear location dimensioning with respect to the centre of gravity [7]
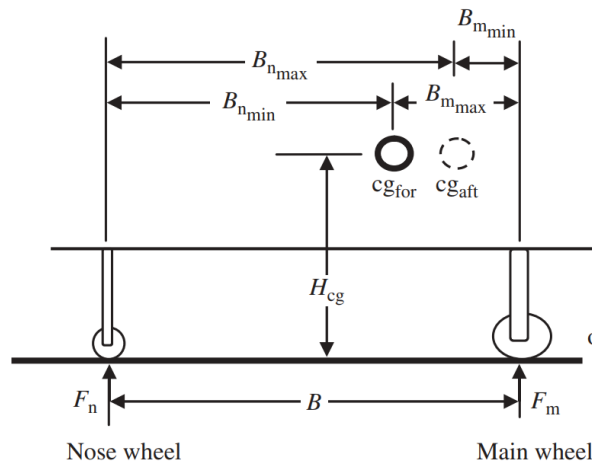
Figure 14 - landing gear location dimensioning with respect to a varying centre of gravity location [7]

$$F_m = \frac{B_n}{B} W_{To} \qquad (2\text{-}87)$$

$$F_n = \frac{B_m}{B} W_{To} \qquad (2\text{-}88)$$

$$F_{m_{max}} = \frac{B_{n_{max}}}{B} W_{To} \qquad (2\text{-}89)$$

$$F_{m_{min}} = \frac{B_{m_{min}}}{B} W_{To} \qquad (2\text{-}90)$$

$$F_{n_{max}} = \frac{B_{n_{min}}}{B} W_{To} \qquad (2\text{-}91)$$

$$F_{n_{min}} = \frac{B_{m_{min}}}{B} W_{To} \qquad (2\text{-}92)$$

Tip-over prevention

The tip-over prevention requirement effects the wheel track of the aircraft, but also the wheelbase. The wheel track is the distance between the most right and most left main landing gear. To prevent an aircraft from tipping over a wider/greater wheel track is desired, but this is not always desired from a design standpoint. This method is able to determine the minimum wheel track, dependent on the wheelbase of the aircraft and the height of the centre of gravity above the ground.

The method presented by Sadraey is based on the guideline that the 'tip-over-angle' must be greater than 25°. The tip-over-angle are two angles that characterize the landing gear, these can be seen in Figure 15. The smallest of the two is the more critical one.

The first is, as shown in Figure 15a, the angle measured from, when looking at the aircraft top view, the line passing through the main gears (say the left one) and the nose gear, and the line that runs from the centre of gravity of the aircraft which cross each other at a distance equal to the height of the aircraft's centre of gravity above the ground.

The second angle, which is shown in Figure 15b, is measured from, when looking from the front of the aircraft, the centre of gravity to the point where either of the main landing gear contacts the ground with respect to a vertical line drawn from the centre of gravity.
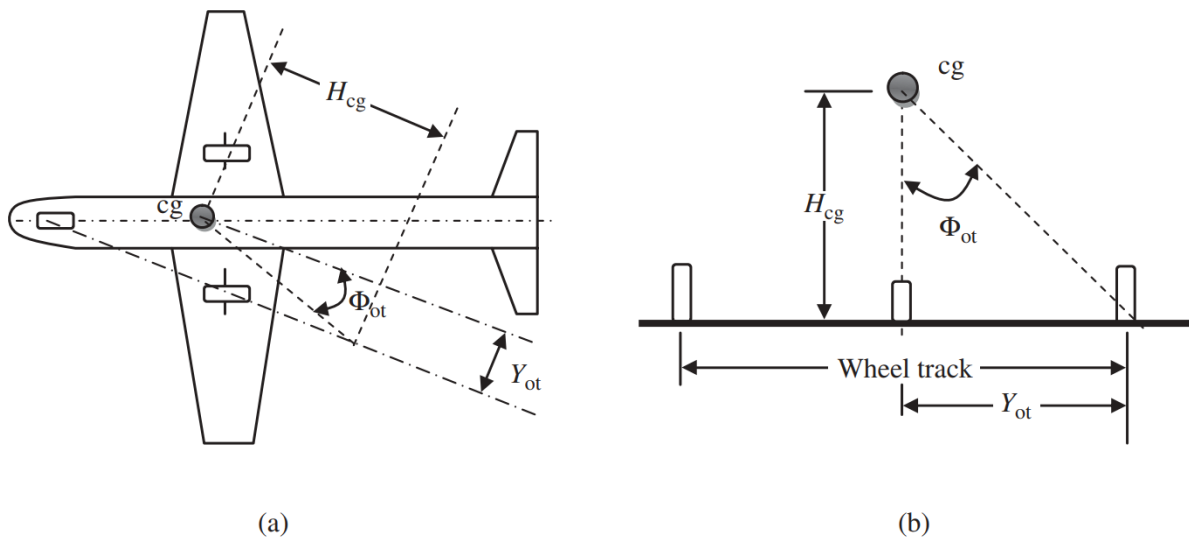
Figure 15 - Tip-over-angle (Φ_{to}) for a tricycle landing gear,
(a) Φ_{to} based on the top view, and (b) Φ_{to} based on the front view [7]

2.9.2 Gudmundsson

Gudmundsson [1] presents the same technique as presented by Sadreay, although Gudmundsson does have several discrepancies with the method of Sadreay. These discrepancies will be presented in this chapter.

The first main discrepancy lies with the take-off rotation analysis, here Gudmundsson, as shown in Figure 16, gives a guideline on the angle that should be used for the clearance angle which the landing gear must achieve of either the stall angle of attack or 15°.
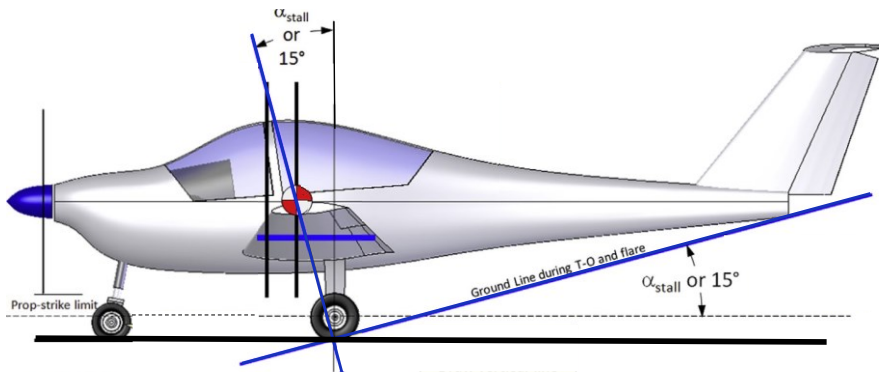
Figure 16 - take-off rotation landing gear placement [1]

The second discrepancy lies in the tip-over-angle analysis, here Gudmundsson, as shown in Figure 17, gives a guideline for the tip-over-angle specifically land- and aircraft carrier-based aircraft. This is, with the same reference frame as Sadreay, 27° and 36°, respectively.
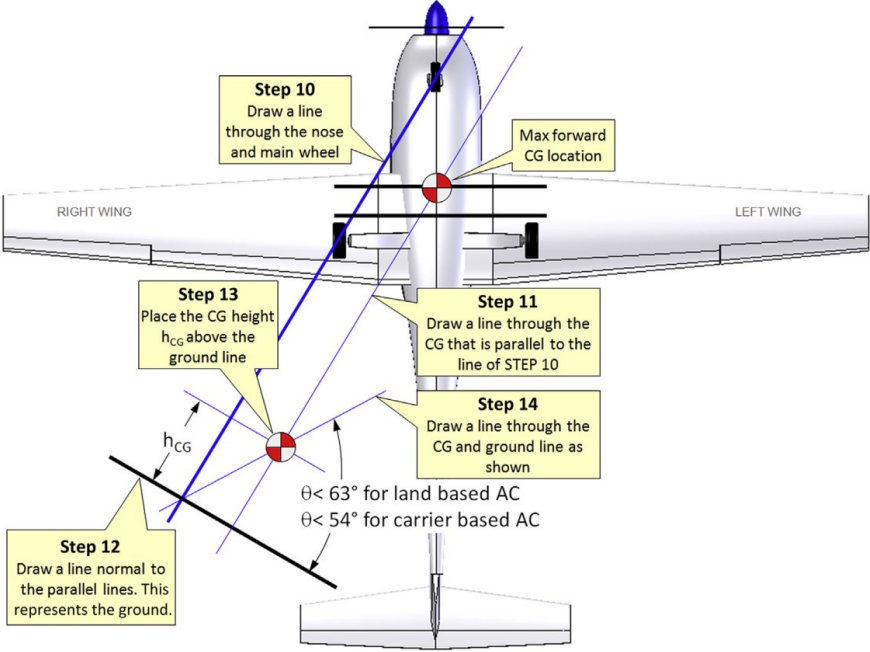
Figure 17 - Tip-over-angle (Φ) according to Gudmundsson [1]

The third and last main discrepancy lies in the guidelines for the minimum and maximum load on the nose landing gear. Gudmundsson gives a minimum load of 10% and a maximum load of 20%. This is with the argument that when the load on the nose landing gear exceeds 20%, rotating during the take-off becomes more challenging and when this load is less than 10%, porpoising can become an issue (the periotic increasing and decreasing load on the nose gear due to dynamic effects).

3. Methodology

This chapter will describe the methods implemented in the toolchain program, together with a description of why these methods are chosen.

3.1 Toolchain Requirements

This chapter presents the requirements for the type of UAV the toolchain must be able to design. These requirements have been provided by the DLR as a verification method to see if the toolchain can analyse the desired type of aircraft. The requirements for the aircraft are shown in Table 3.

Reviewing the requirements in Table 3, the following functional requirements can be set up for the toolchain itself, which the toolchain must comply with;

Table 2 - toolchain requirements

ID	Requirement
Tool - 1	Shall be able to design a UAV that can take-off both conventional and vertically.
Tool - 2	Shall be able to design a UAV that can weigh up to 25kg.
Tool - 3	Shall be able to design a UAV that has a wingspan up to 3m.
Tool - 4	Shall be able to design a UAV that has a maximum airspeed of 35m/s.
Tool - 5	Shall be able to design a UAV that has a fixed wing.
Tool - 6	Shall be able to design a UAV that has two payload bays, one in the nose of the aircraft, and one with access to the bottom of the fuselage.
Tool - 7	Shall be able to take into account the dimensions of the main payload bay.
Tool - 8	Shall be able to design a UAV that has a (main) payload capacity of 4 kg.
Tool - 9	Shall be able to design a UAV that has a (secondary) payload capacity of 0.2 to 0.8 kg.
Tool - 10	Shall be able analyze the static stability of the UAV with all possible payload configurations.
Tool - 11	Shall be able to design a UAV that has an electronics bay, which has access to the bottom of the fuselage.

Table 3 - aircraft requirements for the toolchain

ID	Requirement	Type
Air - 1	The operation shall be possible within the open category	Mission
Air - 1.1	The MTOM shall be smaller than 25kg	Mission
Air - 1.2	During operations, the UA shall not drop any material	Mission
Air - 2	SORA 2.5 certification according to SAIL IV shall be possible	Mission
Air - 2.1	max. dimension shall be <= 3m	Mission
Air - 2.2	max. velocity shall be <= 35 m/s	Mission
Air - 3	An integration of a parachute shall be possible	Derived
Air - 4	The configuration shall be capable of performing VTOL	Mission
Air - 5	The design shall be a fixed wing design	Mission
Air - 6	The operation shall be possible with the FPV pilot station	Mission
Air - 6.1	The system shall have a Walksnail FPV system	Mission
Air - 7	The system shall have a payload mounting below the fuselage which can carry up to 4kg payload	Mission
Air - 7.1	The system shall have stable flight behavior with any payload configuration according to payload limits	Mission
Air - 7.2	The max. Payload volume, when retractable, shall be not smaller than 200mm x 200mm x 200mm	Mission
Air - 8	The system shall have a payload mounting in the nose region which can carry a payload between 0.2 and 0.8 kg	Mission
Air - 9	The system shall be controlled by a Pixhawk 6x autopilot	Mission
Air - 10	The system shall have a LiDAR altitude system	Mission
Air - 11	The system shall have a means to measure the air speed	Mission
Air - 12	The system shall have a means to measure the angle of attack	Mission
Air - 13	The system shall have a means to measure the side slip angle	Mission
Air - 14	The system shall have a GPS antenna	Mission
Air - 15	The system shall have drone ID equipment	Mission
Air - 16	The system shall have a means to estimate the remaining flight time and range	Mission
Air - 17	The system shall have two separate RC links.	Mission
Air - 17.1	One of the RC links shall provide direct control of the system	Mission

3.2 Toolchain Flowchart

The design process realized by the toolchain is based on the process presented by Gudmundsson in 2.2.1. The design process of Gudmundsson is modified to suit a computer-based design method better. The modification include the reordering and combining of multiple steps presented by Gudmundsson and leaving out other steps which are not (as) applicable to the design of a small research-intended UAV. The modified design process is presented in Figure 18 as a flowchart.
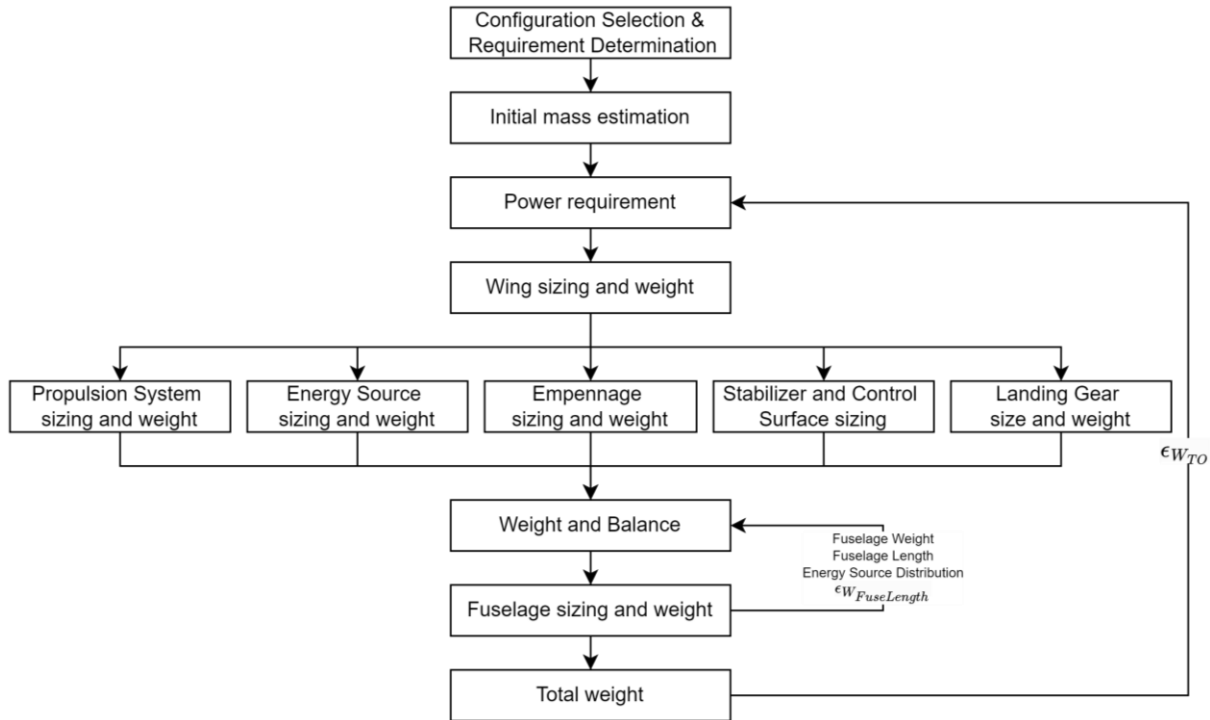
Figure 18 - Toolchain Flowchart

The flowchart initiates with the configuration and requirement determination, this is where the user defines what the UAV should do and how the UAV should look like.

The remaining part of the flowchart will be run automatically by the toolchain and will output the parameters which the user can use as the start point for additional analyses or the preliminary design of the UAV

The following subchapters will present the methods employed in the flowchart.

3.3 UAV Configuration

The toolchain is set to create a UAV with a conventional wing, pusher propeller, and twin-boom tail configuration with an inverted U-tail, a visualization of which, with varying number of VTOL motors, is given in Figure 19. This configuration was selected by implementing a trade-off between 5 configurations that can fulfil the goals set for the UAV in 3.1. This trade-off can be seen in Appendix B – UAV Configurations together with a detailed description of the configurations mentioned in trade-off table and a description on how these configurations are rated. The advantages of this configuration are the following:

- An unobstructed view forward for the front payload bay, due to the forward flight propeller mounting on the rear of the fuselage,
- Convenient mounting opportunities for the VTOL propulsion system, due to the twin-boom design
- The efficiency and reliability of a conventional wing
- Less turbulent flow over the horizontal stabilizer, due to the inverted U-tail configuration

Figure 19 - toolchain UAV configuration

3.4 Module Methods

This chapter will describe the methods in detail that are implemented in the modules of the toolchain, together with why it was chosen to use these.

3.4.1 SUAVE

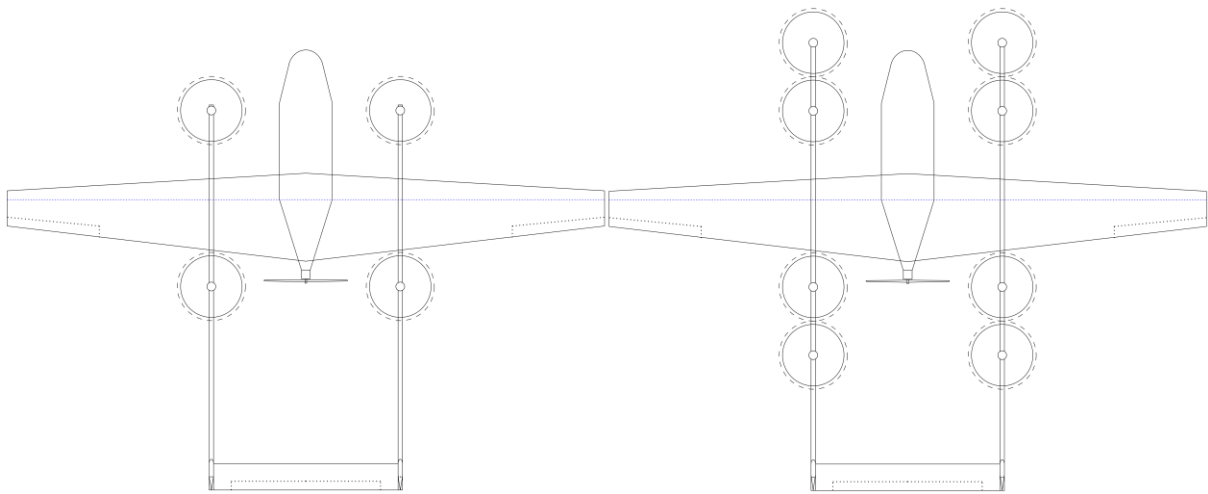It was chosen not to implement the SUAVE program due to two main reasons, the first is that through further research and user experience it has shown that the program requires data on the desired UAV which can not be known in the early conceptual design phase. The other reason is that the program requires extensive knowledge on the functions within the program in order to craft a sound design. Meaning that in the timeframe of this project it would not have been feasible to research how to implement the SUAVE program with the potential risk that the program would not be able to be used for the use case of this project.

An additional aspect on why it was chosen not to use SUAVE is the extend/customizability of a custom toolchain. This is due to all information and knowledge on how the program was created/methods employed are known and can thus be, relatively, easily be modified for a custom purpose.

3.4.2 Initial Mass Estimation

The initial mass estimation is determined using the database Janes [11]. This database contains data on the MTOM, Payload Mass, Range, Endurance, and other parameters of existing UAVs for several use cases. The MTOM of these UAVs ranges from 1.9 kg to 14628 kg. The contents and structure of this database will be further discussed in Appendix C – Data Collection.

A database is used to calculate the initial take-off mass of the UAV due to the ability of the user to specify which dependencies to base the mass calculation on. This has the advantage of being able to base the mass calculation on, what for the UAV, is the most important dependency that will influence the take-off mass. Furthermore, the database that is used can be altered by the user to provide a specific range of existing UAV masses and other dependencies to give a more appropriate result as the take-off mass.

The alternative method, the mass-fraction-based method described in chapter 2.4.1, has the limitation that the result of the calculation is only dependent on the payload mass, together with the weight of the crew. Due to a UAV not carrying crew, this term can be ignored. By only basing the take-off weight on the payload weight can give a highly inaccurate output. This can happen when the desired UAV does not correlate with the average of the other parameters of the UAVs on which the mass-fraction method was based.

The flowchart, shown in Figure 20, visualizes what happens in the initial mass estimation module.
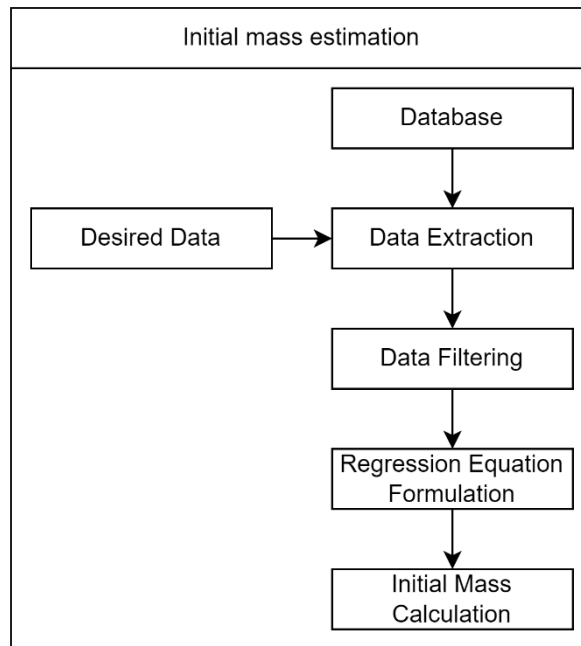
Figure 20 - Flowchart Initial Mass Estimation Module

3.4.2.1   Initial Weight Estimation Method

The method used to determine the initial Maximum Take-Off Mass (MTOM), for the desired UAV is realized by linearly regressing the applicable data from the specified database into an equation dependent on the desired parameters. The regression method is done by feeding the applicable data into either the "polyfit()" function provided by Numpy [14], if the user selects two dependencies for the regression process, or fed into the "curve_fit()" function provided by Scipy [15], if the user selects three dependencies for the regression process.

After the regression equations have been set up, these can be filled in with the parameters given by the user to output the initial mass estimation result.

The initial mass estimation module does not only output the initial mass estimation, but it also outputs the regression equation that was determined, together with the r^2 error value associated with the regression equation. This ensures that the user can either document and/or check if the modules gave reasonable intermediate results.

The Initial Mass Estimation module has the capability to generate a first and second order polynomial equation by taking one or two dependencies to determine the MTOM of the UAV. The determination of the first and second-order equations depending on one dependency, (2-2) and (2-3) respectively, are created by the NumPy [14]. The first and second-order equations depend on two dependencies, (2-4) and (2-5) respectively, are created by the SciPy [15].

By giving the user choice of the order of the regression equation, and number of dependencies, adds flexibility on how the code is implemented. In addition to this, it gives the opportunity for the code can be reused for similar purposes.

The advised method of determining the regressed formula for the initial take-off mass is to regress the MTOM toward the Payload Mass with a regression equation of the second order. This was determined by analyzing the data presented in the database, Janes. When this is desired, the dependency on Range can be added to the regression equation. Applying this method has resulted in a relative error between the regression equation and the utilized data of $r^2 = 0.827$, with 1 being ideal.

Formulas

The regression equations that can be used are based on the following linear regression equations [12]:

$$z = \beta_0 + \beta x \qquad\qquad (2\text{-}2)$$

$$z = \beta_0 + \beta_1 x + \beta_2 y \qquad\qquad (2\text{-}3)$$

$$z = \beta_0 + \beta_1 x + \beta_2 x^2 \qquad\qquad (2\text{-}4)$$

$$z = \beta_0 + \beta_1 x + \beta_2 y + \beta_3 x^2 + \beta_4 y^2 + \beta_5 xy \qquad\qquad (2\text{-}5)$$

Assumptions

- The initial mass estimation module functions with the assumption that the data on the existing UAV within the Janes database are similar in the characteristics of their end-use. Furthermore, the assumption is that Janes contains a high enough number of data points to accurately generate a regressed equation that can be used to estimate the MTOM for the desired UAV.
- From implementing the previously described method it is found that more accurate result is given when the β_0 component is left out. This represents the more traditional method of determining the initial mass (by mass fractions) more closely due to this lack of β_0 term in this method, this is also represented in the method presented by Sadraey in 2.4.1.1. When β_0 is included in the regression equation, this indicates that the aircraft must have a mass even without any requirement, like payload capacity or range. This can give a MTOM with a significant mass offset, mainly when a low payload and/or range is set as requirements. This is due to the data on the UAVs in Janes.

3.4.3   Power Requirement

This chapter will present the influence that performance requirements have on the required power, with respect to the weight of the aircraft. This applies for each of the mission segments for both forward, as for vertical flight.

The flight segments that will be discussed are the; Take-off, Climb, Cruise, Loiter, and Descent. In practice, the Landing segment is part of the mission as well, but this is not considered in this analysis, due to insignificant amounts of power is required during this segment. The only case the Landing segment would require a significant amount of power is when the UAV must perform a Landing abort. The power required during the abort is assumed to be equal to the conventional Take-off segment, STOL, or VTOL manoeuvre. These instances will not be taken into account for the total amount of energy that is required during a mission. In Figure 21 till Figure 24 visualizations are given in of the flight segments within the typical mission profiles. An overview of the methods utilized in the power requirement module is shown in Figure 25.
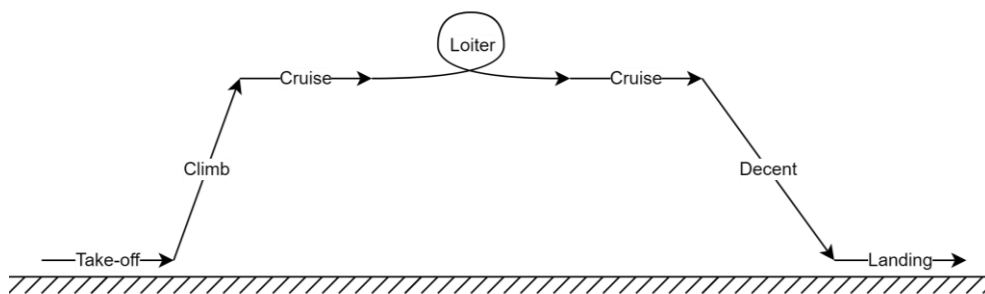

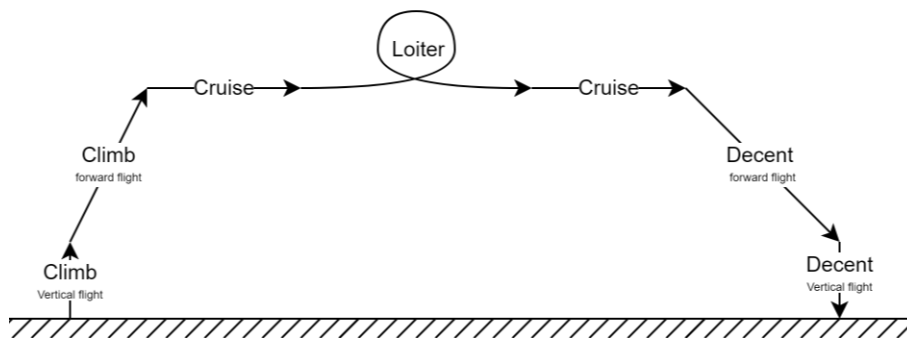*Figure 21 – pure forward flight mission profile, alternate destination*

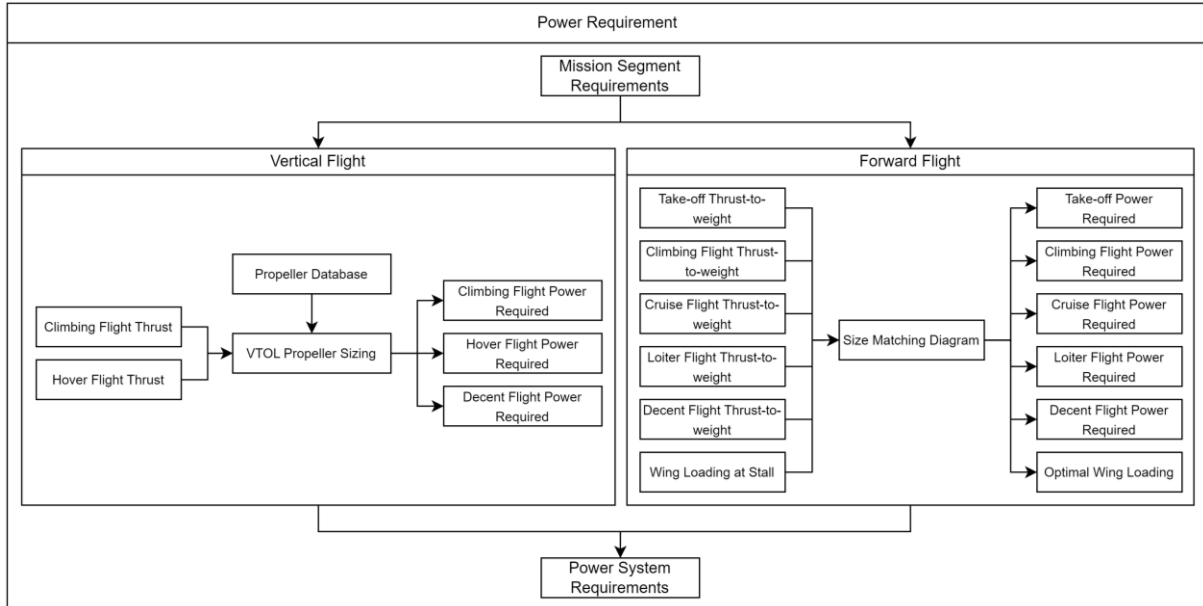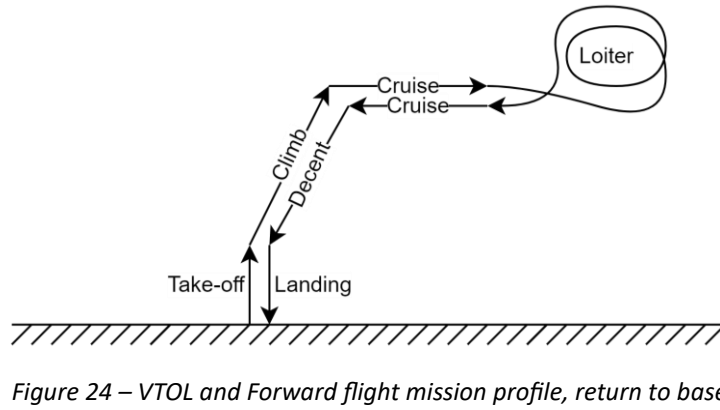*Figure 22 – VTOL and Forward flight mission profile, alternate destination*

Figure 23 – pure forward flight mission profile, return to base

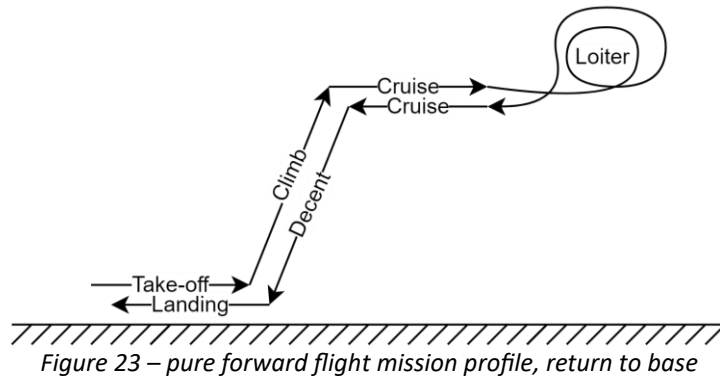*Figure 24 – VTOL and Forward flight mission profile, return to base*

Figure 25- Flowchart Power Requirement Module

3.4.3.1　Forward Flight Power Requirement Method

The power requirement for each forward flight segment is calculated numerically by means of determining the thrust-to-weight ratio for each segment with respect to a range of wing loadings. The goal of determining the thrust-to-weight ratio for each segment is to be able to determine the optimal wing surface area and the thrust/power the propulsion system must be able to provide. This method is based on one described by Sadraey (chapter 4, [7]) utilizing the formulas described by Gudmundsson (chapter 3, [1]). The method described by Sadraey is as follows;

1. Determine the thrust(-to-weight) requirement equations for each flight segment as a function of wing loading. The mission segments taken into account are: Take-Off run $(T/W_{S_{To}})$ with (2-50), climb (T/W_{climb}) with (2-51), cruise (T/W_{cruise}) with (2-52), loiter (T/W_{loiter}), descent $(T/W_{descent})$, service ceiling $(T/W_{ceiling})$ with (2-53), steady turn $(T/W_{Steady\ turn})$ with (2-54), and $(T/W_{V_{max}})$ with (2-59).
2. Determine the W/S_{stall} specific to the airfoil (initially) chosen with (2-55).
3. Plot the thrust(-to-weight) requirements as a function of wing loading in one graph, this graph is called a size-matching diagram. An example of a matching diagram is shown in Figure 26. The visualization can give a clear indication on which of the specified flight segment requirements are most critical to the determination of the wing sizing.
4. Identify the acceptable/viable region within the size-matching diagram. The acceptable region in the sizing diagram is the region that complies with all thrust(-to-weight) requirements, this can be identified both visually and analytically. The blue-shaded region in Figure 26 shows the acceptable region for this example.
5. From the viable region, identify the optimal design points. These are most typically points of intersection of the thrust-to-weight ratio graphs bordering the viable region. The most important requirement of the chosen design point is to choose the point that results in the lowest thrust-to-weight ratio requirement as possible. This will result in a smaller propulsion system, or in other words, a propulsion system that requires less power. This both reduces the final take-off weight of the aircraft, as reducing the amount of energy the aircraft requires for a mission. This ultimately results in a lower cost of the system and operation.
6. From the chosen design point, extract the thrust-to-weight ratio requirement for each flight phase, and the optimum wing loading.
7. Calculate the thrust and wing surface area required dependent on the current (estimation of the) take-off weight of the aircraft. If a propeller-based propulsion system is utilized, calculate the power requirements from the thrust requirements for each flight phase.

This method was chosen because it can determine the optimum wing loading together with the thrust/power requirements whiles considering all forward flight segment requirements. Next to this, the method is based on numeric formulas which have been derived from standard energy conservation equations. These formulas do require several empirically found parameters on the desired aircraft, like the minimal drag coefficient $(C_{D_{min}})$, Oswald efficiency factor (e), wing aspect ratio (AR), take-off drag coefficient $(C_{D_{To}})$, take-off lift coefficient $(C_{L_{To}})$, maximum lift coefficient of the wing $(C_{L_{max}})$, and propeller efficiency (η_{prop}), but these parameters can be updated, either in the conceptual- or preliminary design phase in order to get more accurate results

It was chosen to utilize the formulas given by Gudmundsson over the formulas given by Sadreay due to Sadreay's use of the L/D_{max} variable in the formulas. This term can be estimated but is highly dependent on the type of aircraft and use case of this. Next to this, this term will be difficult to determine during the iteration process of the UAV without performing a detailed aerodynamic analysis. Next to this, Gudmundsson also presents a formula to calculate the thrust(-to-weight) requirements for steady turning flight and cruise flight.

Formulas

The formulas used in the power requirement module are listed below:

Formula		Source	Nr.

$$\frac{T}{W}_{service\ ceiling}^{FF} = \frac{ROC_{ceiling}}{\sqrt{\frac{2}{\rho}(W/S_{wing})\sqrt{\frac{k}{3C_{D_{min}}}}}} + 4\sqrt{\frac{k \cdot C_{D_{min}}}{3}}$$

[1]   (2-53)

$$\frac{T}{W}_{cruise}^{FF} = q\frac{(C_{D_{min}})}{(W/S_{wing})} + \left(\frac{k}{q}\right)(W/S_{wing})$$

[1]   (2-52)

$$\frac{T}{W}_{To}^{FF} = \frac{V_{To}^2}{2g \cdot S_g} + \frac{q \cdot C_{D_{To}}}{(W/S_{wing})} + \mu\left(1 - \frac{q \cdot C_{L_{To}}}{(W/S_{wing})}\right)$$

[1]   (2-50)

$$\frac{T}{W}_{climb}^{FF} = \frac{ROC}{V_{Climb}} + \frac{q}{(W/S_{wing})}C_{D_{min}} + \frac{k}{q}(W/S_{wing})$$

[1]   (2-51)

$$\frac{T}{W}_{steady\ turn}^{FF} = q\left(\frac{C_{D_{min}}}{(W/S_{wing})} + k\left(\frac{n_{turn}}{q}\right)^2 (W/S_{wing})\right)$$

[1]   (2-54)

$$\left(\frac{W}{S_{wing}}\right)_{stall} = \frac{1}{2}\rho V_{stall}^2 \cdot C_{L_{max}}$$

[1]   (2-55)

$$V_{climb} = \sqrt{\frac{2}{\rho}(W/S_{wing})\sqrt{\frac{k}{3C_{D_{min}}}}}$$

[1]   (3-1)

$$P/W = \frac{\frac{T}{W}^{FF} * V}{\eta_{prop}}$$

[3]   (3-2)

$$q = \frac{1}{2}\rho V^2$$

[1]   (3-3)

$$k = \frac{1}{\pi \cdot e \cdot AR_{wing}}$$

[1]   (3-4)

$$e_{strait} = 1.78\left(1 - 0.045(AR_{wing})^{0.68}\right) - 0.64$$

[5]   (3-5)

$$e_{swept} = 4.68\left(1 - 0.045(AR_{wing})^{0.68}\right) \cdot (cos(\Lambda_{LE})^{0.15}) - 3.1$$

[5]   (3-6)

$$n_{turn} = \frac{1}{cos(\phi)}$$

[1]   (3-7)

$$C_{L_{max}} = 0.9 \cdot C_{l_{max}} \cdot cos(\Lambda_{c/4})$$

[5]   (3-8)

Formula variables

$\frac{\text{T}}{\text{W}}^{FF}$	Is the required thrust-to-weight ratio during each forward flight segment [-]
$ROC_{ceiling}$	Is the desired Rate of Climb for at the service ceiling for forward flight, normally 0.508 m/s [m/s]
ρ	Is the local air density [kg/m³]
W/S_{wing}	Is the wing loading of the main wing [N/m²]
k	Is the wing efficiency factor [-]
$C_{D_{min}}$	Is the minimal drag coefficient of an aircraft [-]
q	Is the dynamic pressure [kg/m²]
V_{To}	Is the required take-off airspeed [m/s]
g	Is the gravitational acceleration of earth [m/s²]
S_g	Is the ground run distance designated for the forward flight take-off [m]
$C_{D_{To}}$	Is the drag coefficient of an aircraft during take-off [-]
$C_{L_{To}}$	Is the lift coefficient of an aircraft during take-off [-]
μ	Is the rolling resistance coefficient of the wheels with the ground [-]
ROC	Is the desired Rate of Climb for during climbing forward flight [m/s]
V_{Climb}	Is the optimal airspeed for the aircraft during forward flight climb [m/s]
n_{turn}	Is the load factor introduced by the desired bank angle during a turn [-]
V_{stall}	Is the desired stall airspeed [m/s]
$C_{L_{max}}$	Is the maximum lift coefficient of the main wing stabilizer [-]
P/W	Is the power-to-weight ratio required for a thrust-to-weight ratio [W/N]
V	Is the airspeed [m/s]
η_{prop}	Is the propeller efficiency [-]
e	Is the Oswald factor of the main wing [-]
AR_{wing}	Is the aspect ratio of the main wing [-]
Λ_{LE}	Is the wing sweep at the leading edge of the main wing [°]
ϕ	Is the desired bank angle during a turn [°]
$C_{l_{max}}$	Is the maximum (2D) lift coefficient of the main wing stabilizer [-]
$\Lambda_{c/4}$	Is the wing sweep at the quarter chord of the main wing [°]

Assumptions

The following assumptions and limitations are set;

- The minimum drag coefficient does not significantly change during the different flight segments
- The rate-of-decent during the descent flight phase does not exceed the sink rate during optimal unpowered flight, i.e., the thrust(-to-weight) ratio during the descent phase does not become negative.
- The Take-off power required is calculated by considering how much power it requires to accelerate the UAV to its take-off velocity within a specified ground run/distance. When assuming no wind speed that creates a difference between the airspeed and the ground speed.
- The wing does not contain any high-lift devices that influence the maximum lift coefficient at any segment of the mission.
- The 3D lift coefficient can accurately be estimated by utilizing formula (3-8)
- The Oswald efficiency factor can accurately be estimated by utilizing either formula (3-5) or (3-6)
- The energy required to perform an aborted landing will not be considered in the sizing of the energy source
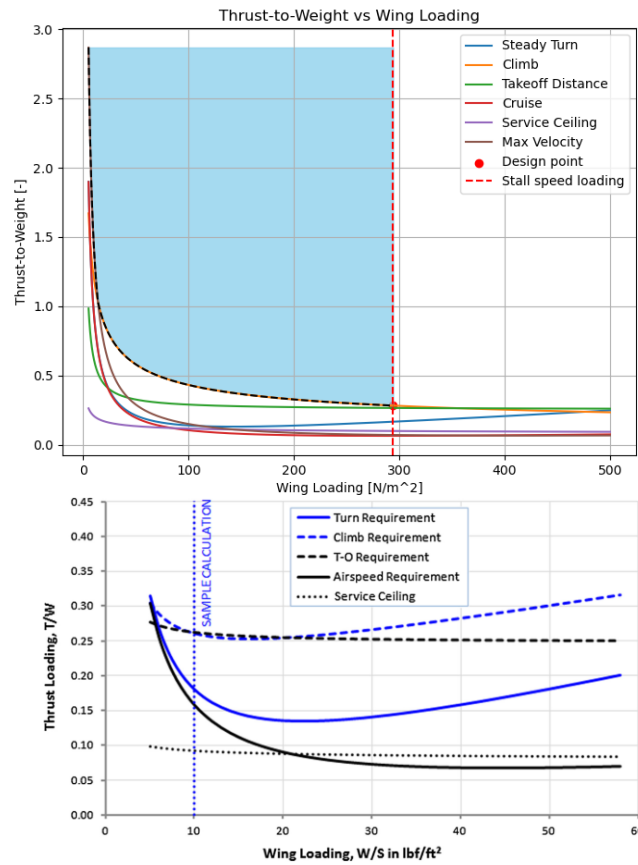
Figure 26 - Size Matching Diagram [1]

Conclusion

By determining the required thrust-to-weight ratios and the wing loading at which the wing will stall, depending on a specified stall speed, the size of the main wing is determined and requirements for the propulsion system are set. Due to the fact that the main wing is a major factor in the overall sizing and geometry of the aircraft, the performance requirements responsible for the sizing of the wing have a direct effect on the overall size and geometry of the aircraft through the thrust-to-weight ratio and the stall wing loading calculations. Hereby answering the research question # 2 for the forward flight performance requirements.

3.4.3.2 Vertical Flight Power Requirement Method

The power requirement for each vertical flight segment is calculated numerically by means of determining the thrust required for the flight segments. The main flight phases are take-off/climb, hover, and descent. The following method is utilized by implementing the formulas ((2-65) - (2-68)) presented by Tyan et al. which are used to calculate both the thrust and power required in the flight phases:

1. Determine the thrust required during the take-off/climb and descent phase of the mission. This is done by using the formula (2-65) which calculates the thrust-to-weight ratio based on the Rate of Climb (RoC^{VTOL}), wing loading, area ratio, and a 20% safety margin accounting for gusts or other situations requiring more thrust. The thrust-to-weight ratio during the descent phase is also determined by utilizing the formula (2-65). This is valid up until the point that the Rate of Descent (RoD^{VTOL}) desired is equal to, or greater than $2 * v_h$, or; $\left(\frac{RoD^{VTOL}}{v_h} \leq 2\right)$. When this is exceeded, the thrust-to-weight ratio required during descent is assumed to be equal to the thrust-to-weight ratio required during hover.
   Formula (2-65) is based on a momentum theory method described by Tyan et al.
   Finally, determine the thrust required by utilizing the current (estimation of the) take-off weight of the aircraft.
2. Determine the thrust required during the hover phase of the mission. The thrust required during hover is, simply, equal to the weight of the aircraft.
3. Determine the disk loading of the lifting rotors, this can be done utilizing the following two sub-methods
4. Manually set a rotor diameter, together with a number of rotors. This can be done when the diameter of the rotor is already known due to the availability of existing parts/experiences. An additional advantage is that it significantly reduces processing time
5. The rotor diameter is determined by finding the optimal Off-The-Shelf (OTS) rotor from a database. This is done by selecting an OTS rotor based on the thrust it is able to produce, the power required to produce that thrust, and if the rotor is within the maximum specified diameter. The database used for this purpose contains experimental data on 432 propellers from APC Propellers [16]. The advantages of this technique is that the determination of the optimum disk loading is based on experimental data, and not solely dependent on the experience of the user. The (major) disadvantage is that the technique requires significantly more processing time to find the optimal rotor.
6. Determine the power required during the different flight phases from the thrust required. This is done by utilizing the formulas (2-65), (2-66), (2-67), and (2-68). Formula (2-68) determines the induced airspeed through the rotor during hover (v_h) dependent on thrust produced per rotor and the disk area of each rotor. Formula (2-67) determines the induced airspeed through the rotor during axial climb/descent (v_i) dependent on the Rate of Climb/Rate of Descent and the induced airspeed during hover. Lastly, the formula determines the (2-66) power required during the different flight phases.

It was chosen to use the formulas stated by Tyan et al. to calculate the power required (2-66) for the vertical flight segments and not to use the formulas stated by Jae-Hyun et al. due to Hyun et al. not including the induced velocity during the hover segment. The induced velocity for a propeller/lifting rotor has a significant impact on the power required, also during hover. The climbing flight power requirement formula stated by Hyun et al. was not used due to limiting the number of different sources within one module in the toolchain. This is to minimize any discrepancies between methods/philosophies used by the different sources.

It was chosen to use the method of initially determining the disk loading by either utilizing a database or having the user specify a maximum rotor diameter. It was chosen not to use formula (2-71) due to the stated accuracy of $R^2 = 0.77$ for the regressed formula for the disk loading of a multi-copter, and

due to the dataset the regressed formula is based on is not applicable to the desired use case for a SUAV with VTOL capabilities. This dataset is constructed from 11 multi-copters with a total mass range between 2 and 18 kg. This dataset is both for a different type of aircraft and has a low number of data points. This makes for a bad representation of what is trying to be simulated.

Formulas

$$\frac{T^{VTOL}}{W}_{climb} = 1.2 \left(1 + \frac{(\rho) \cdot (RoC^{VTOL})^2 \cdot \left(\frac{S_{tot}}{S_{wing}}\right)}{\left(W/S_{wing}\right)} \right) \tag{2-65}$$

$$P_{req}^{VTOL} = \frac{T \cdot v_i}{FoM} \tag{2-66}$$

$$v_i = \frac{1}{2}(RoC^{VTOL}) + \sqrt{\left(\frac{1}{2}(RoC^{VTOL})\right)^2 + v_h^2} \tag{2-67}$$

$$v_h = \sqrt{\frac{T_{single\,rotor}}{2 \cdot (\rho) \cdot \left(S_{rotor_{single}}\right)}} \tag{2-68}$$

$$T_{single\,rotor} = \frac{T}{n_{rotor}} \tag{2-69}$$

$$S_{rotor_{single}} = \frac{T_{max}}{DL * n_{rotor}} \tag{2-70}$$

Formula variables

$\frac{T^{VTOL}}{W}_{climb}$	Is the required thrust-to-weight ratio during climbing vertical flight [-]
ρ	is the local air density [kg/m³]
RoC^{VTOL}	is the desired Rate of Climb for during climbing vertical flight [m/s]
$\frac{S_{tot}}{S_{wing}}$	is the S_ratio for an aircraft [-]
S_{tot}	is the total projected surface area of the entire aircraft [m²]
S_{wing}	Is the surface area of the main wing [m²]
W/S_{wing}	Is the wing loading of the main wing [N/m²]
P_{req}^{VTOL}	Is the power required during vertical flight [W]
T	Is the thrust required during vertical flight [N]
v_i	Is the air inflow velocity into the vertical flight propellers/lifting rotors [m/s]
FoM	is the Figure of Merit of the vertical flight propellers/lifting rotors [-]
v_h	is the induced velocity into the vertical flight propellers/lifting rotors during hover [m/s]
$T_{single\,rotor}$	Is the thrust required during vertical flight of a single propeller/lifting rotor [N]
n_{rotor}	Is the total number of vertical flight propellers/lifting rotors [-]
$S_{rotor_{single}}$	Is the rotor area of a single vertical flight propeller/lifting rotor [m²]
DL	is the disk loading of the vertical flight propellers/lifting rotors [N/m²]

Assumptions

- The vertical flight phases correspond to axial climbing and descending flight.
- The weight of the aircraft does not change during the mission.
- The propeller size determined by the OTS lookup function is representable of the actual optimal propeller to be used

Conclusion

By determining the required thrust-to-weight ratio, the inflow velocity and the induced velocity the power required for the vertical flight phases can be determined. This in turn is used to both size the propellers for the vertical flight propulsion system, but also the weight of this. Hereby answering the research question # 2 for the vertical flight (VTOL) performance requirements.

3.4.4 Wing Sizing and Weight

The Wing Sizing and Weight module has the goal of determining the optimal wing size and the weight that is associated with it. The sizing is done by utilizing the wing loading determined in the Power Requirement module, and the weight is determined from the size of the wing. An overview of the processes utilized in the Wing Sizing and Weight module is shown in Figure 27.
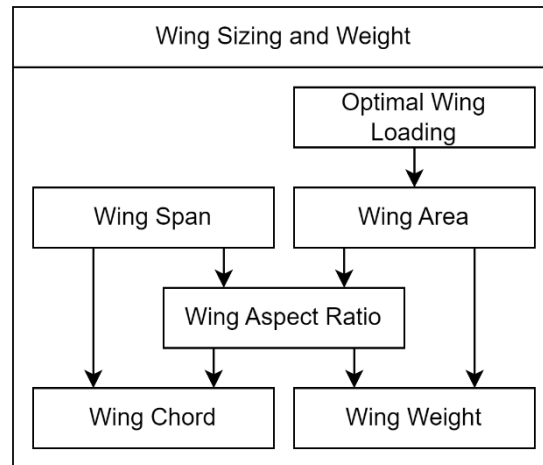

Figure 27 - Flowchart Wing Sizing and Weight Module

3.4.4.1 Wing Sizing and Weight Method

The size and weight of the wing are determined by utilizing the empirical formulas stated by Sadreay. The following method is utilized implementing the formulas ((3-9) - (3-11) and (2-28)) in order to do this;

1. Determine the wing surface area by using (3-9).
2. Determine the aspect ratio and the mean aerodynamic chord of the wing by using (3-10) and (3-11). The wingspan is equal to the maximum wingspan determined by the user.
3. Determine the weight of the wing by using (2-28). The load factor, wing taper ratio, quarter chord sweep, and wing material are all inputs of the user. The thickness-to-chord ratio is determined by the airfoil chosen by the user.

It was chosen to use the empirically derived formulas presented by Sadreay in 2.5.2.4 to calculate the size and weight of the wing. It was chosen to use empirically derived formulas to determine the weight of the wing due to the amount of data that is available at this point of the designing process. An alternative for the empirically derived formulas is the mass fraction-based formula. This only takes into consideration the payload weight of the aircraft, but not the previously determined wing loading, for example. The other alternative is to use an analytical method of determining the weight. For this method a (detailed) geometry is required, together with a form of structural analysis. This is not feasible with the data available at this point. Thus, the empirically derived formulas are the best suitable method.

The formulas presented by Sadraey are chosen because the formulas can be customized to become applicable for the use case of this report, as well as for other use cases when desired. The most applicable class of aircraft the formulas of Sadraey can be customized to is for "Remotely controlled model" aircraft. This class of aircraft is most typically a small, unmanned, low-intermediate performance aircraft, which correlates very well with the use case of this report.

Another viable alternative is the formulas presented by Yi and Heping in 2.5.2.5. Formula (2-28), the primary formula in calculating the weight of the wing, is specially made for HALE UAVs, which are, most

typically, larger, unmanned, intermediate-high performance aircraft. It was ultimately chosen for utilizing the formulas presented by Sadraey due to how applicable the formula is and the potential to simulate other types of aircraft classes.

Formula

Formula	Source	Nr.
$$S_{wing} = \frac{W_{To}}{(W/S_{wing})}$$	[9]	(3-9)
$$AR_{wing} = \frac{b^2}{S_{wing}}$$	[7]	(3-10)
$$C_{wing} = \frac{S_{wing}}{b}$$	[7]	(3-11)
$$W_{wing} = (S_{wing}) \cdot C_{wing} \cdot (t/C_{max}) \cdot (\rho_{mat}) \cdot \left(K_{\rho_{wing}}\right) \cdot \left(\frac{AR_{wing} \cdot n_{ult}}{\cos \Lambda_{c/4}}\right)^{0.6} \cdot \left(\lambda_{wing}\right)^{0.04} \cdot g$$	[7]	(2-28)

Formula variables

S_{wing}	Is the surface area of the main wing [m²]
W_{To}	Is the total take-off weight [N]
W/S_{wing}	Is the wing loading of the main wing [N/m²]
AR_{wing}	Is the aspect ratio of the main wing [-]
b	Is the span of the main wing [m]
C_{wing}	Is the Mean Aerodynamic Chord of the main wing [m]
t/C_{max}	Is the maximum thickness-to-chord ratio of the main wing airfoil [-]
ρ_{mat}	Is the density of a material [kg/m³]
$K_{\rho_{wing}}$	Is the density factor for the wing specific to the method of Sadraey [-]
n_{ult}	Is the desired maximum ultimate load factor [-]
$\Lambda_{c/4}$	Is the wing sweep at the quarter chord of the main wing [°]
λ_{wing}	Is the taper ratio of the main wing [-]
g	Is the gravitational acceleration of earth [m/s²]

Assumptions

- The main wing has a strait, constant taper
- The wing has a singular airfoil which is applied to the entire wing
- Any effects of dihedral does not have a significant influence on the performance of the wing

3.4.5 Propulsion System Sizing and Weight

The Propulsion System Sizing and Weight module determines the optimal propulsion system size for both the vertical- and forward flight segments, and the weight that is associated with these. The sizing is done by utilizing the maximum thrust requirements determined in the Power Requirement module, and the weight is determined from the sizing of the propulsion system components. An overview of the processes utilized in the Propulsion System Sizing and Weight module is shown in Figure 28.
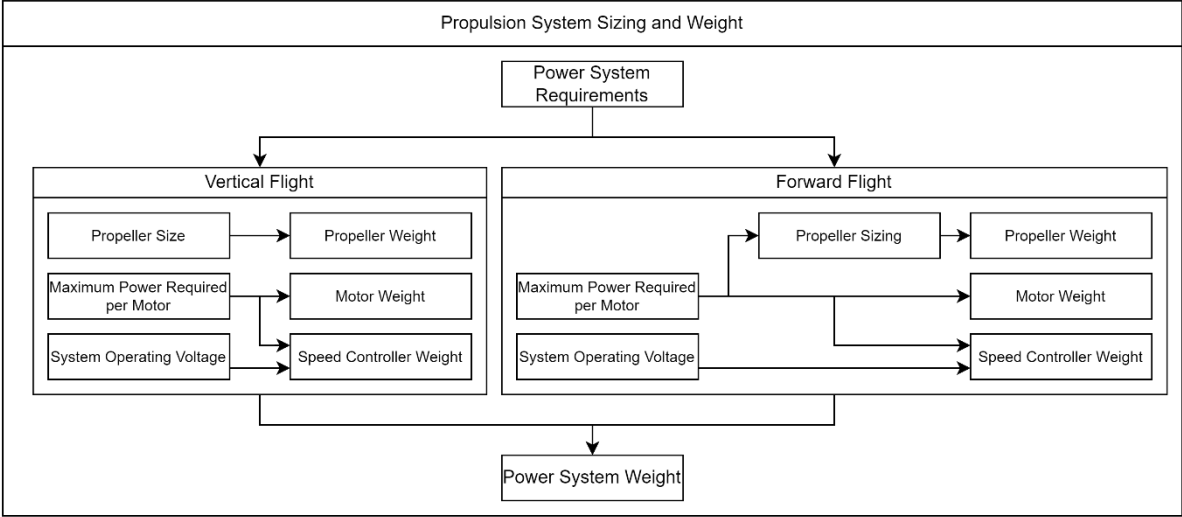

Figure 28 - Flowchart Power System Sizing and Weight Module

3.4.5.1 Forward and Vertical Flight Propulsion System Sizing and Weight Method

It was chosen to use the empirically derived formulas presented by Tyan et al. in 0 to calculate the size and weight of the propellers for both vertical and forward flight. And to use the formulas presented by Jae-Hyun et al. in 2.5.2.6 to calculate the weight of the ESCs and motors for both vertical and forward flight.

This combination of formulas was chosen because the method presented by Tyan et al. to calculate the size and weight of the propeller presented limitations during the implementation of these formulas. The most prominent issue with the method is that the KV rating must first be calculated in order to determine the size of the propeller. Due to the formulas being used have been derived empirically, each implementation of a formula carries an uncertainty due to the error between the regressed formula and reality. The formulas for the determination of the weight of the propellers are not used by Jae-Hyun et al. due to the stated minimum and maximum diameter of the propellers. These are $0.1 - 0.7m$ for the forward flight propeller and $0.3 - 1.0m$ for the vertical flight propeller. Especially the minimum diameter requirement of 0.3m for the vertical flight propeller is a prominent limiting factor which makes the formulas presented by Tyan et al. more advantageous.

The chosen method was implemented according to the following steps:

1. Determine the propeller size according to formula (2-48) which depends on a factor (k_p) associated with the number of blades of the propeller and the amount of power the propeller is predicted to consume (P_{max}).
2. Determine the weight of all propellers according to the formula (2-47) which depends on the desired propeller material (k_{mat}), an adjustment factor (k_{prop}), number of blades of the propeller (n_{blades}), the propeller diameter (D_{prop}) the amount of power the propeller is predicted to consume (P_{max}).
3. Determine the weight of each motor according to the formulas (2-38) and (2-39) which depends on the amount of power the propeller/motor is predicted to consume (P_{max}).

4. Determine the weight of each ESC according to formula (2-40) which depends on the amount of power the propeller/motor is predicted to consume (P_{max}) and the system's operating voltage (U).

Formula

$$D_{prop} = k_p \sqrt[4]{(P_{max})} \tag{2-48}$$

$$W_{prop} = \left((6.514 * 10^{-3}) \cdot (k_{mat}) \cdot (k_{prop}) \cdot (n_{prop}) \cdot (n_{blades})^{0.391} \cdot \left(\frac{(D_{prop}) \cdot (P_{max})}{1000(n_{prop})} \right)^{0.782} \right) \cdot g \tag{2-47}$$
$$\cdot 1000$$

$$W_{motor}^{VTOL} = \left((0.196 * 10^{-5})(P_{max}^{VTOL})^2 + 0.201(P_{max}^{VTOL}) + 5.772 \right) * \frac{g}{1000} \tag{2-38}$$

$$W_{motor}^{FF} = \left((-0.922 * 10^{-5})(P_{max}^{FF})^2 + 0.196(P_{max}^{FF}) + 23.342 \right) * \frac{g}{1000} \tag{2-39}$$

$$W_{ESC} = \left((0.324 * 10^{-2})\left(\frac{P_{max}}{U}\right)^2 + 0.847\left(\frac{P_{max}}{U}\right) + 1.532 \right) * \frac{g}{1000} \tag{2-40}$$

Formula variables

D_{prop}	Is the diameter of a propeller/lifting rotors [m]
k_p	Is the propeller/lifting rotors multiplication factor depending on the number of propeller blades [-]
P_{max}	Is the maximum power required for a propeller/lifting rotors for all the mission segments [W]
W_{prop}	Is the total weight of the propeller(s)/lifting rotor(s) [N]
k_{mat}	Is the material multiplication factor for the material of the propeller/lifting rotors [-]
k_{prop}	Is a scale multiplication factor of a propeller/lifting rotors, take a value of 15 for a propeller with a P_{max} of less than 50 hp (37.285 kW) [-]
n_{prop}	Is the total number of propellers/lifting rotors [-]
n_{blades}	Is the number of blades on the propellers/lifting rotors [-]
W_{motor}^{VTOL}	Is the weight of a vertical flight motor [N]
W_{motor}^{FF}	Is the weight of a forward flight motor [N]
W_{ESC}	Is the weight of an Electric Speed Controller (ESC) [N]
U	Is the operating Voltage of the propulsion system [V]

Assumptions

- The motors are not to exceed a maximum power predicted consumption of 12 kW per motor.
- The propellers used must have either 2, 3, or 4 blades.
- The diameter of the forward flight propeller can be sized by only depending on the number of blades and the amount of power which the propeller will receive from the motor.

3.4.6　Energy Source Sizing and Weight

The Energy Source Sizing and Weight module determines the optimal Energy Source size for both the vertical- and forward flight segments, and the weight that is the result of the sizing analysis. The sizing of the energy source is done by utilizing the data on the power consumption during the flight mission segments. An overview of the processes utilized in the Propulsion System Sizing and Weight module is shown in Figure 29.
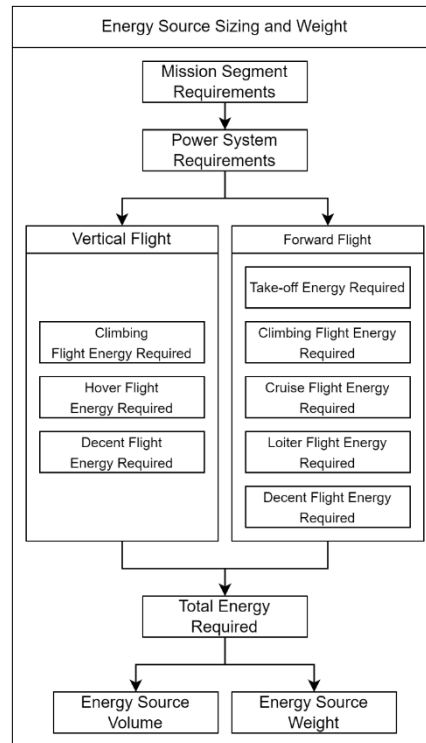

Figure 29 - Flowchart Energy Source Sizing and Weight Module

3.4.6.1　Energy Source Sizing and Weight Method

The method utilized is based on the one presented by Tyan et al. in 0. This method takes the following steps and uses the following formulas:

1. Determine the weight of the battery for each flight segment with the duration, power required, specific energy of the battery, and the efficiency of the battery according to formula (2-49).
    In the absence of other data, the following parameters may be used; a specific energy of the battery (E_{spec}) of 140 Wh/kg [17], battery efficiency of 70% [2], and a useful battery fraction of 90% [18]. These parameters are based on the lithium-polymer battery, due to the frequent use in small UAVs.
2. Determine the total weight of the battery by summing all flight segment battery weights.
3. Determine the volume of the battery, according to the formula (3-12).
    In the absence of other data, the following parameters may be used; energy density $(E_{volumetric})$ of 202.5 Wh/l [17]. This energy density was based on the lithium-polymer battery, due to the frequent use in small UAVs.

This methodology was selected due to the absence of superior alternatives.

Formula

$$W_{bat} = \left(\frac{t \cdot P}{(E_{spec}) \cdot (\eta_{bat}) \cdot (f_{usable})} \right) \cdot g \qquad\qquad (\,2\text{-}49\,)$$

$$V_{bat} = \frac{W_{bat}}{(E_{spec}) \cdot (E_{volumetric}) \cdot g} \qquad\qquad (\,3\text{-}12\,)$$

Formula variables

W_{bat}	Is the weight of a battery [kg]
t	Is the duration of one entire mission segment [sec]
P	Is the power required during of one entire mission segment [W]
η_{bat}	Is the efficiency of the battery [-]
f_{usable}	Is the useful fraction of the battery capacity [-]
g	Is the gravitational acceleration of earth [m/s²]
V_{bat}	Is the volume of a battery [m³]
E_{spec}	Is the specific energy storage capacity of a battery [Wh/kg]
$E_{volumetric}$	Is the volumetric energy storage capacity of a battery [Wh/l]

Assumptions

- The storage capacity of batteries is directly correlated with both the weight and volume of the battery
- No additional volume has been taken into account for subsystems which support the batteries
- The batteries utilized in the UAV can be shaped and sized as required, as a 'rubber battery'

3.4.7 Empennage Sizing and Weight

The Empennage Sizing and Weight module determines the optimal empennage size, and the weight that is the result of the sizing process. The optimal Empennage size is one which complies with the used stability margins and one that minimizes the amount of lift the main wing must produce. This means that the empennage must minimize its own weight, but also the amount of negative lift it produces to stabilize the aircraft. An overview of the processes utilized in the Empennage Sizing and Weight module is shown in Figure 30.
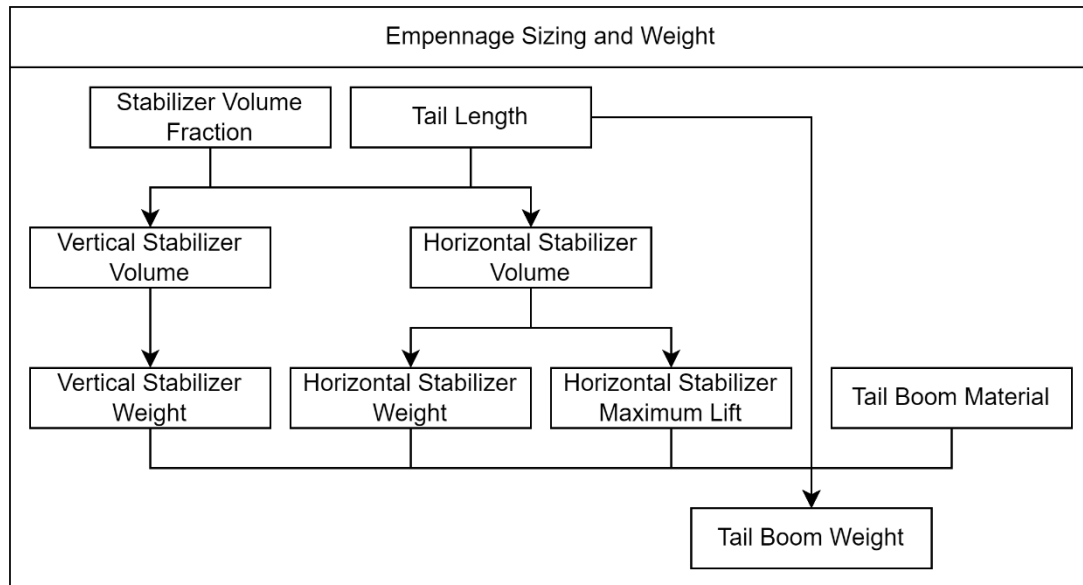

Figure 30 - Flowchart Empennage Sizing and Weight Module

3.4.7.1 Empennage Sizing and Weight Method

The method utilized is based on the method presented by Gudmundsson in 2.6.1 and Sadraey in 2.5.2.4. The method described by Gudmundsson is specifically derived for a conventional tail configuration, not a twin-boom U-tail. Due to this the method must be modified. In a conventional stabilizer configuration, the vertical stabilizer is a single vertical surface/stabilizer. In the twin-boom U-tail configuration, the vertical stabilizer consists of two vertical surfaces/stabilizers. In order to keep the configuration applicable for both the method and the chosen configuration, it is assumed that the summed surface area of both the vertical stabilizers must be equal to the surface area determined by the volume fraction method of Gudmundsson. And to calculate the weight of the stabilizers, this surface area is divided between the two vertical stabilizers, and thus will still be applicable for the twin-boom U-tail configuration.

Originally the tail length, from the quarter chord of the main wing to the quarter chord of the stabilizers, was determined by minimizing the wetted area. This was under the assumption that the fuselage supporting the tail had a significant wetted area with respect to the wetted area of the stabilizers. For the twin-boom U-tail configuration, this is not the case. The tail booms supporting the stabilizers are long thin tubes with an insignificant wetted area, thus the tail length optimization method of Gudmundsson will result in unrealistic answers.

Thus, the determination of the tail length must be modified, it can initially be determined done by utilizing statistical data on previously developed aircraft. This data is on the ratio between the overall length of the aircraft (l_{tot}) and the length of the tail-boom (l_{tail}). The data for this method is provided by Sadraey [7], and is shown in Table 4. This method can be used as a starting point to do the stability analysis but must be revised and optimized when more data becomes available. The method utilized for optimizing the length of the tail is the optimizer function of SciPy to modify the

length to minimize the weight of the empennage section, together with the negative lift the horizontal stabilizer must produce to stabilize the aircraft. In other words, minimize the amount of lift the main wing must produce during flight.

Table 4 - Typical values of $(l_{tail})/(l_{tot})$, or l/L for various aircraft configurations [7]

No.	Aircraft configuration/type	l/L
1	An aircraft whose engine is installed at the nose and has an aft tail	0.6
2	An aircraft whose engine(s) are installed above the wing and has an aft tail	0.55
3	An aircraft whose engine is installed at the aft fuselage and has an aft tail	0.45
4	An aircraft whose engine is installed under the wing and has an aft tail	0.5
5	Glider (with an aft tail)	0.65
6	Canard aircraft	0.4
7	An aircraft whose engine is inside the fuselage (e.g., fighter) and has an aft tail	0.3

Processing the data, for the case that the length of the fuse is known from the quarter chord of the main wing and forward, this ratio states that the tail boom will be: $l_{tail} = l_{fuse_{c/4\ forward}} \cdot \frac{0.45}{1-0.45}$ (3-13) for a configuration with the engine aft of the fuselage, and the tail aft of the main wing.

A topic that also must be taken into account with determining the tail-boom lengths is the placement and diameter of the vertical flight propellers. These should not interfere with the stabilizers nor with the main wing, to prevent any significant interference, mechanical as well as aerodynamic, the tail length from the trailing edge of the main wing to the leading edge of the stabilizers must be larger than the diameter of the vertical flight propeller with a safety margin. This safety margin must be either 25 mm (added to the radius of the propeller) or a factor of 1.10 (10%) multiplied by the diameter of the vertical flight propeller. This added size of the propeller is called; c_{prop}. The c_{prop} safety margin around the propellers is also visualized in Figure 31. This same margin is applied to the forward vertical-flight motors and propellers. These must not interfere mechanically nor aerodynamically with the main wing, an additional requirement for the placement of the forward vertical-flight motors and propellers is that they must have an equal X distance to the quarter chord as the rear vertical-flight motors and propellers. This is to ensure the forward and rear vertical-flight motors and propellers have a minimal thrust difference they must produce during vertical flight. When determining the length of the tail boom the length required to mount the forward vertical-flight motors and propellers should be taken into account.

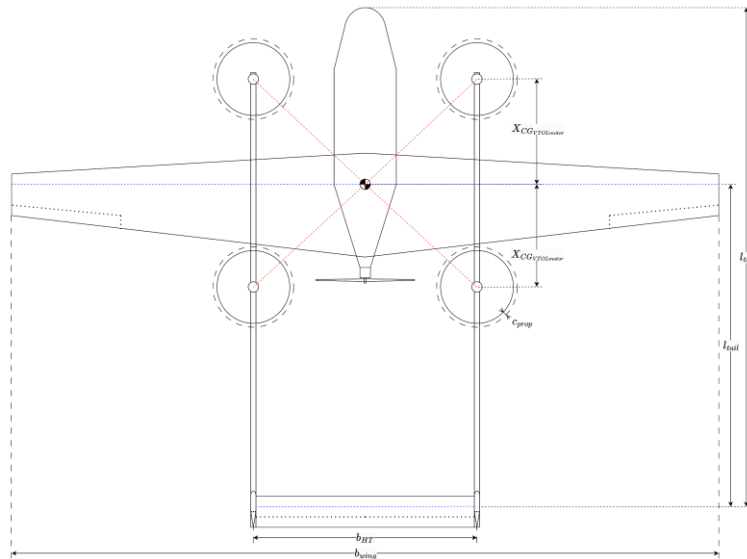When the aircraft is not required to take-off vertically, this topic does not have to be taken into account.

Figure 31 – UAV configuration, Top view

To determine the weight of the stabilizers, the empirically derived formulas presented by Gudmundsson are implemented. These are used according to the following steps and formulas:

1. Determine the tail length, using either formula (2-76) or (3-13), (3-14), and (3-15). When using the formulas (3-13), (3-14), and (3-15), use the greater value of the formulas.
2. Determine the surface area of the stabilizers, using formulas (2-72) and (2-74)
3. Determine the span and chord of the stabilizers, using the formulas(2-73) and (2-75)
4. Determine the weight of the stabilizers, using formulas (2-29) and (2-30)

During the determination of the span and chord of the stabilizers, the diameter of the forward flight propeller, together with the vertical flight propeller must be taken into account to avoid mechanical as well as aerodynamic interference. The identical safety margin method is applied as for the length of the tail booms.

The tail boom weight is calculated according to the following steps and formulas:

1. Determine the maximum force the horizontal stabilizer is able to produce by producing lift, using the formulas (3-8) and (3-16)
2. Determine the weight (W) of the horizontal- and vertical stabilizer with the maximum load factor (n) applied, using formula (3-17)
3. Determine the maximum moment within the tail booms (m_{tail}) due to the forces acting on the stabilizers, with formula (3-18)
4. Determine the minimum wall thickness of the round tail booms with the outer diameter and material assumed/set, thus the optimum inner diameter of the booms, use a safety factor (SF) of 2.5, with formula (3-19)
5. Determine the total tail boom length, also including the length required to mount the forward vertical-flight motors and propellers using formulas (3-20) or (3-21), use the greater value.
6. Determine the weight of the tail booms depending on the density of the material set, with formula (3-22)

Formula

$$W_{ht} = (S_{ht}) \cdot (C_{ht}) \cdot (t/C_{max_{ht}}) \cdot (\rho_{mat}) \cdot (K_{\rho_{ht}}) \cdot \left(\frac{AR_{ht} \cdot n_{ult}}{\cos \Lambda_{c/4}}\right)^{0.6} \cdot (\lambda_{ht})^{0.04} \cdot (\bar{V}_{ht})^{0.3} \cdot \left(\frac{C_e}{C_{ht}}\right)^{0.4} \cdot g \qquad (2\text{-}29)$$

$$W_{vt} = (S_{vt}) \cdot (C_{vt}) \cdot (t/C_{max_{vt}}) \cdot (\rho_{mat}) \cdot (K_{\rho_{vt}}) \cdot \left(\frac{AR_{vt} \cdot n_{ult}}{\cos \Lambda_{c/4}}\right)^{0.6} \cdot (\lambda_{vt})^{0.04} \cdot (\bar{V}_{vt})^{0.2} \cdot \left(\frac{C_r}{C_{vt}}\right)^{0.4} \cdot g \qquad (2\text{-}30)$$

$$S_{ht} = \frac{\bar{V}_{ht} \cdot S_{wing} \cdot C_{wing}}{l_{tail}} \qquad (2\text{-}72)$$

$$b_{vt} = \sqrt{AR_{ht} \cdot S_{ht}} \qquad (2\text{-}73)$$

$$S_{vt} = \frac{\bar{V}_{ht} \cdot S_{wing} \cdot b_{wing}}{l_{tail}} \qquad (2\text{-}74)$$

$$b_{vt} = \sqrt{AR_{vt} \cdot S_{vt}} \qquad (2\text{-}75)$$

$$l_{tail} = \sqrt{\frac{2(S_{wing}) \cdot \left((\bar{V}_{ht}) \cdot (C_{wing}) + \bar{V}_{vt} \cdot (b_{wing})\right)}{\pi(R_1 + R_2)}} \qquad (2\text{-}76)$$

$$l_{tail} = l_{fuse_{c/4\,forward}} \cdot \frac{0.45}{1 - 0.45} \qquad (3\text{-}13)$$

$$l_{tail} = (D_{prop}^{VTOL}) \cdot c_{prop} + \frac{3}{4} c_{wing} + \frac{1}{4} c_{ht} \qquad (3\text{-}14)$$

$$l_{tail} = D_{prop}^{VTOL} + c_{prop} + \frac{3}{4} c_{wing} + \frac{1}{4} c_{ht} \qquad (3\text{-}15)$$

$$L_{tail_{max}} = \frac{1}{2} (\rho_0) \cdot (V_{max})^2 \cdot (S_{ht}) \cdot (C_{L_{max}}) \qquad (3\text{-}16)$$

$$W_{effective} = W \cdot n \qquad (3\text{-}17)$$

$$m_{tail} = \sum (F \cdot x) \qquad (3\text{-}18)$$

$$D_{tailboom_{inner}} = \left((D_{tailboom_{out}})^4 - \frac{64 \cdot m_{tail_{max}} * \frac{D_{tailboom_{out}}}{2} \cdot SF}{\pi \cdot \sigma_{yield}}\right)^{\frac{1}{4}} \qquad (3\text{-}19)$$

$$l_{tailboom} = l_{tail} + \frac{1}{2} (D_{prop}^{VTOL}) \cdot c_{prop} + \frac{1}{4} (c_{wing}) \qquad (3\text{-}20)$$

$$l_{tailboom} = l_{tail} + \frac{1}{2} (D_{prop}^{VTOL}) + c_{prop} + \frac{1}{4} (c_{wing}) \qquad (3\text{-}21)$$

$$W_{tailboom} = \pi \cdot (l_{tailboom}) \cdot (\rho_{mat}) \cdot \frac{(D_{tailboom_{out}})^2 - (D_{tailboom_{inner}})^2}{4} \qquad (3\text{-}22)$$

Formula variables

W_{ht}	Is the weight of the horizontal stabilizer [kg]
S_{ht}	Is the surface area of the horizontal stabilizer [m²]
C_{ht}	Is the Mean Aerodynamic Chord of the horizontal stabilizer [m]
$t/C_{max_{ht}}$	Is the maximum thickness-to-chord ratio of the horizontal stabilizer airfoil [-]
ρ_{mat}	Is the density of a material [kg/m³]
$K_{\rho_{ht}}$	Is the density factor for the horizontal stabilizer specific to the method of Sadraey [-]
AR_{ht}	Is the aspect ratio of the horizontal stabilizer [-]
n_{ult}	Is the desired maximum ultimate load factor [-]
$\Lambda_{c/4_{ht}}$	Is the wing sweep at the quarter chord of the horizontal stabilizer [°]
$\bar{V}_{ht}$	Is the horizontal stabilizer volume fraction [-]
$\frac{C_e}{C_{ht}}$	Is the horizontal stabilizer chord to elevator chord ratio [-]
g	Is the gravitational acceleration of earth [m/s²]
W_{vt}	Is the weight of a vertical stabilizer [kg]
S_{vt}	Is the surface area of the vertical stabilizer [m²]
C_{vt}	Is the Mean Aerodynamic Chord of the vertical stabilizer [m]
$t/C_{max_{vt}}$	Is the maximum thickness-to-chord ratio of the vertical stabilizer airfoil [-]
ρ_{mat}	Is the density of a material [kg/m³]
$K_{\rho_{vt}}$	Is the density factor for the vertical stabilizer specific to the method of Sadraey [-]
AR_{vt}	Is the aspect ratio of the vertical stabilizer [-]
n_{ult}	Is the desired maximum ultimate load factor [-]

$\Lambda_{c/4_{vt}}$	Is the wing sweep at the quarter chord of the vertical stabilizer [°]
$\bar{V}_{vt}$	Is the vertical stabilizer volume fraction [-]
$\dfrac{C_r}{c_{vt}}$	Is the vertical stabilizer chord to rudder chord ratio [-]
S_{wing}	Is the surface area of the main wing [m²]
C_{wing}	Is the Mean Aerodynamic Chord of the main wing [m]
b_{wing}	Is the span of the main wing [m]
R_1	Is the radius of the fuselage at the mounting point of the stabilizers to the tail [m]
R_2	Is the (maximum) radius of the fuselage at the mounting point of the main wing [m]
l_{tail}	Is the length of the tail from the quarter chord of the main wing to the quarter chord of the stabilizers [m]
$l_{fuse_{c/4\,forward}}$	Is the length of the fuselage forward of the quarter chord of the main wing [m]
D_{prop}^{VTOL}	is the diameter of a vertical flight propeller/lifting rotor [m]
c_{prop}	Is the safety margin around the propellers is also visualized in Figure 26 to minimize/eliminate both mechanical and aerodynamic interference with other aircraft components [-] or [m] (explained in 3.4.7.1)
c_{wing}	Is the local chord of the wing [m]
c_{ht}	Is the local chord of the horizontal stabilizer [m]
$L_{tail_{max}}$	Is the maximum lift the horizontal stabilizer is able to produce [m]
ρ_0	Is the air density at sea level [kg/m³]
V_{max}	Is the maximum desired airspeed [m/s]
$C_{L_{max}}$	Is the maximum lift coefficient of the horizontal stabilizer [-]
$W_{effective}$	Is the effective weight of a component, meaning the apparent weight also due to additional acceleration factors [N]
n	Is the desired maximum load factor [-]
$D_{tailboom_{inner}}$	Is the inner diameter of the tail boom [m]
$D_{tailboom_{out}}$	Is the outer diameter of the tail boom [m]
$m_{tail_{max}}$	Is the maximum moment which will be applied to the tail boom [Nm]
SF	Is a safety factor, when not otherwise specified, use a value of 1.5
σ_{yield}	Is the yield strength of a material [Pa]
$l_{tailboom}$	Is the total length of a tail boom [m]

Assumptions

- Both the horizontal- and the vertical stabilizers are constant-chord lifting surfaces. If the lifting surfaces of the aircraft are tapered rather than having a constant chord, place the Mean Geometric Chord of the lifting surfaces on the quarter chord line for the constant-chord lifting surface.
- The tail length for both the horizontal- and the vertical stabilizers are equal.
- The summed vertical stabilizer surface area of both stabilizers in the inverted U-tail configuration can be represented by the total surface area of the single vertical stabilizer of a conventional tail configuration.
- By minimizing the weight of the tail, together with the minimizing the lift the tail must produce during flight, a stable tail length value can be determined by the optimization method

3.4.8 Stabilizer and Control Surface Sizing

The Control System Sizing module has the goal of determining an initial estimation of the size of the Control System. An overview of the processes utilized in the Control System Sizing module is shown in Figure 32.
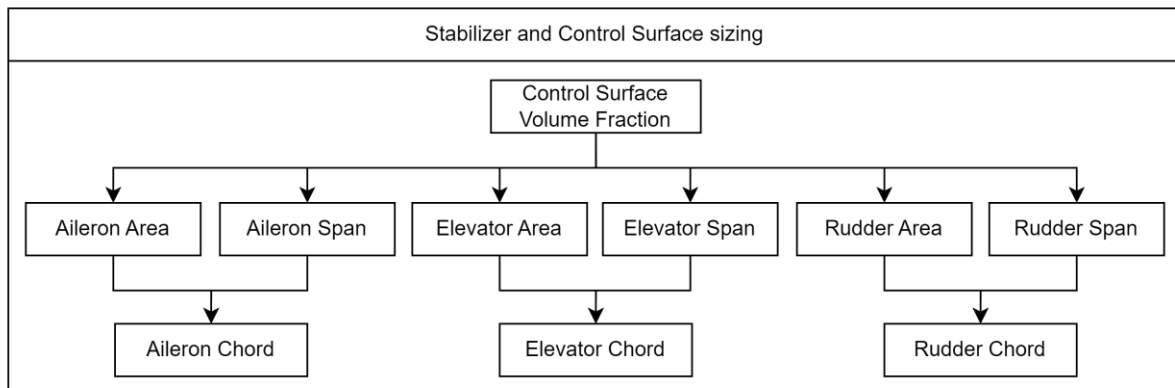

Figure 32 - Flowchart Control Surface Sizing Module

3.4.9 Control System Sizing Method

The method utilized is based on the method presented by Sadraey, in 2.6.2. The method is originally derived to be utilized for a conventional tail configuration. After reviewing the technique no modifications must be made to determine the size of the control surfaces for a twin-boom U-tail aircraft configuration.

The size is determined by implementing three sets of formulas while only two are required to determine the size of the control surfaces. In order to avoid conflicting parameters, initially only the control surface area and chord are determined. The output of which are checked if the control surface span that is required for these parameters are viable. If this is not the case, then the control surface chord and span are modified to achieve a viable result while maintaining the determined control surface area. These are implemented according to the following steps and formulas:

1. Determine the surface area for the control surfaces, with the formulas (2-77), (2-78), and (2-79).
2. Determine the Mean Aerodynamic Chord of each control surfaces, with the formulas (2-83), (2-84), and (2-85).
3. Check if the span of the control surfaces is viable, if this is not the case, then modify the control surface chord and span to achieve a viable result while maintaining the determined control surface area.

Assumptions
- The rudder surface area and rudder chord are determined for both vertical stabilizers, not as one combined rudder surface. (this is to prevent any conflicts due to the twin-boom U-tail configuration)

3.4.10 Landing Gear Sizing and Weight

The Landing Gear Sizing and Weight module has the goal of determining the length for both the main and nose gear of the UAV and the weight that is associated with this. An overview of the processes utilized in the Landing Gear Sizing and Weight module is shown in Figure 33.
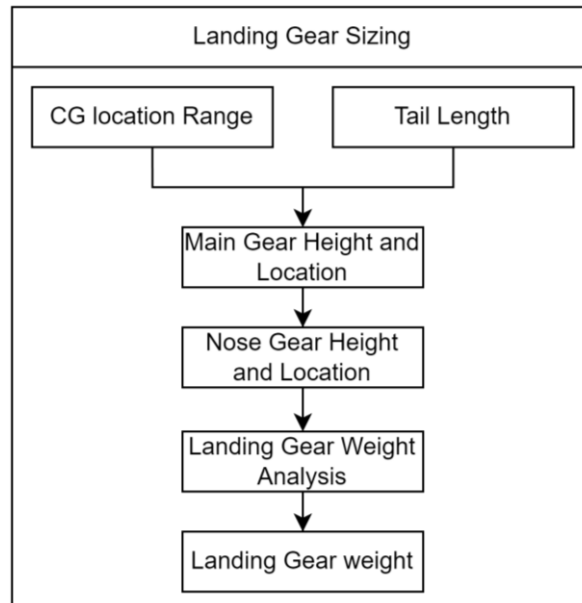

Figure 33 - Flowchart Landing Gear Weight Module

3.4.10.1 Landing Gear Sizing and Weight Method

The method utilized is based on techniques presented by Sadreay and Gudmundsson, their techniques utilize the following steps and formulas to determine the size, location, and weight of the landing gear:

1. Determine if the forward flight propeller has sufficient clearance during ground operations by using formula (3-23) and comparing the $R_{prop_{eff}}$ with the height of the main payload $h_{payload}$ (this is due to the top of the main payload is at the same level as the attachment point of the landing gear, thus is the bottom of the payload the first point of risk contacting the ground) with the same added ground clearance height as for the propeller.
2. Determine if the forward flight propeller has sufficient clearance during the take-off rotation by applying the assumed attitude angle (α_{To}), if this is not the case, redefine the (α_{To}), using formulas (3-23) and (3-24).
3. Determine the location $(X_{LG_{main}})$ in [m] and length $l_{LG_{main}}$ in [m] of the main landing gear based on the centre of gravity range (with respect to the quarter chord of the wing), the tail length $(X_{tail_{end}})$ in [m], and the take-off angle of attack (α_{To}), using formulas (3-25) and (3-26).
4. Determine the location $(X_{LG_{nose}})$ in [m] of the nose landing gear based on the centre of gravity range (with respect to the quarter chord of the wing), and the desired load fraction on the nose landing gear (f_{nose}) according to Gudmundsson, using formula (3-27).
5. Determine the length of the nose landing gear $(l_{LG_{nose}})$ in [m] dependent on the height of the main payload bay $h_{payload}$ in [m], using formula (3-28).
6. Determine the weight of the main and nose landing gear by means of utilizing the formula (2-32) presented by Sadraey. This will result in a weight for the entire landing gear system. Divide the weight of the entire landing gear between the nose and main gear in order to determine the weight contribution for the centre of gravity location of the aircraft.

It was chosen to base the utilized method of determining the location of the main and nose gear on the techniques of both Sadreay and Gudmundsson due to their similarities and that the combination of the techniques resulted in a better overall technique.

The formulas utilized for the location determination are, mostly, self-derived from simple trigonometry and the relations between the variables in the formulas are visualized in Figure 34.

The weight of the landing gear is determined by utilizing the formula (2-32) presented by Sadraey to determine the weight of the entire landing gear due to it having the most relevant specified use case. This use case is for "Remotely controlled model" aircraft. Due to the separate weight being required for the centre of gravity location of the entire aircraft, it is assumed that the separate gears have an equal weight. Thus, the nose gear weighs 1/3 the weight of the entire landing gear system, and in turn the main gear 2/3 the weight of the entire landing gear system. It may be assumed that the main gear strut assemblies weigh the same as the nose gear assembly, due to the main gear and nose gear being of similar build and configuration. The major difference between the two is that the majority of the weight of the aircraft is carried by the main gear, which results in a necessity for a stronger gear. And that the nose gear is able to rotate to enable the aircraft to steer on the ground, which necessitates a mechanism to rotate the gear. These two primary differences result in an approximately equal weight for the separated gear strut assemblies.
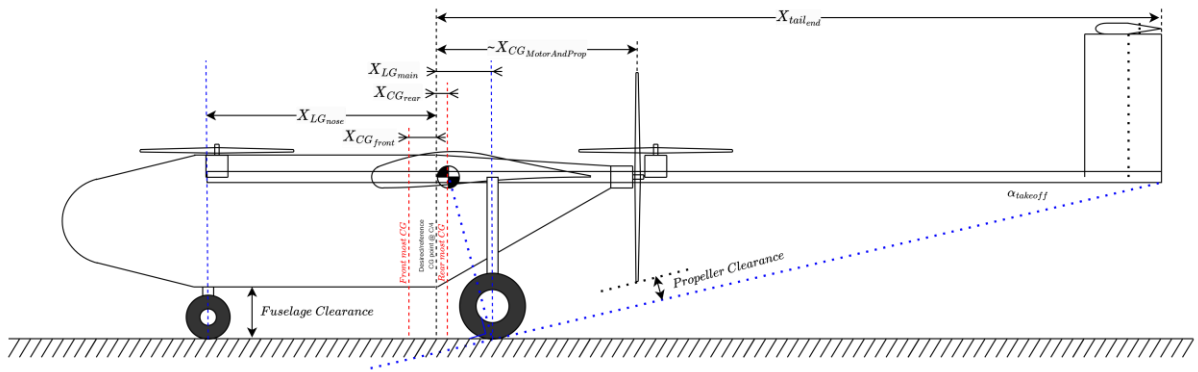

Figure 34 - Landing gear placement and height analysis

Formula

$$W_{LG} = (K_L) \cdot (K_{ret}) \cdot (K_{LG}) \cdot (W_L) \cdot \left(\frac{l_{LG}}{b}\right) \left(n_{ult_L}\right)^{0.20} \tag{2-32}$$

$$R_{prop_{eff}} = prop_{clearance} * \cos(\alpha_{To}) + R_{prop} \tag{3-23}$$

$$\alpha_{prop_{clearance}} = \tan^{-1}\left(\frac{R_{prop_{eff}}}{X_{tail_{end}} - X_{CG_{MotorAndProp}}}\right) \tag{3-24}$$

$$X_{LG_{main}} = \left(\left(X_{tail_{end}} - X_{CG_{aft}}\right) \cdot (\sin(\alpha_{To}))^2\right) + X_{CG_{aft}} \tag{3-25}$$

$$l_{LG_{main}} = \left(\left(X_{tail_{end}} - X_{CG_{aft}}\right) \cdot (\sin(\alpha_{To}) * \cos(\alpha_{To}))\right) \tag{3-26}$$

$$X_{LG_{nose}} = \left(\frac{f_{main}}{f_{nose}}\right) \cdot \left(X_{LG_{main}} - X_{CG_{front}}\right) + X_{CG_{front}} = \left(\frac{1 - f_{nose}}{f_{nose}}\right) \cdot \left(X_{LG_{main}} - X_{CG_{front}}\right) + X_{CG_{front}} \tag{3-27}$$

$$l_{LG_{nose}} = \left(h_{payload} \cdot k_{h_{fuse}}\right) - l_{LG_{main}} \tag{3-28}$$

Formula variables

W_{LG}	Is the weight of the main landing gear [N]
K_L	Is the landing implementation factor, 1.8 for a navy aircraft and 1.0 for a land-based aircraft [-]
K_{ret}	Is the retraction factor, for non-retractable gear and 1.07 for a retractable landing gear [-]
K_{LG}	Is the landing gear weight factor, refer to Appendix D – Sadraey Empirical Weight Factors for an applicable value [-]
W_L	Is the weight of the aircraft at landing [N]
n_{ult_L}	Is the desired maximum ultimate load factor at landing [-]
$l_{LG_{main}}$	Is the length of the main gear, from the ground to where the gear will mount to the aircraft [m]
$l_{LG_{nose}}$	Is the length of the nose gear, from the ground to where the gear will mount to the aircraft [m]
R_{prop}	Is the radius of the propeller [m]
$R_{prop_{eff}}$	Is the effective radius of the propeller, thus including clearance factor(s) [m]
$prop_{clearance}$	Is the minimal desired distance between the propeller and the ground when both the main gear and the end of the tail touch the ground as shown in Figure 34 [m]
α_{To}	Is the maximum desired angle at which the aircraft will take-off as shown in Figure 34 [°]
$\alpha_{prop_{clearance}}$	Is the angle required to ensure the propeller does not strike the ground before the tail strikes the ground together with that the main gear touches down measured from the end of the tail as shown in Figure 34 as the α_{To} [°].
$X_{tail_{end}}$	Is the x-distance which the end of the tail, the first part of the tail that will strike the ground on the take-off rotation, from the quarter chord of the main wing [m]
$X_{CG_{MotorAndProp}}$	Is the x-distance which the forward flight motor and propeller are located from the quarter chord of the main wing [m]
$X_{LG_{main}}$	Is the distance of the main gear to the quarter chord of the main wing [m]
$X_{LG_{nose}}$	Is the distance of the nose gear to the quarter chord of the main wing [m]
$X_{CG_{aft}}$	Is the most aft position of the CG for all possible payload configurations to the quarter chord of the main wing [m]
$X_{CG_{front}}$	Is the most forward position of the CG for all possible payload configurations to the quarter chord of the main wing [m]
f_{main}	Is the desired weight fraction which acts on the main landing gear [-]
f_{nose}	Is the desired weight fraction which acts on the nose landing gear [-]
$h_{payload}$	Is the height of the main payload [m]
$k_{h_{fuse}}$	is the fuselage component height factor, this adds additional height to each component for space for miscellaneous parts like bulkheads, cable management and other subsystems. A preliminary value of 1.10 is assumed to make the length of each component 10% higher than necessary [-].

Assumptions

- The extension and compression of the landing gear is assumed to be neglectable.
- The centre of gravity of the aircraft is at the same height as the attachment points of the main landing gear, thus the centre of the wing thickness at the quarter chord, as shown in Figure 34.
- No other structures on the UAV will have the risk of impacting the ground during ground operations and take-off rotation than the (end of the) tail, forward flight propeller, or the fuselage itself.
- There is enough volume in the fuselage to have the nose landing gear collapse into.
- The initial value for the take-off rotation angle (α_{To}) utilized in step 2, in formula (3-23), is approximately equal to the $\alpha_{prop_{clearance}}$ which formula (3-24) determines.
- The weight of the separate landing gear strut assemblies are equal to each other; thus, the nose gear weighs 1/3 the weight of the entire landing gear system, and in turn the main gear 2/3 the weight of the entire landing gear system.

3.4.11 Weight and Balance

The mass and balance analysis of an aircraft analyses the distribution of the weight within an aircraft with respect to a reference point. With the goal of determining if the centre of gravity of the entire aircraft is within a range viable for flight. By doing this, this method analyses the influence that the requirements have on the previously presented methods and how this might influence the weight distribution of the entire aircraft. And thus, also how the components must be arranged to achieve a viable balance of the aircraft. The Weight and Balance method does this in conjunction with the fuselage sizing and weight method, described in 3.4.12. This chapter will describe the method utilized to do this following the flowchart shown in Figure 35.
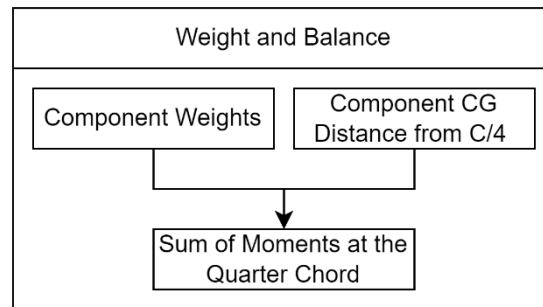
Figure 35 - Flowchart Weight and Balance Module

3.4.11.1 Weight and Balance Method

The method utilized is based on moment equations to determine the location of the centre of gravity of the entire aircraft. The moment equations are dependent on the weight of the component and its distance from the reference point. In this case, this reference point is the main wing root quarter chord point. These distances are visualized in Figure 37. The steps taken to determine the location of the centre of gravity are listed below.

1. Determine the moment contribution for each component by multiplying the weight of the component with the distance it's located away from the quarter chord, note, when the component is located forward from the quarter chord point distance must be taken as negative. Sum these moment contributions to determine the summed moment around the quarter chord $(\sum m)$. This is done by using formula (3-29).
2. Determine the distance for which the summed moments equal zero by using formula (3-30). This determines the location of the X-location CG of the entire aircraft with respect to the quarter chord (X_{CG}).

The layout of the components in the fuselage has a large influence on the balance analysis, the layout employed is shown in Figure 37. The following subchapters will describe the reasoning for the layout of the components within the fuselage.

Main Payload

It was chosen to locate the main payload bay forward of the quarter chord of the wing to minimize the frontal area of the UAV. Due to the main payload bay being the main contributing factor to the height of the fuselage, locating the payload bay forward of the quarter chord of the wing, thus forward of the main spar of the wing, will reduce the frontal area of the fuselage. This, in turn, is advantageous to reducing the amount of drag the fuselage creates.

Battery

The batteries for the UAV are split between two battery bays. It has been chosen to do this, to be able to balance the aircraft by determining the optimal distribution of the battery weight between the two bays. This eliminates, in most cases, the need for either counterbalance weights or fuselage/tail extensions to balance the aircraft. The counterweights are highly effective in balancing an aircraft but have the disadvantage of, most commonly, being otherwise useless weight. The extension of either the fuselage or the tail to balance the aircraft is also a widely used method, but this increases the wetted area of the aircraft, which increases the frictional drag.

Forward Payload

The forward payload bay is located in front of both the forward battery bay and the main payload bay, this is in order to allow the forward payload to have an unobstructed view forward of the aircraft.

Formula

$$\sum m = \sum_i W_i \cdot X_{CG_i} \qquad\qquad (\ 3\text{-}29\ )$$

$$X_{CG} = \frac{\sum m}{W_{To}} \qquad\qquad (\ 3\text{-}30\ )$$

Formula variables

$\sum m$	Is the sum of moments around the quarter chord of the main wing [Nm]
W_i	Is the weight of each individual component [N]
X_{CG_i}	Is the x-distance the component is away from the quarter chord of the main wing [m]
X_{CG}	Is the x-distance the Centre of Gravity (CG) is away from the quarter chord of the main wing [m]
W_{To}	Is the total take-off weight [N]

Assumptions
- The CG location of the forward flight motor and the propeller is at the base, or the location where the forward flight motor is mounted to the fuselage. Due to no applicable motor height determining method available.
- The CG location of the landing gear does not significantly change during flight in the case that the landing gear is able to retract.

Conclusion

The mass and balance of the aircraft is determined by the summation of the weights multiplied by the distance from a reference point for all components and systems within the aircraft and determining how these must modified in location for a viable balance of the aircraft. The modification of location of the components is done with two methods, one is redistributing the batteries between two battery bays, and the other is to extend either the nose or the tail of the fuselage. This allows for an automated analysis of the balance of the aircraft which results in an optimal placement of the components. Hereby answering the research question # 3.
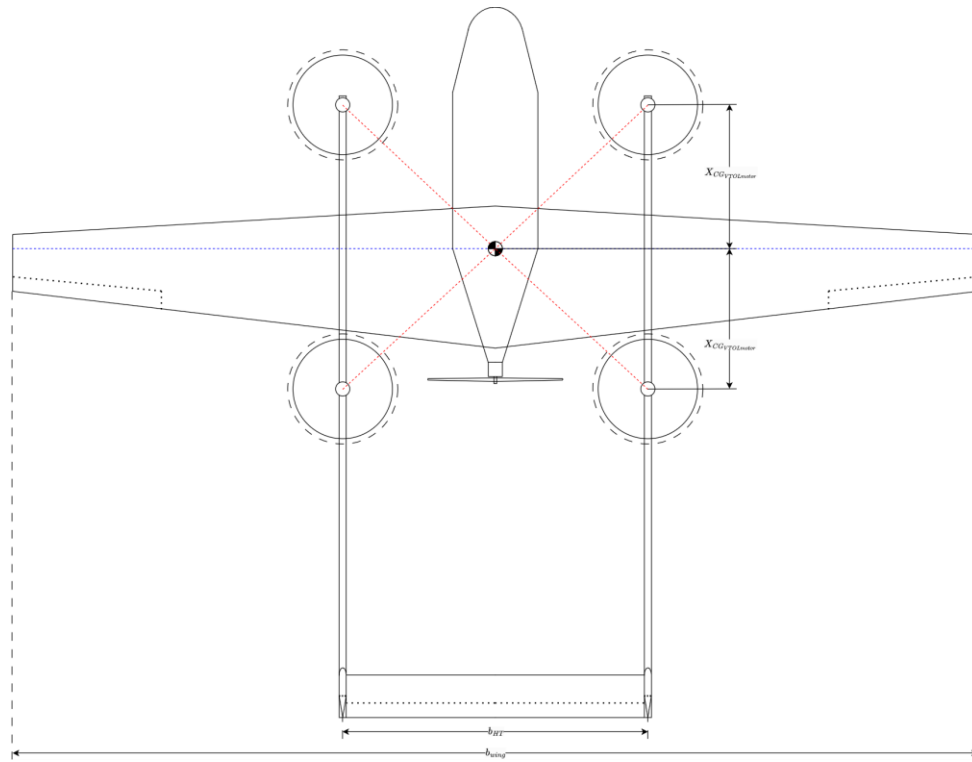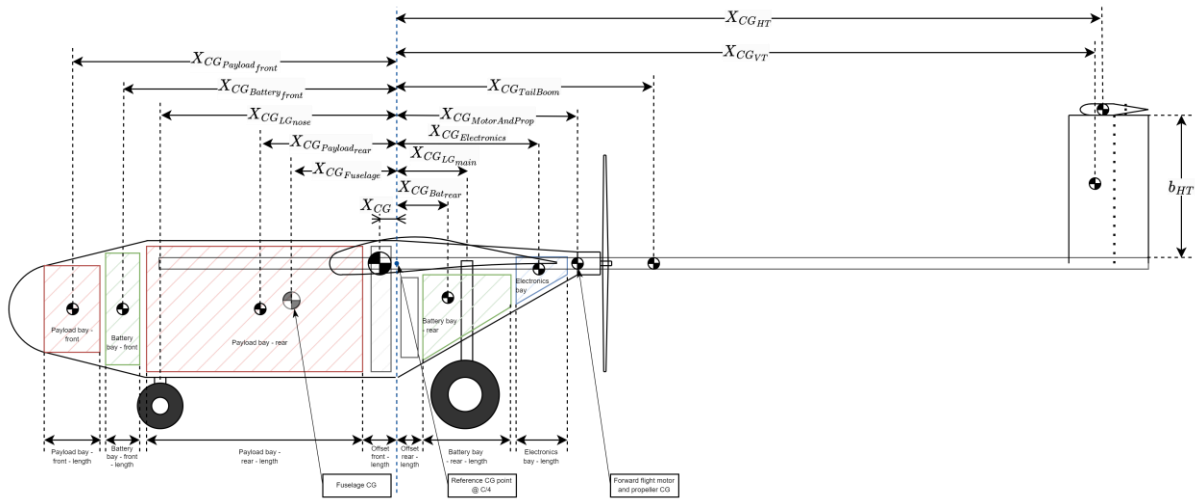
Figure 36 - UAV component location, top view.

Figure 37 - UAV component location, side view.

3.4.12   Fuselage Sizing and Weight

The Fuselage Sizing and Weight module determines what the minimal dimensions of the fuselage should be to contain all the required components and to balance the aircraft around the desired balance point. This is done in conjunction with the Weight and Balance module described previously. This is also shown in the flowchart in Figure 38.
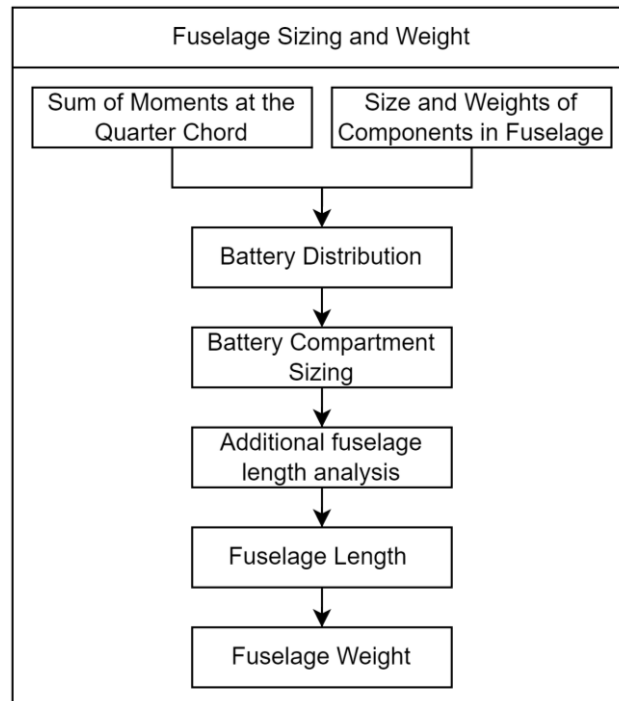

Figure 38 - Flowchart Fuselage Sizing and Weight Module

3.4.12.1   Fuselage Sizing and Weight Method

The method utilized for the Sizing and Weight of the fuselage is described in more detail in the following steps:

1. List the components and the dimensions of each that must be integrated into the fuselage.
2. Determine the placement of each component with respect to the quart chord point of the wing.
3. Determine the optimal battery distribution between the two battery bays.
4. Analyse if any additional length must be added to the fuselage to offset the components to minimize the moment around the quarter chord point.
5. Determine the total length of the fuselage with formula (3-31).
6. Determine the weight of the fuselage with formula (2-31).
7. After one iteration; determine the absolute relative error between the current and the previously determined fuselage weight with formula (3-32) [19].

A circular dependency is present in the determination of the weight of the fuselage with the Weight and Balance module presented in 3.4.11. Due to this dependency between the two modules an iterative loop must be set up to minimize the effects of the circular dependency. This loop will continue until a weight convergence with a prespecified desired relative error is reached.

The formula used to calculate the weight of the fuselage, formula (2-31), is derived empirically by Sadraey based on data on existing aircraft with a conventional fuselage-tail configuration. This is not the case for the UAV which is desired to be developed by this method described in this chapter. It is however assumed that the weight of the fuselage calculated in this method is representable with the formula presented by Sadraey. This is due to, when the conventional fuselage is turned around, i.e. the nose, thus also the motor, is pointing aft, like a pusher configuration, does not affect the types of loads

which the fuselage experiences. These loads can be due to aerodynamics, payload weight, moments transferred from the main wing, and the weight and thrust of the motor. The only major difference is the direction of most of these loads acting in a different direction, with respect to the conventional fuselage.

3.4.12.2 Formula

$$\sum l_{fuse} = \sum l_{components} \cdot k_{l_{fuse}} \qquad (\,3\text{-}31\,)$$

$$W_{fuse} = \left(l_{fuse}\right) \cdot (2 \cdot R_2)^2 \cdot (\rho_{mat}) \cdot \left(K_{\rho_{fuse}}\right) \cdot (n_{ult})^{0.25} \cdot (K_{inlet}) \cdot g \qquad (\,2\text{-}31\,)$$

$$\varepsilon_{To} = \left|\frac{W_{To_{new}} - W_{To_{old}}}{W_{To_{new}}}\right| \qquad (\,3\text{-}32\,)$$

Formula variables

l_{fuse}	is the total length of the fuselage [m]
$l_{components}$	is the length of each component located in the fuselage [m]
$k_{l_{fuse}}$	is the fuselage component length factor, this adds additional length to each component for space for miscellaneous parts like bulkheads, cable management and other subsystems. A preliminary value of 1.10 is assumed to make the length of each component 10% longer than necessary [-].
W_{fuse}	Is the weight of the fuselage [N]
R_2	Is the (maximum) radius of the fuselage at the mounting point of the main wing [m]
ρ_{mat}	Is the density of a material [kg/m³]
$K_{\rho_{fuse}}$	Is the density factor for the fuselage specific to the method of Sadraey [-]
n_{ult}	Is the desired maximum ultimate load factor [-]
K_{inlet}	Is the multiplication factor given for certain types of air inlets, specific to the method of Sadraey [-]
g	Is the gravitational acceleration of earth [m/s²]
$\varepsilon_{W_{fuse}}$	Is the percentual error between the current take-off weight and the previously determined fuselage weight [-]
$W_{fuse_{new}}$	Is the current determined fuselage weight [N]
$W_{fuse_{old}}$	Is the previously determined fuselage weight [N]

3.4.12.3 Assumptions

- During the analysis for the optimal battery distribution, the fuselage weight, nor CG does not change of magnitude or location.
- The weight of the fuselage can be determined by using an empirical formula derived for a conventional fuselage.
- The relative error of the fuselage length will have a decreasing trend with an increasing number of iterations.

3.4.13 Total Weight

The Total Weight module determines the total weight of the entire aircraft and calculates the error factor between the previous and current total weight. This process is shown in a flowchart in Figure 39.
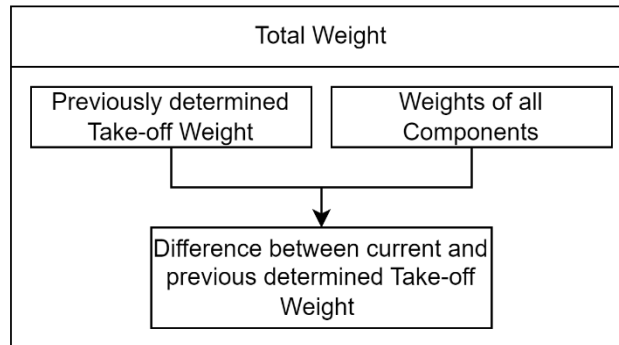

Figure 39 - Flowchart Total Weight Module

3.4.13.1 Total Weight Determination Method

The method used for the Total Weight determination is described in more detail in the following steps:

1. List the weights of all the components, together with the quantity of each component within the aircraft.
2. Determine the total weight of the aircraft by using formula (3-33).
3. Determine the absolute relative error between the current and the previously calculated take-off weight with formula (3-34).

The new total weight can be output as the final determined take-off weight or can be reinserted into the toolchain in order to initiate or continue an iteration loop which continues until a weight convergence with a prespecified desired relative error is reached. Utilizing this method results in more accurate answers due to the several circular dependencies throughout the process of determining the total take-off weight. For example, the thrust requirement module is directly dependent on the value of the take-off weight, and without an iteration loop, or other method of updating this value, can give highly skewed answers.

3.4.13.2 Formula

$$W_{To} = \sum_i W_i \cdot n_i \qquad\qquad (\,3\text{-}33\,)$$

$$\varepsilon_{To} = \left| \frac{W_{To_{new}} - W_{To_{old}}}{W_{To_{new}}} \right| \qquad\qquad (\,3\text{-}34\,)$$

Formula variables

W_{To}	Is the total take-off weight of the aircraft [N]
W_i	Is the weight of a component [N]
n_i	Is the quantity of the component in the aircraft [-]
ε_{To}	Is the percentual error between the current take-off weight and the previously determined take-off weight [-]
$W_{To_{new}}$	Is the current determined take-off weight [N]
$W_{To_{old}}$	Is the previously determined take-off weight [N]

3.4.13.3 Assumptions

- The relative error of the take-off weight will have a decreasing trend with an increasing number of iterations.

3.4.14 Required Input Parameters

This chapter will present the parameters which are required as inputs to the toolchain for normal operation of the toolchain. Next to this, the parameters that can be put in to increase the accuracy of the toolchain are also presented.

The required parameters are shown below in Table 5.

Table 5 - Required input parameters

Parameter	Unit
Payload Weight (maximum & minimum) (forward & main)	N
Payload Width (forward & main)	m
Payload Height (forward & main)	m
Payload Length (forward & main)	m
Maximum Wingspan	m
VTOL capability	Yes/No
Range	m
Loiter Duration	sec
Hover Duration	sec
Take-Off distance	m
Rate-of-Climb (forward flight)	m/s
Rate-of-Climb (vertical flight)	m/s
Maximum velocity	m/s
Cruise velocity	m/s
Stall velocity	m/s
Flight Altitude (forward flight)	m
Accent Altitude (vertical flight)	m
Airfoil main wing t/C	[-]
Airfoil main wing $C_{l_{max}}$	[-]
Operating voltage	V
Propeller maximum diameter (vertical flight)	m

The parameters which are optional to put in are shown below in Table 5.

Parameter	Unit
Airfoil horizontal stabilizer t/C	[-]
Airfoil horizontal stabilizer $C_{l_{max}}$	[-]
Airfoil vertical stabilizer t/C	[-]
Material main wing	[-]
Material horizontal stabilizer	[-]
Zero-lift drag (prediction)	[-]
Number of propeller blades(forward & vertical flight)	[-]
Service Ceiling Altitude	m
Electronics Weight	N
Propeller Clearance	m
Steady-Turn bank angle	°

3.5 Verification Methods

In order to verify the methods employed by the toolchain design program which are described in the chapter 3.4, the toolchain will be given the requirements of an existing aircraft. The output of the toolchain will be compared to this reference aircraft. Any discrepancies between the predicted parameters (bases on the characteristics of the reference aircraft), like the weight of the aircraft components and the propulsion system requirements, will be analyzed and will explain why these differences might be present. In the following subchapter the aircraft, the Prometheus, which will be used as a reference for the verification process will be described. Furthermore, the differences between this aircraft and the chosen configuration that is analyzed in the toolchain will be presented. Together with this, mitigation techniques for potential discrepancies that might present themselves in the analysis will be discussed in 3.5.1.2.

3.5.1   Prometheus

The Prometheus, a small UAV, shown in Figure 40, employed by the DLR for research purposes, will be used to perform the verification process. The DLR has collected a substantial amount of data on the performance of the Prometheus during the research studies it has gone through. This data, which is presented in 3.5.1.1, will be used to compare the data produced by the toolchain to determine if the toolchain is able to output valid results. The data that is put into the toolchain will be the following:

- The payload capacity
- Payload dimensions
- Propulsion system weight
- Desired rate of climb
- The maximum wingspan
- Electronics weight

Figure 40 - Prometheus UAV employed by the DLR for research [20]

The Prometheus is a small UAV with a maximum take-off mass of 35 kg and is powered by a 5.9 kW gasoline two-stroke two-cylinder 85cc boxer engine. It is configured with a pusher-style propeller-based propulsion system together with a twin-tail-boom H-tail configuration. The aircraft was originally designed for several use cases, two of which are to test systems that are associated with aerial refuelling and sensor integration. The most important performance and geometric characteristics are shown in Table 6 and Table 7.

Table 6 – Prometheus performance characteristics [21]

Payload Mass	7,69	[kg]
Engine Power	5,9	[kW]
Stall speed	15	[m/s]
Maximum speed	60	[m/s]
Cruise speed	42	[m/s]
Range	450	[km]
Endurance	3	[h]

3.5.1.1 Prometheus Specifications

The specifications on the Prometheus will be presented in this subchapter.

Dimensions

The Prometheus has the following dimensions:

Table 7 – Prometheus geometric characteristics [21]

Measurement	Dimension
Wingspan	3.250 m
Total length	2.230 m
Total height	0.820 m
Fuselage length	1.40 m
Fuselage height (max)	0.30 m
Fuselage width (max)	0.32 m
Landing gear length	0.25 m
Wing area	1.085m²
Mean Aerodynamic Chord	0.3485 m
Aspect Ratio	9.44 [-]
Horizontal stabilizer area	0.224 m²
Vertical stabilizer area (total)	0.3616 m²
Horizontal stabilizer span	0.640 m
Vertical stabilizer span	0.620 m
Tail length	1.15 m
Elevator span	0.64 m
Rudder span	0.55 m
Aileron span	0.70 m
Elevator chord	0.075 m
Rudder chord	0.10-0.08 m
Aileron chord	0.075-0.050 m
Elevator area	0.048 m²
Rudder area (total)	0.099 m²
Aileron area (total)	0.0875 m²
Propeller diameter	0.61 m {24 inch}
Landing Gear Length	0.25 m
Airfoil main wing	NACA 4415

An overview of the planform of the Prometheus is shown in Figure 41 below.
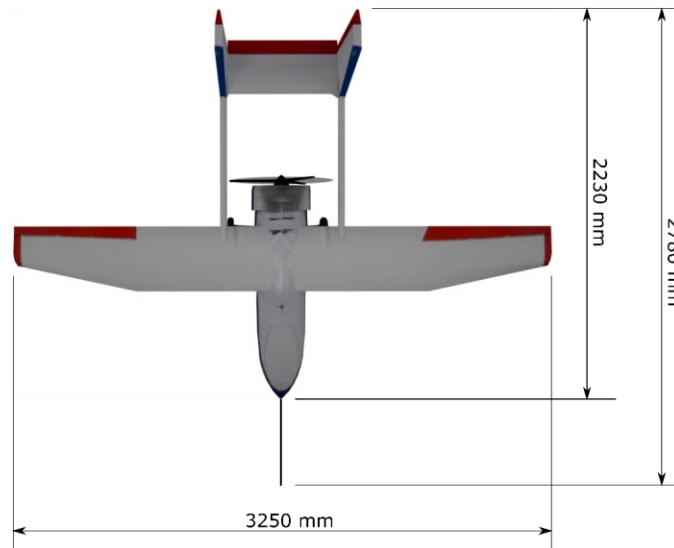
Figure 41 – Dimensions of the Prometheus UAV [image created by Stefan Krause, DLR ULF]

Weights

The Prometheus has the following weights for each component:

Table 8 - Prometheus component position and masses [21]

Section	Mass [kg]	x-position [m]	y-position [m]	z-position [m]
Fuselage	1,388	0,875	0,000	0,410
Wing	3,096	0,970	0,000	0,490
Tailboom L	0,243	1,495	-0,350	0,450
Tailboom R	0,243	1,495	0,350	0,450
Hor.Tail	0,448	2,014	0,000	0,450
Ver.Tails L	0,331	2,088	-0,350	0,540
Ver.Tails R	0,331	2,088	0,350	0,540
Nose L/G	0,541	0,410	0,000	0,060
Main L/G L	0,494	1,000	-0,200	0,060
Main L/G R	0,494	1,000	0,200	0,060
RC devices	0,860	0,600	0,000	0,470
Computer	0,500	0,600	0,000	0,310
Engine	2,880	1,250	0,000	0,430
Propeller	0,250	1,395	0,000	0,430
Muffler	0,700	0,971	0,000	0,290
Electricity	0,400	0,120	0,000	0,350
Fuel	3,000	0,840	0,000	0,330
Payload	7,690	0,360	0,000	0,390
Total	23.889			

The position of the components of the Prometheus is relative to the following reference frame:
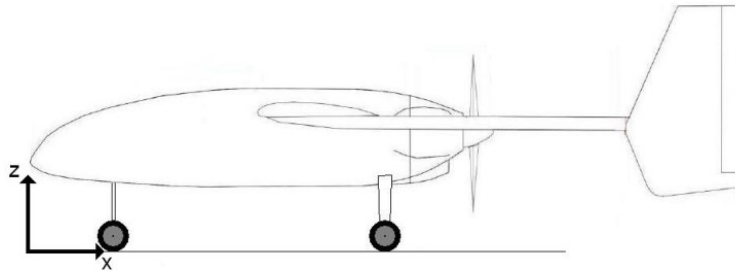
Figure 42 - Prometheus component location reference frame [21]

3.5.1.2 Configuration Discrepancies

The Prometheus has three major differences compared to the configuration chosen for the toolchain, these are; the propulsion system type, tail-configuration, and the VTOL capability. This chapter will describe these differences between the configuration chosen in the toolchain and the configuration of the Prometheus, and how the effects of the differences will be mitigated.

Propulsion system difference mitigation

The propulsion system type of the Prometheus is a gasoline two-stroke two-cylinder 85cc boxer engine. The propulsion system chosen for the toolchain is an electric-powered system. This difference affects the weight of both the engine/motor, but also the weight of the energy source. This is a fuel tank for the gasoline engine and batteries for the electric system. The difference lies within the weight of both systems which mainly affects the range of the aircraft.

The chosen mitigation technique for this difference is to determine an equivalent range the Prometheus would have if the propulsion system were electric-based with the same mass as the current gasoline-based system. One additional problem with this technique is that the mass of the propulsion system reduces during a mission for the gasoline-based system due to the fuel being burned and expelled from the aircraft. This effect will be assumed to have a minimal effect on the range of the aircraft in the gasoline configuration. This can be assumed due to the relatively small fuel mass that the Prometheus is able to carry compared to its MTOM. The equivalent range for the electric Prometheus is determined in Appendix E – Prometheus Performance Determination.

Tail configuration difference mitigation

The tail configuration employed by the Prometheus is a twin-tail-boom H-tail configuration, and the tail configuration employed by the toolchain is a twin-tail-boom inverted-U-tail configuration. The difference is visualized in Figure 43.

Figure 43 - Tail configuration difference

It is assumed that the effect of this difference between the tail configuration does not have a substantial effect on the outcome of the toolchain analysis. The only difference between the two configurations is, when viewing the size and weight determination techniques, is an additional multiplication factor presented by Raymer in chapter 0. However, the chosen method to determine the weight of the

stabilizers of Sadraey does not consider this difference of configuration to significantly affect the weight of the stabilizers.

VTOL capability

The Prometheus is developed to be a forward flight UAV, this means that the Prometheus is not able to verify the VTOL capability-related modules within the toolchain. This will have to be done by using another aircraft.

3.5.1.3   Conclusion

The methods utilized by the toolchain will be verified by comparing the results of the methods of the toolchain with the weight, propulsion system requirements, and geometry parameters of the Prometheus UAV. This is done by having the performance parameters, payload requirements, and mission requirements of the Prometheus put into the toolchain as input parameters. Next, the outputs are compared by percentual difference and discussed why these might differ between the implemented toolchain method and reality. Hereby answering research question # 5.

4. Verification

The verification process can be subdivided into 3 parts, the first is the collection of the data which the verification process will be conducted with, and next is the analysis itself, which is performed by the toolchain utilizing the methods described in 3.4. Lastly is the comparison between the expected outputs of the toolchain and the actual outputs of the toolchain. These topics will be discussed in this chapter.

4.1 Verification Method Data Collection

The verification method will use data on the Prometheus UAV, which is summarized in a table in Table 9. The expected results of the analysis are the parameters collected in Table 6 and Table 8 of chapter 3.5.1, but are summarised in Table 10.

Table 9 – Prometheus data, toolchain input parameters for the verification analysis

Parameter	Value	Source
Payload Weight	75.44 N	Derived (from the Payload mass)
Payload Width	0.20m	Measured
Payload Height	0.20 m	Measured
Payload Length	0.40 m	Measured
Range	85227 m	Derived (described in Equivalent Electric Propulsion System)
Rate-of-Climb	20.1 m/s	Derived (described in Theoretical Maximum Rate-of-Climb)
VTOL capability	No	[21]
Maximum velocity	60 m/s	[21]
Cruise velocity	41 m/s	[21]
Stall velocity	15 m/s	[21]
Electronics Weight	17.27 N	Derived (from the RC devices, Computer, Electricity mass in Table 8)
Airfoil main wing	NACA 4415	[21]
Airfoil vertical stabilizer	NACA 0006	[21]
Airfoil horizontal stabilizer	NACA 0006	[21]
Airfoil horizontal stabilizer $C_{l_{max}}$	0.8	[21]
Operating voltage	22.2 V	Assumed

Table 10 – Prometheus data, expected toolchain parameters

Parameter	Value
Total Aircraft Weight	234.35 N
Wing Area	1.085 m²
Aspect Ratio	9.44 [-]
Mean Aerodynamic Chord	0.3485 m
Horizontal Stabilizer Area	0.224 m²
Vertical Stabilizer Area (total)	0.3616 m²
Horizontal Stabilizer Span	0.640 m
Vertical Stabilizer Span	0.620 m
Fuselage Length	1.40 m
Tail Length	1.15 m
Elevator Area	0.048 m²
Rudder Area (Total)	0.099 m²
Aileron Area (Total)	0.0875 m²
Propeller Diameter	0.61 m
Landing Gear Length (main)	0.25 m
Fuselage Weight	13.62 N
Wing Weight	31.35 N
Tail-boom Weight (individual)	2.383 N
Horizontal Stabilizer Weight	4.395 N
Vertical Stabilizer Weight (individual)	3.247 N
Propulsion System + Energy Storage + Propeller Weight	67.00 N
Theoretical Battery Weight	44.79 N
Landing Gear Weight (Nose)	5.307 N
Landing Gear Weight (Main) (individual)	4.846 N

4.2 Analysis Results

This chapter presents the outputs of the toolchain based on the inputs previously described, and will compare these outputs with the expected results (Figure 44, Figure 45, and Table 11) and will discuss the most prominent/significant discrepancies between the values.
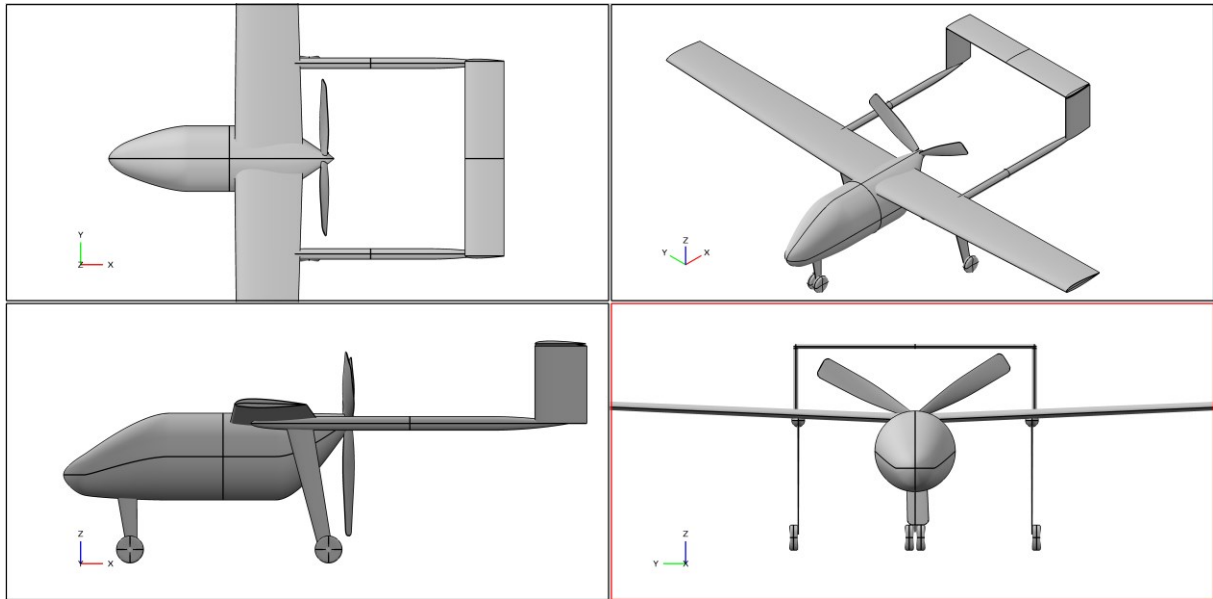
Figure 44 - Visualization of the generated UAV
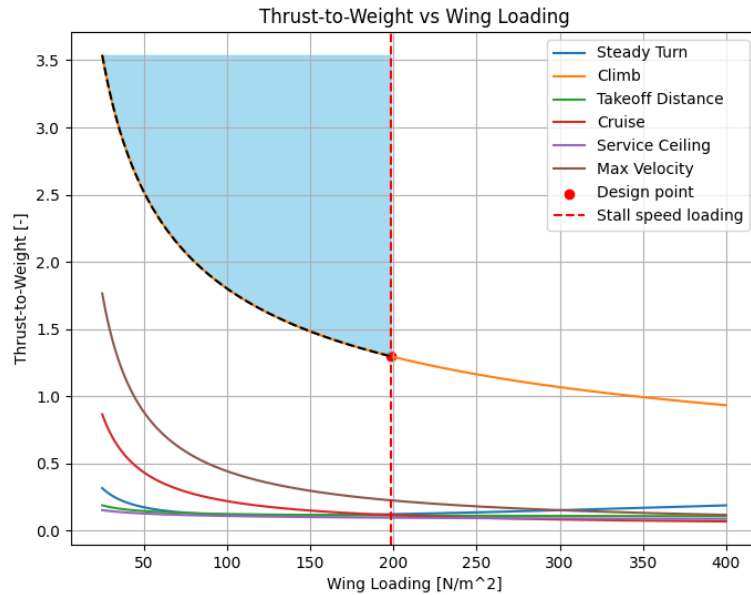
Figure 45 – size matching diagram for the Prometheus analysis

Table 11 – Processed Prometheus data , together with the expected processed parameters

Parameter	Expected Value	Generated Value	Percentual Difference
Total Aircraft Weight	234.35 N	196.577 N	16.12%
Wing Area	1.085 m²	0.996 m²	8.20%
Aspect Ratio	9.44 [-]	10.607 [-]	-12.36%
Mean Aerodynamic Chord	0.3485 m	0.306 m	12.20%
Horizontal Stabilizer Area	0.224 m²	0.174 m²	22.32%
Vertical Stabilizer Area (total)	0.3616 m²	0.106 m²	70.69%
Horizontal Stabilizer Span	0.640 m	0.975 m	-52.34%
Vertical Stabilizer Span	0.620 m	0.562 m	9.35%
Fuselage Length	1.40 m	1.042 m	25.57%
Fuselage Height	0.30 m	0.3253 m	-8.43%
Fuselage Width	0.32 m	0.3253 m	-1.66%
Tail Length	1.15 m	1.227 m	-6.70%
Elevator Area	0.048 m²	0.048 m²	0.00%
Rudder Area (Total)	0.099 m²	0.026 m²	73.74%
Aileron Area (Total)	0.0875 m²	0.075 m²	14.29%
Propeller Diameter	0.61 m	0.875 m	-43.44%
Landing Gear Length (main)	0.25 m	0.472 m	-88.80%
Fuselage Weight	13.62 N	5.876 N	56.86%
Wing Weight	31.35 N	16.356 N	47.83%
Tail-boom Weight (individual)	2.383 N	2.446 N	-2.64%
Horizontal Stabilizer Weight	4.395 N	0.936 N	78.70%
Vertical Stabilizer Weight (individual)	3.247 N	0.265 N	91.84%
Propulsion System + Energy Storage + Propeller Weight	67.00 N	60.935 N	9.05%
Theoretical Battery Weight	44.79 N	40.03 N	10.63%
Landing Gear Weight (Nose)	5.307 N	5.117 N	3.58%
Landing Gear Weight (Main) (individual)	4.846 N	5.117 N	-5.59%

4.2.1 Verification Discrepancy Analysis

As can be seen in Table 11 a percentual difference ranging between 91.84% and -88.80% is present between the expected data and the Generated data. The most significant of the discrepancies will be discussed below:

Vertical Stabilizer Area (total)

The vertical stabilizer area differs by a percentage of 70.69% from the expected value. This in turn directly affects the outcome of the Rudder Area (Total) and the Vertical Stabilizer Weight analysis, which has a similar 73.74% and 91.84% difference, respectively. The main contributing factor to the determination of the vertical stabilizer area is the stabilizer volume-fraction coefficient, which is assumed to be 0.04, which is implemented into the formula (2-74). This value is sourced from the book of Gudmundsson and is meant to be utilized for a General Aviation class aircraft with a single propeller.

Due to the large, potential, differences between GA-single engine and small UAVs, more research must be conducted to verify if this value for the stabilizer volume-fraction coefficient is fully applicable to the small UAV aircraft class. An additional potential cause of the large percentual difference is that the Prometheus could have been designed with an intentionally larger vertical stabilizer. This can be

supported by the fact that the Prometheus was originally designed to research systems utilized during aerial refueling where high-accuracy flight is required.

Propeller Diameter

The method utilized to determine the diameter of the forward flight propeller is solely dependent on the maximum amount of power the motor will provide to the propeller to propel the aircraft. The, relatively large/powerful, propulsion system mounted on the Prometheus means that the method utilized by the toolchain resulted in a large propeller diameter.

Since the propeller diameter is in reality not solely dependent on the power of the motor, but on several other factors, like desired efficiency, propeller pitch, operating rotation speed, and others, can lead to large discrepancies between reality and the method employed. A solution for this might be to find/create another method which does consider the previously mentioned factors to determine a more accurate propeller size.

Due to the forward flight propeller being mounted between the two tail booms means that in order to maintain clearance between the propeller and the booms the horizontal stabilizer must take into account the propeller diameter. This is visualized in Figure 45. This results in the large stabilizer span, and thus the large percentual difference is shown in Table 11.

Landing Gear

The landing gear length is (also) dependent on the size of the propeller, this is due to the clearance required during take-off rotation, which is discussed in 3.4.10 and visualized in Figure 34. Due to the analyzed propeller diameter being larger than the Prometheus results in a larger required landing gear for the analyzed UAV. It is however noteworthy that the weight does not reflect this same difference as the length does. This might be due a discrepancy between the weight calculation reference landing gear configuration and the one employed on the Prometheus.
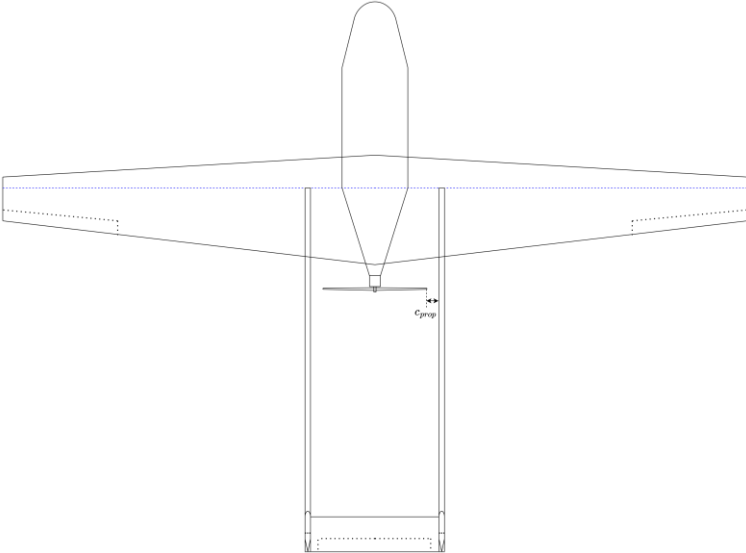
Figure 46 - UAV configuration, Top view

Fuselage Weight

The fuselage weight determined by the toolchain differs by 56.86% from the weight of the fuselage of the Prometheus. Possible causes for this might be a difference in the parameters which are used to calculate the fuselage weight, like the fuselage length, fuselage height and width, and the material used for the fuselage. But the fuselage length differs by 27.57%, the height and width of the fuselage only differ by -8.43% and -1.66%, respectively, and the material used for the structure is glass fibre for both the Prometheus and the toolchain. This only leaves that the formula provided by Sadraey gives an output which does not represent the Prometheus well. This is most likely due to either other design philosophies between the aircraft Sadraey analyzed and the designers of the Prometheus, or a differing target configuration. Sadraey based the weight formula on small UAVs with a conventional configuration, which the Prometheus is not. Further research must be conducted to determine where the discrepancy originates and how this can be adjusted.

Wing Weight

The wing weight determined by the toolchain differs by 48.82% from the weight of the Prometheus. The causes of this difference might be a difference between the maximum load factor used during the design process of the Prometheus, and a difference in designing methodology between the designers of the Prometheus and the UAVs analyzed by Sadraey. Lastly, a difference in the parameters which are used to calculate the wing weight. Like the wing area, mean aerodynamic chord, airfoil thickness, wing material, wing sweep, or wing taper.

The difference in wing weight is most probably not caused by a difference in parameters put into the weight determination formula provided by Sadraey. This is due to the parameters put into the weight determination formula differing with a maximum percentage of -15.74% or are identical to the characteristics of the actual wing.

More research must be conducted to determine where the discrepancy originates and how to correct this.

Horizontal Stabilizer Weight

The weight of the horizontal stabilizer determined by the toolchain has a difference of 80.50% from the weight of the stabilizer of the Prometheus. This can be caused by the fact that the actuation of the elevator of the Prometheus is done by two (relatively big) servos mounted to the horizontal stabilizer. This increases the weight of the stabilizer. Another reason might be that the fact that the tail configuration of the Prometheus (a twin-tail-boom H-tail configuration) has a greater effect on the weight of the stabilizer than first anticipated, this needs to be researched further to answer this.

Total Aircraft Weight

The percentual difference between the total aircraft weight determined by the toolchain and of the Prometheus only differ with 16.12%. Which for a conceptual design is a very close estimate of the total weight. The cause that this weight is so close is that the main weight-contributing components like the batteries and the propulsion system have a very similar weight as of the Prometheus.

5. Conclusion

A toolchain has been developed capable of generating a conceptual design for a small UAV with VTOL capabilities. This toolchain can estimate the size and weight of a small UAV with VTOL capabilities with a very limited amount of requirements and preexisting known parameters. This toolchain is a Python program that employs methods based on statistical data, empirically derived equations, design guidelines, and basic energy and drag models to determine the basic parameters required to initiate the preliminary design process of the desired UAV. These methods are most commonly determined based on previously developed aircraft of a similar class and use case. To implement these methods and get a valid answer an automated process is desired which solves these circular dependences. Which leads to the answer of the main research question:

"How can the conceptual design phase for a fixed-wing, VTOL-capable UAV be automated based on a given set of requirements?"

The conceptual design phase for a fixed-wing UAV can be automated by creating a toolchain. This toolchain is based on the answers to the following research questions:

1. What types of automated conceptual design analysis programs exist and what is the primary use case of these programs within the aviation industry?
   o Several tools have been created to automate the conceptual design process for aircraft, like the program SUAVE, which is further described in chapter 2.3. But the vast majority of the tools are created within a company and are either not shared due to the effort it requires to create such a program or must be purchased in order to use the program.
2. How do flight performance requirements affect the sizing, and geometry of a UAV?
   o The flight performance requirements primarily affect the amount of thrust the propulsion system must produce in various situations, this is in turn reflected in the size and weight of the propulsion system and the supporting systems around it. Details on how the performance requirements affect the design of the UAV can be found in chapter 3.4.3.
3. How is the design of a UAV influenced by a set of requirements on the weight and balance of the UAV?
   o The mass and balance of an aircraft is essential for the stability of the aircraft, the toolchain employs two methods to ensure that the balance point, or the CG of the aircraft is located at a specific point, these methods are described in detail in chapter 3.4.11.
4. Which requirements are necessary, and how will these be processed to result in a realistic and desired conceptual UAV design?
   o In order to run the toolchain, requirements on the desired UAV are necessary, these requirements are presented in chapter 3.4.14, which is supported by the chapters 3.4.2 till 3.4.13.
5. How can the conceptual designs generated by an automated conceptual design analysis program be verified?
   o The toolchain can be verified by employing the toolchain to determine the conceptual design parameters of an existing UAV and compare these parameters given by the toolchain with the actual parameters of the UAV, this process is described in more detail in chapter 3.5.

6. Future Work

In order to expand and/or continue on the methods described in this report, certain topics, limitations, and assumptions can be improved on, these will be mentioned in this chapter.

Statement of Assumptions and Limitations

A major limitation of the methods described in this report is that these are specifically selected and, in some cases, modified to fit the conceptual design process of a small UAV with a conventional wing, pusher propeller, and twin-boom tail configuration with an inverted U-tail. In order to analyze other configurations these methods must be reviewed if these are also applicable.

A topic for improvement within this project would be to verify that the toolchain can generate a realistic conceptual design for aircraft other than the Prometheus. This can eliminate uncertainties in the verification process in this report. Like, to answer the question of were the differences between the expected and the actual outcomes of the toolchain due to the slight difference in configuration, due to the Prometheus representing an abnormal aircraft of its size and configuration, or that the methods used caused these differences.

A summary of the assumptions made and limitations set by the methods used are shown in Appendix F – Statement of Assumptions and Limitations.

References

[1]   S. Gudmundsson, General Aviation Aircraft Design: Applied Methods and Procedures, Oxford: Elsevier Inc., 2014.

[2]   J. Gundlach, Designing Unmanned Aircraft Systems: A Comprehensive Approach, Reston: American Institute of Aeronautics and Astronautics, Inc., 2012.

[3]   J.-H. An, D.-Y. Kwon, K.-S. Jeon, M. Tyan and J.-W. Lee, "Advanced Sizing Methodology for a Multi-Mode eVTOL UAV Powered by a Hydrogen Fuel Cell and Battery," Aerospace, 2022.

[4]   L. Nicolai and G. Carichner, Fundamentals of Aircraft and Airship Design, vol. 1, Reston: American Institute of Aeronautics and Astronautics, Inc., 2010.

[5]   D. Raymer, Aircraft Design: A Conceptual Approach, Reston: American Institute of Aeronautics and Astronautics, Inc., 2018.

[6]   Roskam, Airplane Design - part 5: Component Weight Estimation, Lawrence: DARcorporation, 2018.

[7]   M. H. Sadraey, Aircraft Design A Systems Engineering Approach, Chichester: John Wiley & Sons, Ltd, 2013.

[8]   M. Tyan, N. Nguyen, S. Kim and J. Lee, "Comprehensive preliminary sizing/resizing method for a fixed wing – VTOL electric UAV," Elsevier Masson SAS, 2017.

[9]   Z. Yi and W. Heping, "A Study Structure Weight Estimating for High Altitude Long Endurance (HALE) Unmanned Aerial Vehicle (UAV)," School of Aeronautics, Northwestern Polytechnical University, Xi'an, 2006.

[10] DLR, "DLR Braunschweig," 2024. [Online]. Available: https://www.dlr.de/en/dlr/locations-and-offices/braunschweig.

[11] SUAVE, "SUAVE 2.5: Design Dreams Come Alive," [Online]. Available: https://suave.stanford.edu/index.html. [Accessed 06 2024].

[12] L. Kracke, "Entwicklung und Implementierung einer Methodik zur Massenabschätzung im Entwurfsprozess von unbemannten Luftfahrzeugen," DLR, Braunschweig, 2023.

[13] J. S. S. S. Chatterjee, Handbook of Regression Analysis, New Jersey: John Wiley & Sons, inc., 2013.

[14] A. Sprague, "Finite Element Method," Wiliam E. Boeing Department of Aeronautics & Astronautics, [Online]. Available: https://www.aa.washington.edu/about/impact/FEM. [Accessed 05 2024].

[15] numpy, "numpy.org," 2024. [Online]. Available: https://numpy.org/. [Accessed 05 2024].

[16] scipy, "scipy.org," 2024. [Online]. Available: https://scipy.org/. [Accessed 05 2024].

[17] A. Propellers, "APC Propeller," 2024. [Online]. Available: https://www.apcprop.com/technical-information/performance-data/. [Accessed 08 05 2024].

[18] H. Energy, "Harding Energy Lithium," [Online]. Available: https://www.hardingenergy.com/lithium-2/. [Accessed 05 2024].

[19] "BU-808: How to Prolong Lithium-based Batteries," Battery University, [Online]. Available: https://batteryuniversity.com/article/bu-808-how-to-prolong-lithium-based-batteries. [Accessed 05 2024].

[20] O. Learning, "Relative And Percent Error Formula," OnlineMath Learning.com, [Online]. Available: https://www.onlinemathlearning.com/relative-error-formula.html. [Accessed 05 2024].

[21] S. Krause, "Prometheus - Air-to-air refueling/automatic catcher," Braunschweig.

[22] S. Walbers, "Simulating the Prometheus UAV," Deutsches Zentrum für Luft- und Raumfahrt e.V, Braunschweig, 2005.

[23] K. Gonet, "Flugmechanische Auslegung eines UAV Demonstrators (Unmanned Air Vehicle)," DLR, Braunschweig, 2003.

Appendices

The following appendices provide additional material/information that supports the main text of this report. These materials include the original assignment description for this report, detailed descriptions of the Unmanned Aerial Vehicles (UAVs) considered for implementation into the toolchain described in the report, information on the databases utilized in the toolchain described in this report, and lastly, additional information on parameters presented by other sources that are used during the weight determination analysis of the UAV.

Appendix A – Assignment Description

Institut für Flugsystemtechnik

DLR e. V.   Institut für Flugsystemtechnik
             Lilienthalplatz 7, 38108 Braunschweig

Institut
Fachgebiet

Professor

Name	Lennart Kracke
Telefon	+49 (0)531 295 1022
Telefax	
E-Mail	lennart.kracke@dlr.de

Assignment of the graduation project for Mr. Ivo Poelma
-Draft-

08.01.2024

Matrikel-Nr.:   ???   Studiengang: Master Luft- und Raumfahrttechnik

E-Mail: ivopoelma@gmail.com

Project title:

Development and implementation of a toolchain for the analysis and conceptual design of fixed wing UAVs

Background:

Unmanned aircraft have become an important extension to aviation. The scalable nature of UAS permits the utilization of these systems over a wide range of operations. Possible scenarios are flights over disaster areas, maintenance of power supply lines or oil pipelines, traffic supervision, or missions in unsecure areas.
The desired missions for future UAS are typically complex and require different capabilities. For this reason, fundamental research in many fields of UAS is still needed. The department for unmanned aircraft systems at the DLR Institute of Flight Systems promotes the development by conducting research in the following areas:

- Robust flight control and mission control solutions for systems operating under high uncertainty
- Sensor fusion and environmental perception
- Optical navigation
- Machine Learning
- UAS integration into the existing airspace
- Detect and avoid
- Airworthiness
- Drone defense
- Technical solutions for systems with very small space, weight, and power requirements

A key aspect of these applications and their corresponding methods are modern aerial vehicles, including the different sub-systems and supporting processes. For this reason, the department operates a variety of experimental unmanned aircraft. Beside a fleet of unmanned helicopters and multicopters of different sizes, autonomous fixed-wing aircraft and parachute load deposing systems are available for research. In order to acquire suitable UAVs for the research projects to come, it is desirable to develop a toolchain for the analysis and design of UAV. By doing so, the department is enabled to evaluate and reverse engineer the performance characteristics of different configurations as well as providing tailored solutions for a given mission profile.

UAV Proteus I & II at the DLR National Experimental Test Center for Unmanned Aircraft Systems in Cochstedt (Source: DLR)

Assignment:

The aim of this student research project is to develop and implement a toolchain for the analysis and design of fixed-wing UAVs. The toolchain is to be developed in Python and should cover at least the following aspects on a conceptual design level:

- Initial unmanned aircraft sizing
- Unmanned aircraft geometry and configurations
- Aerodynamics
- Mass and Balance
- Propulsion Systems
- Flight Performance

The following points need to be addressed in detail by the graduation report:
o Literature research on existing methods and tools for the design of fixed-wing UAVs
o Theoretic background of the used methods for the analysis of certain systems
o Documentation of the developed code with special focus on the software architecture
o Validation of the toolchain on one of the existing unmanned aircraft in the department
o Documentation of the findings in a scientific report in accordance with the requirements of the university and the quality specifications of the DLR Institute of Flight Systems

Duration: 6 months

The student research project is being carried out at the German Aerospace Center (DLR) in Braunschweig. The information made accessible during the course of the internship is confidential.

Supervisor:
Lennart Kracke

Erstprüfer:

Name Professor

_____
    Unterschrift

Appendix B – UAV Configurations

This appendix presents the configurations that were considered to be implemented in the toolchain analysis. For each of the configurations, a detailed description and a presentation of the (dis)advantages is given in order to support the trade-off table presented in chapter 3.3 and in this appendix.

Configuration 1 – Conventional – Central-fuselage – Pusher
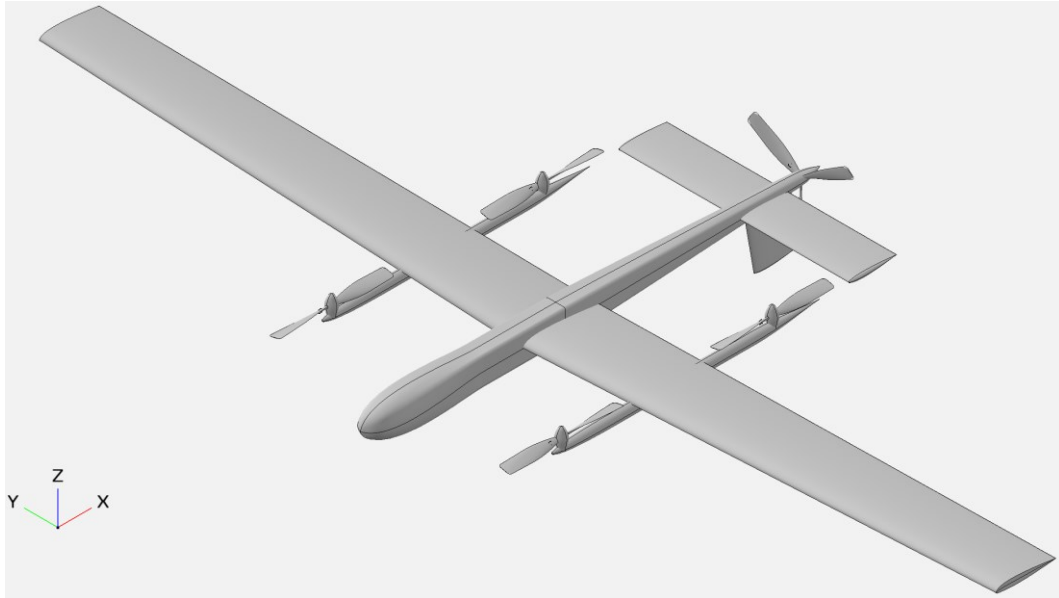
[Conventional Wing – Pusher – Single propulsion system – Single-boom – Inverted Conventional tail]

Description

Configuration 1 is a UAV with a conventional wing, meaning that the main lifting surface is located in front of the horizontal stabilizer. It is fitted with a pusher-style propulsion system which can either be a propeller or a jet-powered system. The propulsion system is mounted to the aft portion of the central fuselage/empennage. The empennage is a conventional tail configuration, meaning that both the vertical and horizontal stabilizers are mounted to the aft portion of the fuselage like a T. The propulsion system for during and transitioning to and from the vertical flight is mounted to the two booms that extend forward and aft from the main wing. This propulsion system will consist of four or more dedicated propellers for vertical flight. The landing gear is in the of a tricycle landing gear, which can either be a retractable- or non-retractable gear.

Advantages

The conventional wing design has been used in the past and present to design the majority of aircraft. This means there is a lot of knowledge of how to design, manufacture, and simulate these types of aircraft. Additionally, the rear-mounted horizontal stabilizer provides predictable lateral control, even near stall conditions.

Due to the pusher propeller configuration, there is a clear forward and sideways view from a typical payload bay location. Additionally, due to the pusher propeller configuration, undisturbed air will flow over the wing and fuselage, which reduces vibrations and decreases drag due to more laminar airflow.

The vertical stabilizer is located below the tail boom, instead of on top which is more common. This is to prevent the forward flight propeller from impacting the ground. Additionally, it prevents rudder blanketing, when the horizontal stabilizer reduces the effective area of the vertical stabilizer at high angles of attack.

Disadvantages

Due to the rear-mounted horizontal stabilizer, it must create downforce in order to stabilize the aircraft. This means that the main wing must create even more lift than the total aircraft's weight, which increases the total amount of drag of the aircraft. Due to the tractor propeller configuration, there isn't a completely clear forward from a typical payload bay location. Additionally, due to the tractor propeller configuration, disturbed air will flow over the wing and fuselage, which causes vibrations and increases drag due to less laminar airflow. Due to the single boom fuselage does not provide mounting options for VTOL motors twin booms must be added to mount the four (or more) VTOL motors that can control the aircraft in vertical flight. Lastly, due to the propulsion system being mounted to the aft of the central fuselage/empennage the risk is increased that the propulsion system impacts the ground. To mitigate this, a higher landing gear can be used, but this adds additional weight.
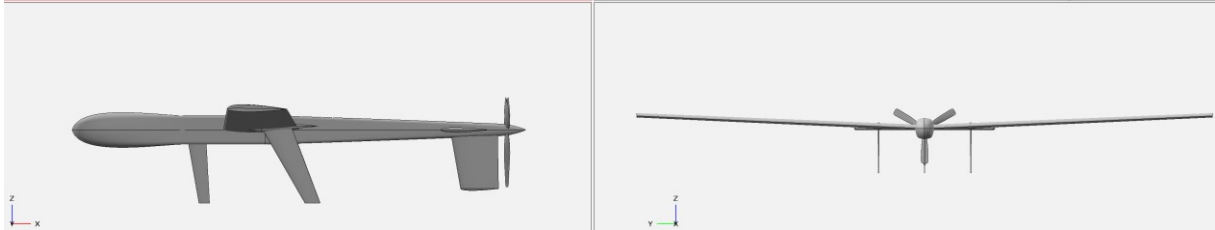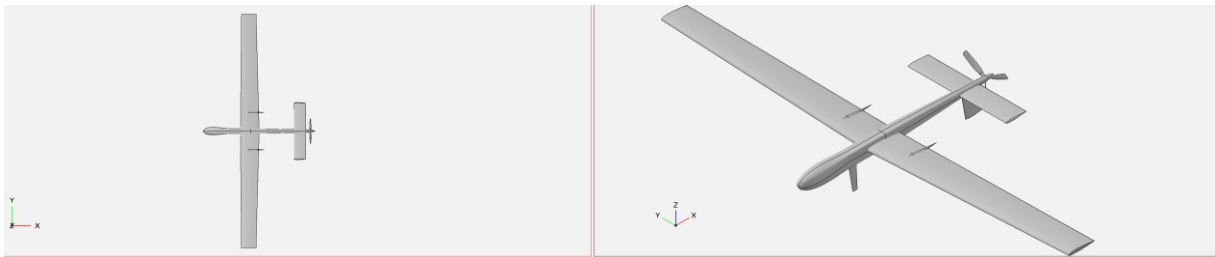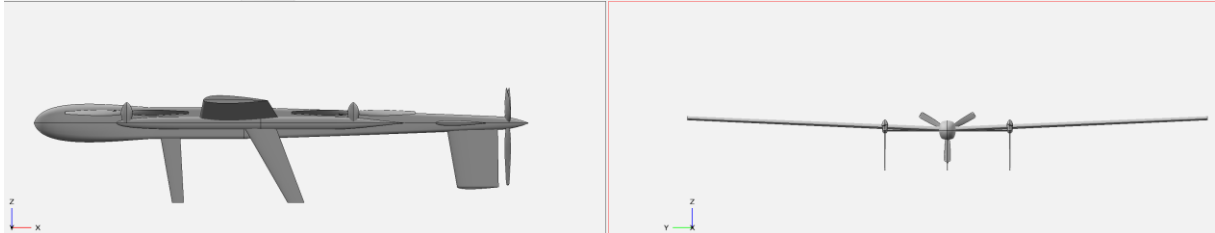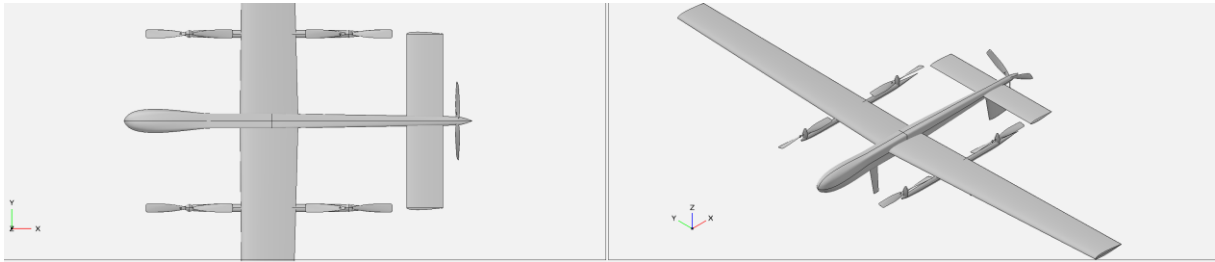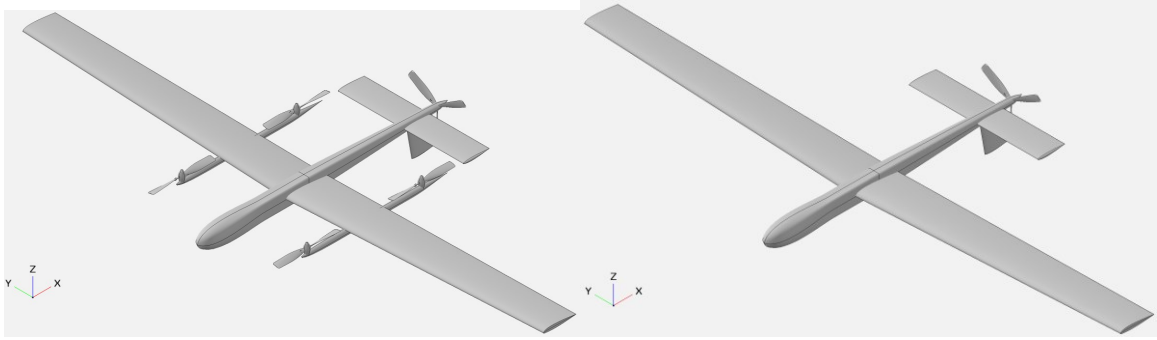
Configuration 2 – Conventional – Twin-boom – Pusher
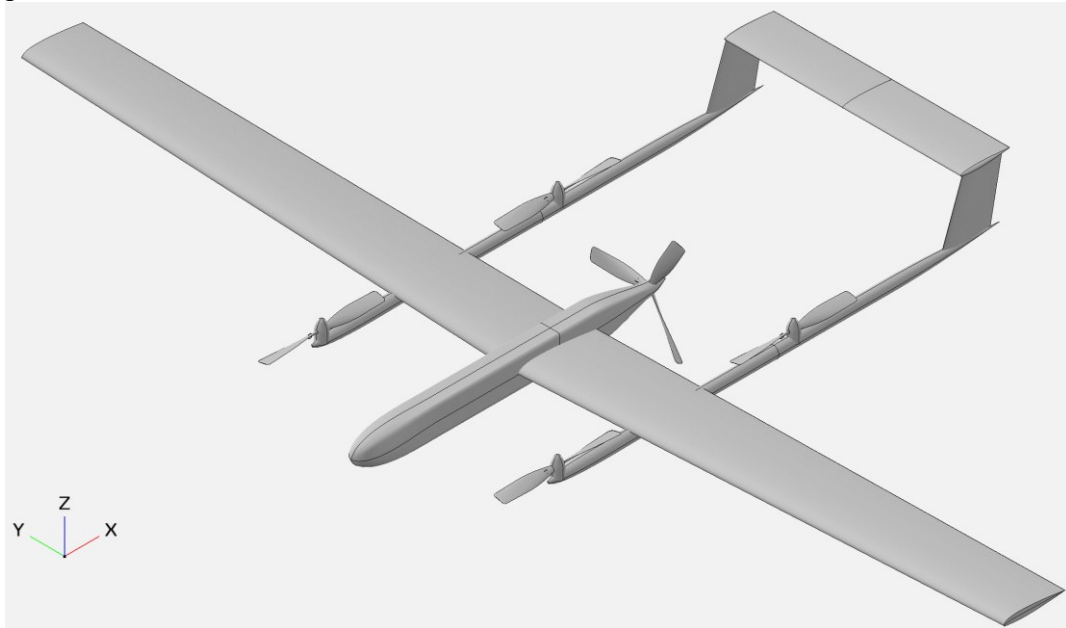
[Conventional Wing – Pusher – Single propulsion system – Twin-boom – Inverted U-tail]

Description

Configuration 2 is a configuration with a conventional wing, meaning that the main lifting surface is located in front of the horizontal stabilizer. It is fitted with a pusher-style propulsion system which can either be a propeller or a jet-powered system. The propulsion system is thus mounted to the aft portion of the central fuselage. The empennage is an inverted U-shaped tail configuration connected to the aircraft utilizing two booms. This means that the horizontal stabilizer is mounted to each upper tip of the vertical stabilizers and that the vertical stabilizers are mounted to the booms which are then mounted to the main wing of the aircraft. The propulsion system for during and transitioning to and from the vertical flight is mounted to the two tail booms and extensions of these that extend forward from the main wing. This propulsion system will consist of four or more dedicated propellers for vertical flight.

Advantages

The conventional wing design has been used in the past and present to design the majority of aircraft. This means there is a lot of knowledge of how to design, manufacture, and simulate these types of aircraft. Due to the pusher propeller configuration, there is a clear forward and sideways view from a typical payload bay location. Additionally, due to the pusher propeller configuration, undisturbed air will flow over the wing and fuselage, which reduces vibrations and decreases drag due to more laminar airflow. The landing gear is in the of a tricycle landing gear, which can either be a retractable- or non-retractable gear.

The twin booms can be extended and used to mount the VTOL motors, this gives a solid mounting of four (or more) motors which can control the aircraft in vertical flight. Additionally, the distance between the motors and the major surfaces of the aircraft (i.e. wings) more efficient vertical flight can be achieved. Next to this, the rear-mounted horizontal stabilizer provides predictable lateral control, even near stall conditions. By incorporating the inverted U-shaped tail configuration, the turbulent prop wash interacts minimally with the horizontal stabilizer which makes for a more steady and efficient flight.

Disadvantages

Due to the rear-mounted horizontal stabilizer, it must create downforce in order to stabilize the aircraft. This means that the main wing must create even more lift than the total aircraft's weight, which increases the total amount of drag of the aircraft.
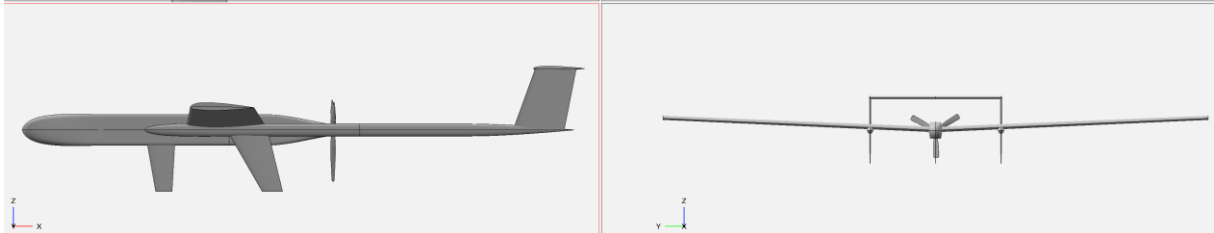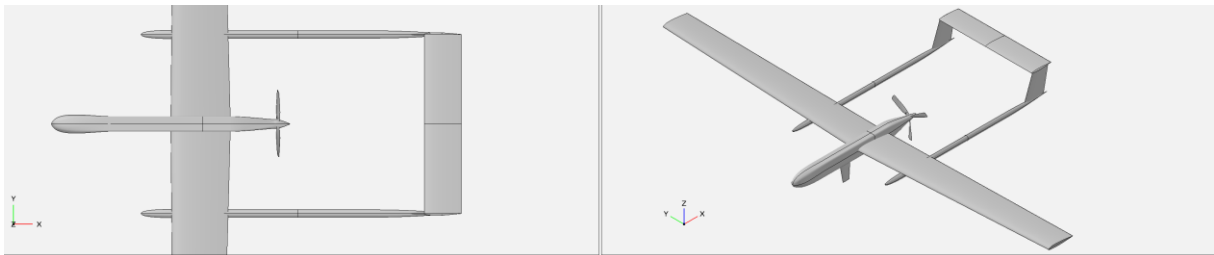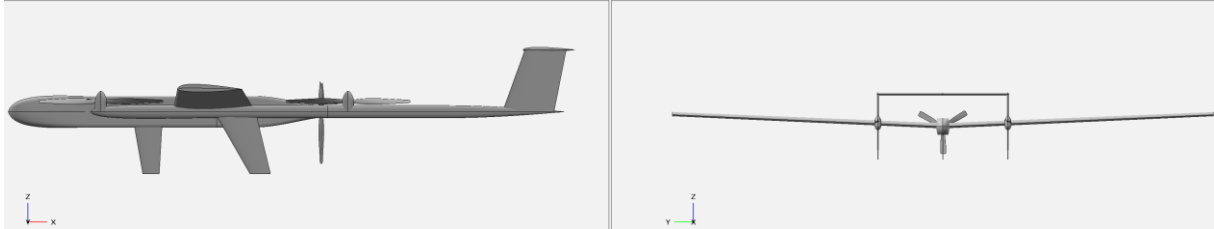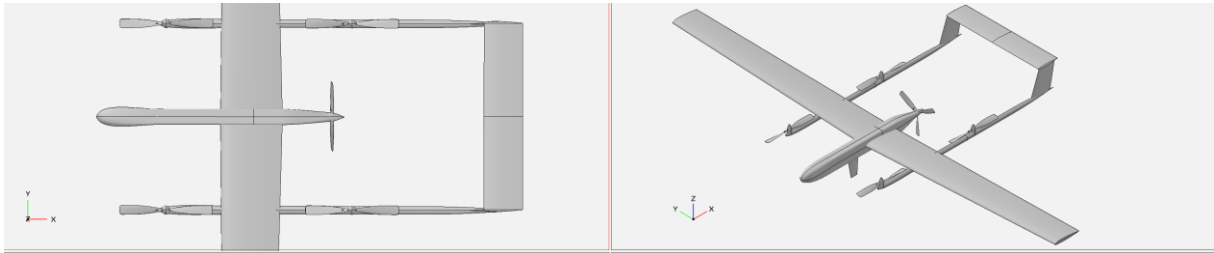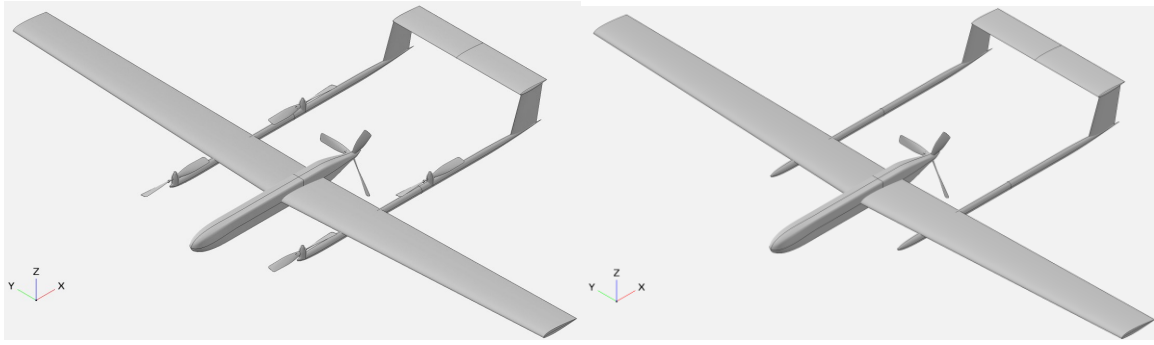
Configuration 3 – Conventional – Twin-boom – Twin-tractor
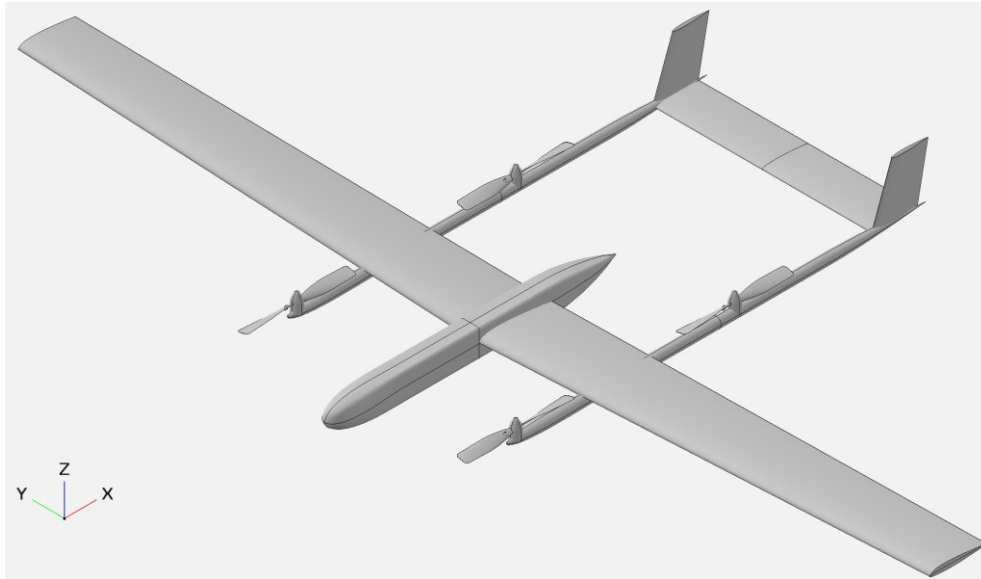
[Conventional Wing – Tractor – Twin propulsion system – Twin-boom – U-tail]

Description

Configuration 3 is a configuration with a conventional wing, meaning that the main lifting surface is located in front of the horizontal stabilizer. It is fitted with a twin tractor-style propeller-powered propulsion system for forward flight (FF). The FF propulsion system is mounted to the forward portion of either boom that also attaches to the main wing, horizontal- and vertical stabilizer. The empennage is a U-shaped tail configuration. This means that the horizontal stabilizer is mounted between either boom and that the vertical stabilizers are mounted to the booms which are then mounted to the main wing of the aircraft. The two FF propulsion systems can tilt to create vertical thrust during, transitioning to and from vertical flight. At least two additional propeller propulsion systems are mounted to the tail booms aft of the main wing. These propulsion systems will consist of two or more dedicated propellers for vertical flight. The landing gear is in the of a tricycle landing gear, which can either be a retractable- or non-retractable gear.

Advantages

The conventional wing design has been used in the past and present to design the majority of aircraft. This means there is a lot of knowledge of how to design and manufacture these types of aircraft.

The twin booms can be extended and used to mount the VTOL motors, this gives a solid mounting of four (or more) motors which can control the aircraft in vertical flight. Additionally, the distance between the motors and the major surfaces of the aircraft (i.e. wings) more efficient vertical flight can be achieved. The rear-mounted horizontal stabilizer provides predictable lateral control, even near stall conditions. Lastly, the two (or more) forward VTOL motors can also be repurposed to be tilted to provide thrust in forward flight. This has the possibility of reducing the weight of the aircraft.

Disadvantages

Due to the rear-mounted horizontal stabilizer, it must create downforce in order to stabilize the aircraft. This means that the main wing must create even more lift than the total aircraft's weight, which increases the total amount of drag of the aircraft. Lastly, the double function of the forward motors also requires a tilting mechanism, which adds more components, failure points, and complexity.
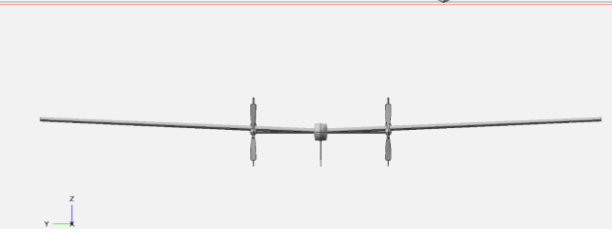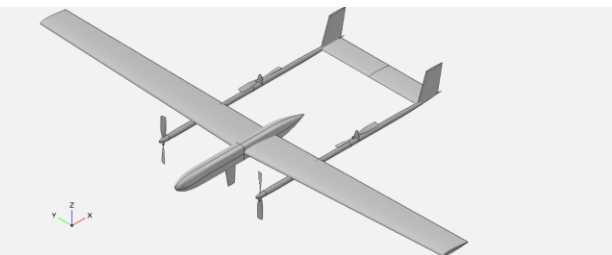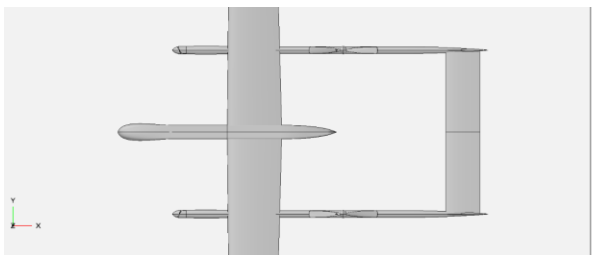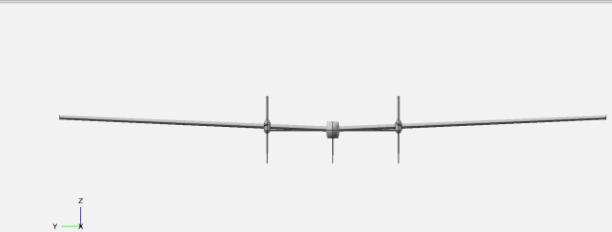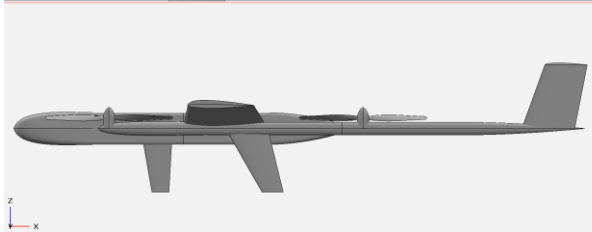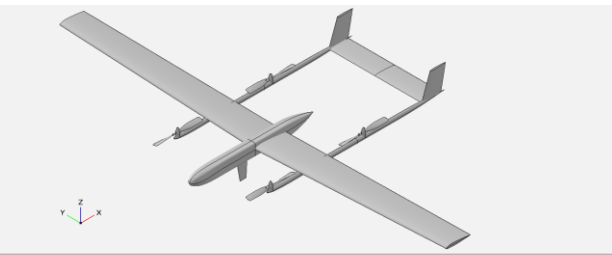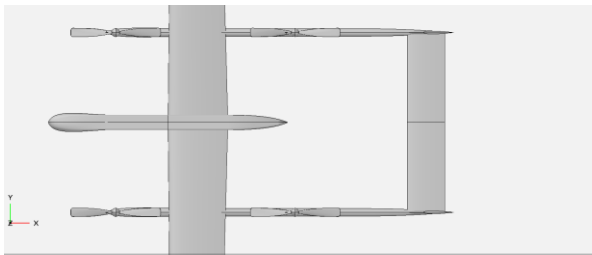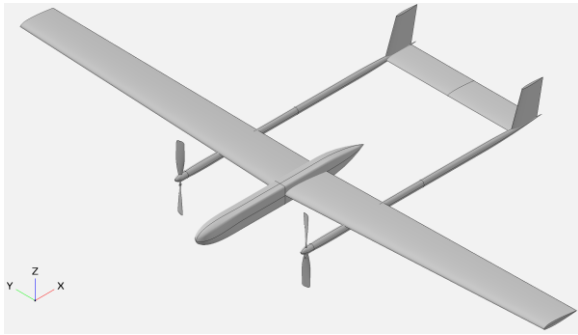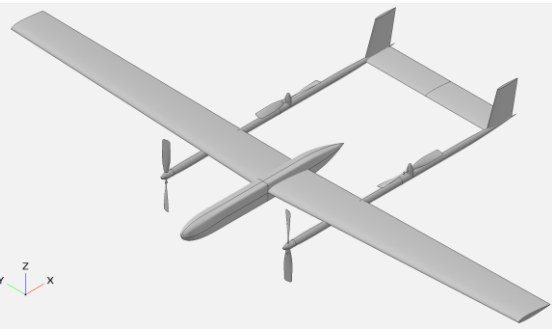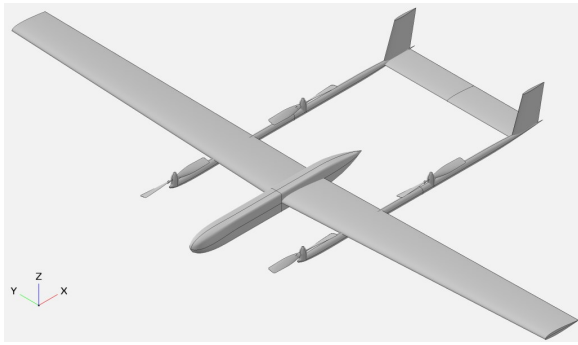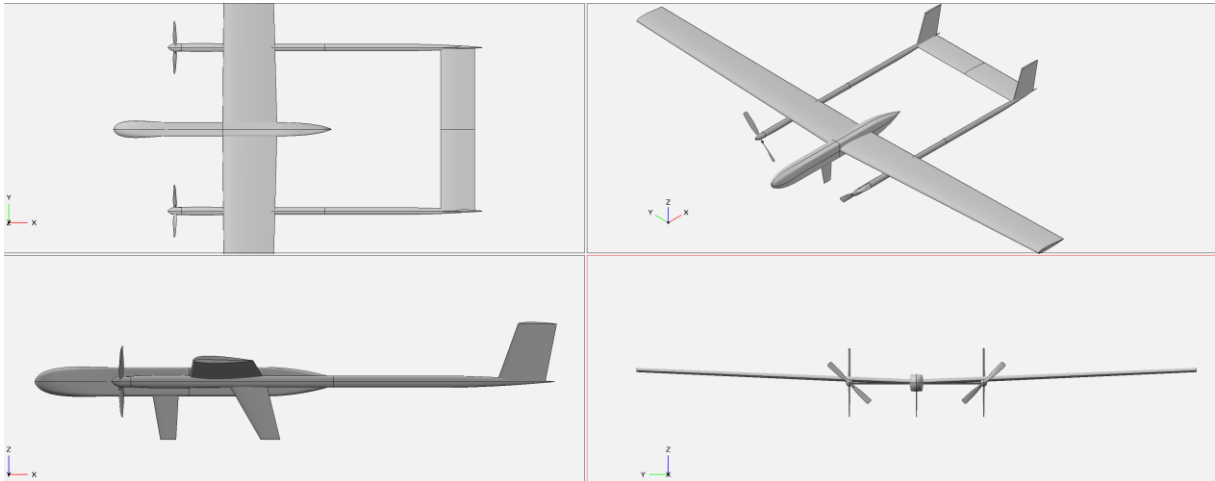
Configuration 4 – Canard - Pusher
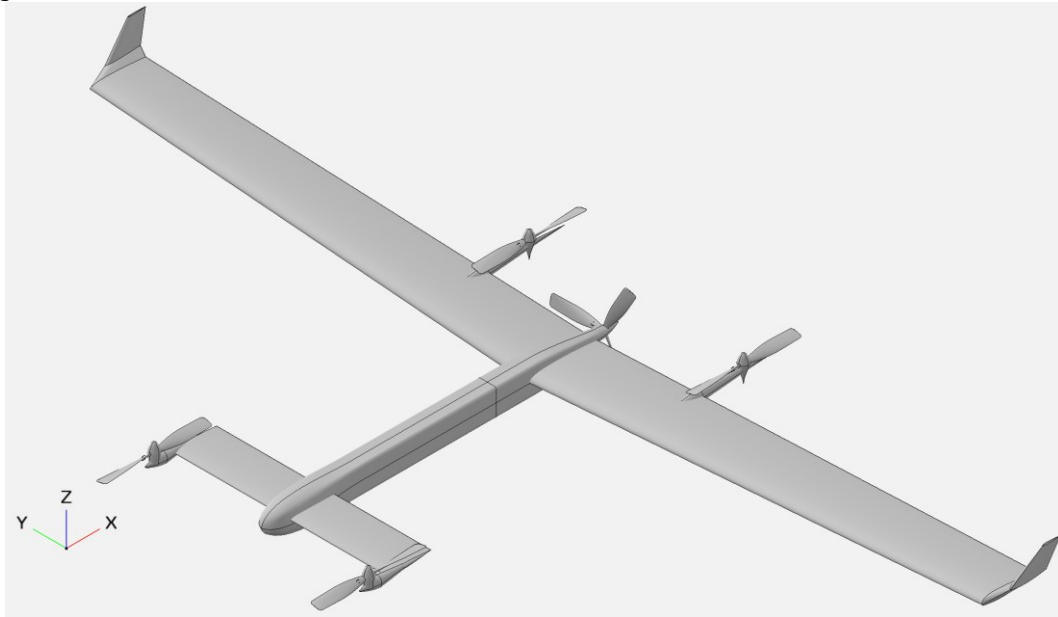
[Canard Wing – Pusher – Single propulsion system – Vertical Stabilizers on Wingtips]
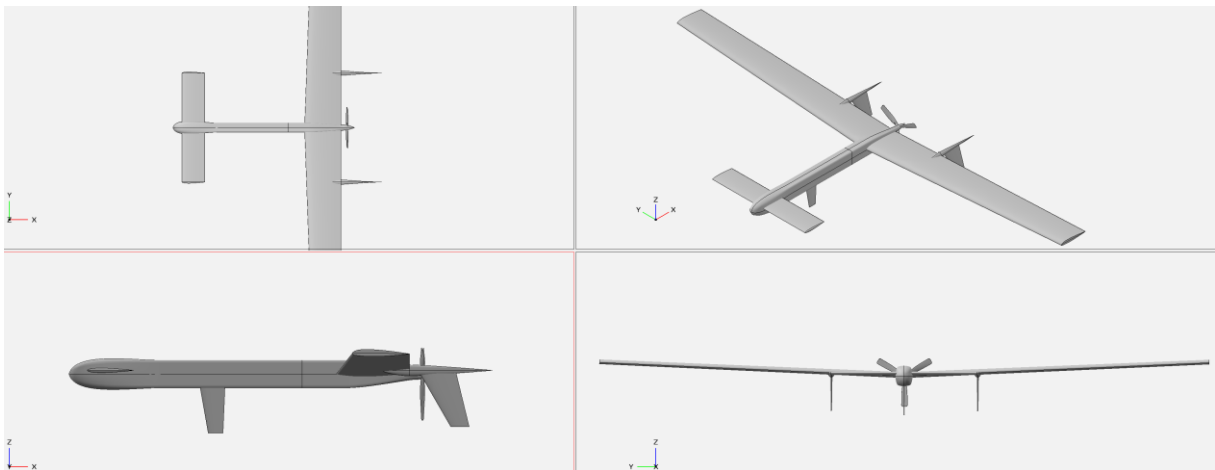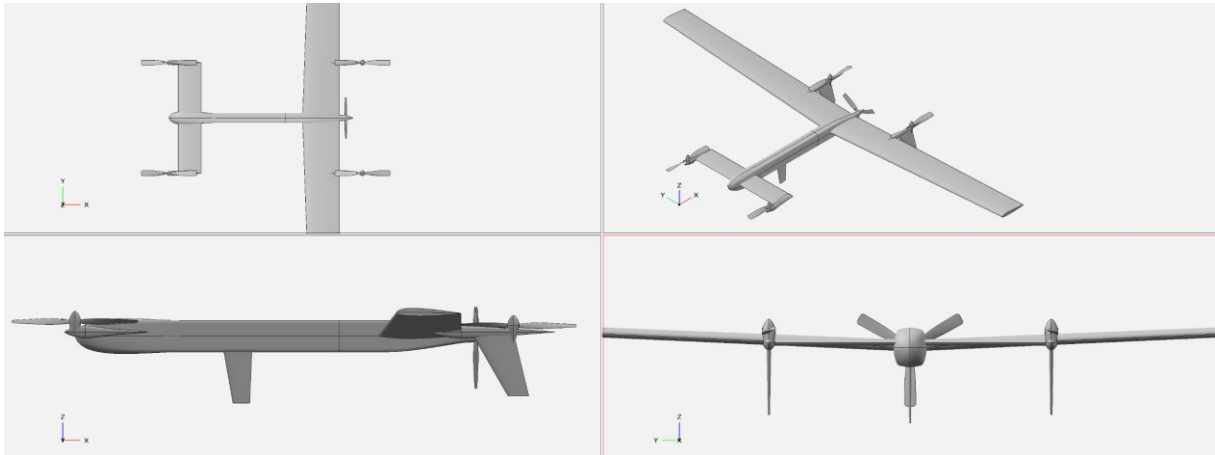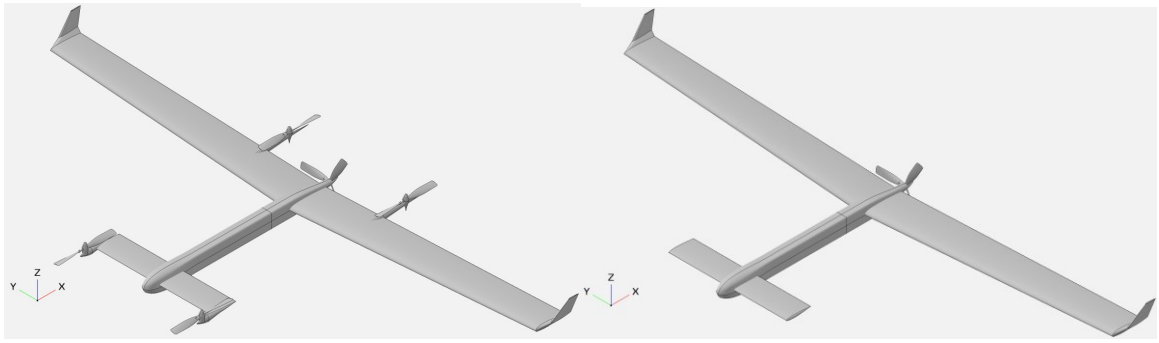
Description

Configuration 4 is a canard configuration, meaning that the main lifting surface is located aft of the horizontal stabilizer. It is fitted with a pusher-style propulsion system which can either be a propeller or a jet-powered system. The propulsion system is mounted to the aft portion of the central fuselage. The lateral control is achieved by the horizontal stabilizers mounted in front of the main wing to the fuselage. Vertical stabilizers can be mounted either at the wingtips to have a double function as drag-reducing devices, and/or can be mounted on the aft end of the fuselage. The propulsion system for during and transitioning to and from the vertical flight is mounted to the main wing and the tips of the canard on nacelles. This propulsion system will consist of four or more dedicated propellers for vertical flight. The landing gear is in the of a tricycle landing gear, which can either be a retractable- or non-retractable gear.

Advantages

The typical primary goal of a canard design is to increase the flight efficiency by having the horizontal stabilizer create lift, instead of downforce which a conventional horizontal stabilizer creates. This either reduces the amount of lift the main wing must create or increases the payload mass that the aircraft can carry. Due to the canard creating lift, the CG must be placed forward of the MAC. This results in that the payload bay can be located on the CG and in a relatively 'open' section of the fuselage due to the lack of major structural members. Lastly, due to the pusher propeller configuration, there is a clear forward and sideways view from a typical payload bay location. Additionally, due to the pusher propeller configuration, undisturbed air will flow over the wing and fuselage, which reduces vibrations and decreases drag due to more laminar airflow.

Disadvantages

Due to the atypical design of a canard configuration, additional steps must be taken to ensure that it is both stable and controllable compared to a conventional aircraft. This is primarily regarding the (near) stall characteristics of a canard configuration.

Configuration 5 – Flying Wing - Pusher
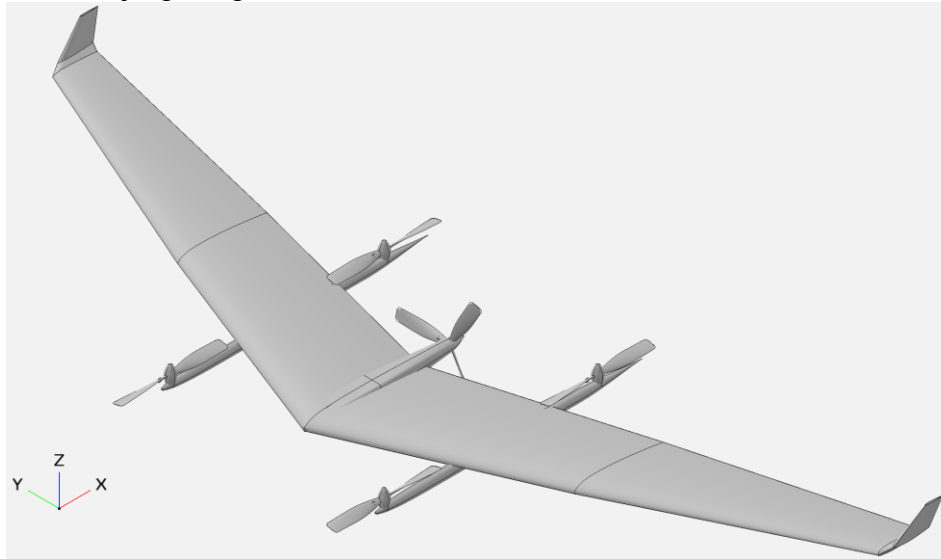
[Flying Wing – Pusher - Single propulsion system – Vertical Stabilizers on Wingtips when necessary]

Description

Configuration 5 is a Flying wing configuration, meaning that the aircraft does not have a distinct fuselage or empennage. The configuration is fitted with a pusher-style propulsion system which can either be a propeller or a jet-powered system. The propulsion system is mounted centrally to the aft portion of the wing. Due to the Flying wing not having a horizontal stabilizer, the lateral control is achieved by doubly using the ailerons as elevators, i.e. elevons. Directional control can either be achieved by wingtips to have a double function as drag-reducing devices, or by split elevons which can create additional drag when required. Or lastly, by utilizing distinct lift and pressure distribution methods. The propulsion system for during and transitioning to and from the vertical flight is mounted to the two booms that that extend forward and aft from the wing. This propulsion system will consist of four or more dedicated propellers for vertical flight. The landing gear is in the of a tricycle landing gear, which can either be a retractable- or non-retractable gear.

Advantages

The typical primary goal of a flying wing design is to increase flight efficiency due to the lack of a fuselage and tail section both weight-wise and drag-wise. This commonly also results in a simpler design and manufacturing process due to a lower number of parts. Due to fewer surfaces being present and the general shape of a typical flying wing, a low radar cross-section aircraft can be developed. Lastly, due to the pusher propeller configuration, there is a clear forward and sideways view from a typical payload bay location. Additionally, due to the pusher propeller configuration, undisturbed air will flow over the wing, which reduces vibrations and decreases drag due to more laminar airflow.
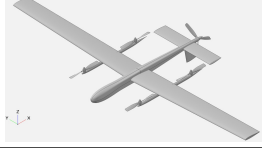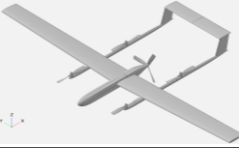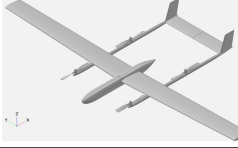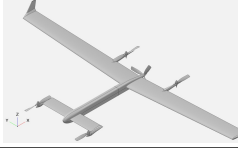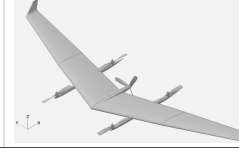
Disadvantages

Due to the lack of a tail section/stabilizer, a flying wing is typically very sensitive to a CG shift, meaning that the CG must be placed accurately in order to achieve stable flight. Next to this, due to the lack of vertical stabilizers and/or lack of directional control landing in a conventional method in a specified direction (with respect to the wind and landing zone) is either challenging or impossible. Lastly, additional steps must be taken to ensure that the flying wing is both stable and controllable compared to an aircraft with a tail section/stabilizer.
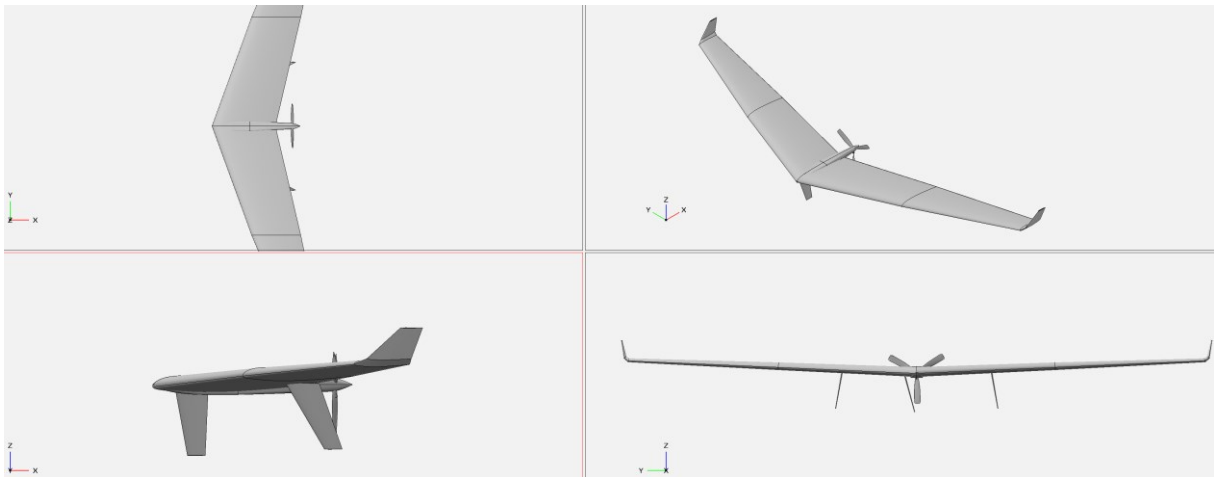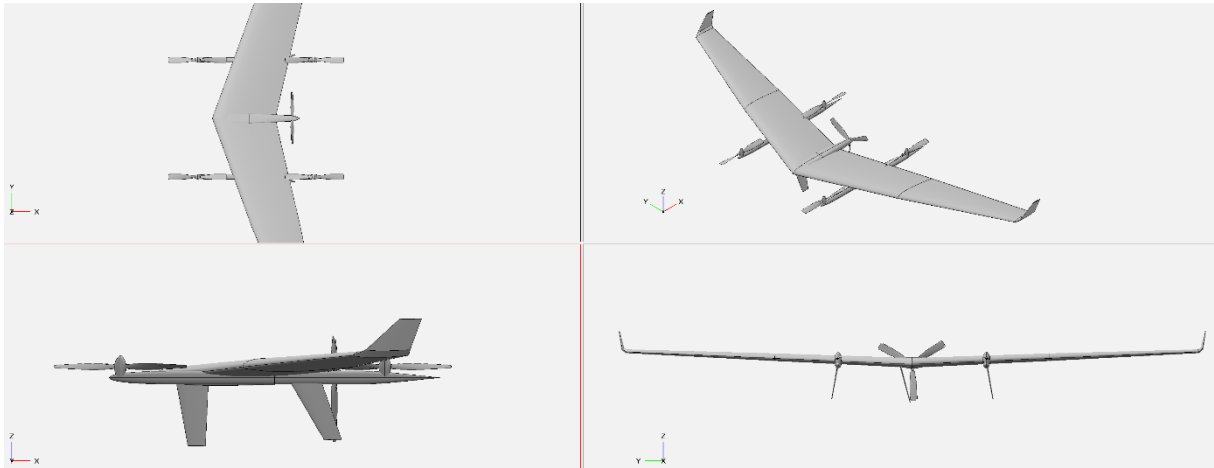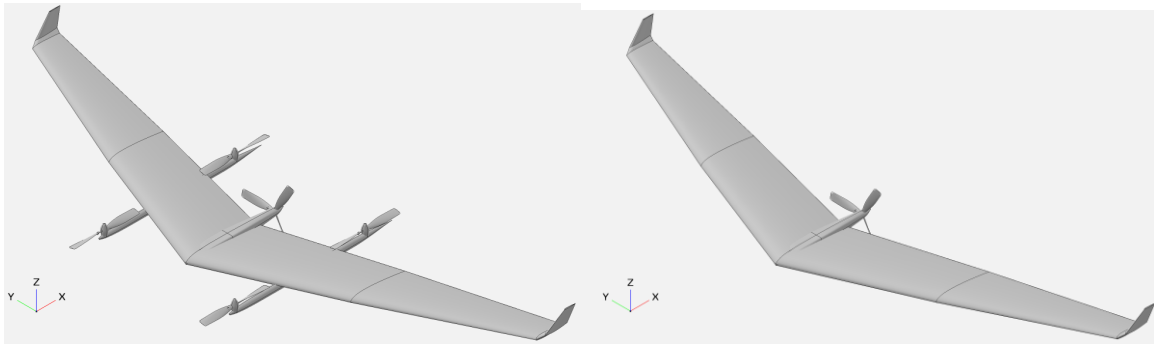
Configuration Trade-Off Table

This chapter will present the trade-off table that is shown below that is used to select the configuration to be used in this report.

Grading criteria (-1, 0, 1)	Weight (1-5)	Design Configurations				
		Conventional-Central_fuselage-Pusher	Conventional-Twinboom-Pusher	Conventional-Twinboom-Twin_Tractor	Canard-Pusher	Flying_Wing-Pusher
Manufacturing Complexity	4	0	0.5	-0.5	0.5	1
Efficiency FF	5	0	0.5	-0.5	0.5	1
Efficiency VTOL	4	0	0.5	0	0	0.5
CG Shift Sensitivity	5	0.5	0.5	0.5	0.5	-1
Lift Capability to Wto ratio	2	0	0	0	0.5	0.5
Favorable (near-)Stall Characteristics	3	1	1	0	0	-1
Conventional Take-off and Landing Capablities	2	-1	1	1	0	0
Transition behavior	4	1	1	0	1	1
Total score	29	7.5	18	0	12	8

The trade-off table above is based on a weight-and -score system. The weights appointed to each grading criterium are determined how influential each criterium is for the requirements set up for the desired UAV presented in 3.1 Toolchain Requirements. With the score of 5 being very influential and 1 being almost not influential. The score given to each configuration for each criterium was based on engineering insight on how well a UAV of this configuration would perform in this aspect, with a score of 1 being that the configuration would perform very well and a score of -1 very poorly all with respect to an average score for all the configurations. As example, the Conventional-Central-Fuselage-Pusher configuration scored a -1 on Conventional Take-Off and landing Capabilities due to this configuration having the forward flight propeller at the trailing tip of the fuselage which only allows from minimal take-off angle of attack while keeping the landing gear to a reasonable length, all to avoid a tail/propeller strike with the ground.

Appendix C – Data Collection

In this appendix the database Janes provided by Krake [11] will be introduced, this will be done by discussing what data is presented in the database, how this was acquired and how this might be used.

Janes

This database called "Janes" contains data on a large number of previously developed UAVs of a wide range of purposes, take-off weights and configurations. This database is based on the book "Jane's All World's Aircraft Unmanned". Due to the fact that Janes solely contains data on previous developed UAVs, the database can be used for either verification methods and/or formula regression methods. Janes contains parameters on 367 UAVs, these parameters are;

- Total length [m]
- Wing span [m]
- Wing area [m²]
- Empty weight [kg]
- Fuel weight [kg]
- Payload weight [kg]
- Maximum take-off weight [kg]
- Cruise speed [km/h]
- Maximum speed [km/h]
- Range [km]
- Endurance [h]
- Service ceiling [m]
- Powerplant type [-]
- Aircraft type [-]

Not all UAVs have data given on all of the previously mentioned parameters.

A method of utilizing the data contained in Janes can be done by various lookup functions which make use of the consistent structure of the database. Which is that the name of the type of parameter is located in the second row of the document and that the respective data is shown in the same column underneath the parameter name. The lookup functions can import the data and various other functions can process this to eventually determine a desired output.

As stated previously, Janes has data on a wide variety of UAVs, to give an example of this range; the maximum take-off weight ranges from 1.9 till 14628 kg, payload weight of between 0.04 and 4500 kg, and a wing span range of between 0.8 and 74 m.

Appendix D – Sadraey Empirical Weight Factors

This appendix presents the different multiplication factors of the formulas provided by Sadraey for the different aircraft classes. Several of these factors are used in chapter 3.4.

Density factors

No.	Aircraft – wing structural installation condition	K_ρ
1	GA, no engine, no fuel tank in the wing	0.0011–0.0013
2	GA, no engine on the wing, fuel tank in the wing	0.0014–0.0018
3	GA, engine installed on the wing, no fuel tank in the wing	0.0025–0.003
4	GA, engine installed on the wing, fuel tank in the wing	0.003–0.0035
5	Home-built	0.0012–0.002
6	Transport, cargo, airliner (engines attached to the wing)	0.0035–0.004
7	Transport, cargo, airliner (engines not attached to the wing)	0.0025–0.003
8	Supersonic fighter, few light stores under wing	0.004–0.006
9	Supersonic fighter, several heavy stores under wing	0.009–0.012
10	Remotely controlled model	0.001–0.0015

No.	Aircraft – tail configuration	$K_{\rho_{HT}}$	$K_{\rho_{VT}}$
1	GA, home-built – conventional tail/canard	0.022–0.028	0.067–0.076
2	GA, home-built – T-tail/H-tail	0.03–0.037	0.078–0.11
3	Transport – conventional tail	0.02–0.03	0.035–0.045
4	Transport – T-tail	0.022–0.033	0.04–0.05
5	Remotely controlled model	0.015–0.02	0.044–0.06
6	Supersonic fighter	0.06–0.08	0.12–0.15

No.	Aircraft	K_{ρ_f}
1	General aviation, home-built	0.002–0.003
2	Unmanned aerial vehicle	0.0021–0.0026
3	Transport, cargo, airliner	0.0025–0.0032
4	Remotely controlled model	0.0015–0.0025
5	Supersonic fighter	0.006–0.009

(Fuselage density factor)

Stabilizer Volume Fractions

No.	Aircraft	Horizontal tail volume coefficient ($\overline{V}_H$)	Vertical tail volume coefficient ($\overline{V}_v$)
1	Glider and motor glider	0.6	0.03
2	Home-built	0.5	0.04
3	GA single prop-driven engine	0.7	0.04
4	GA twin prop-driven engine	0.8	0.07
5	GA with canard	0.6	0.05
6	Agricultural	0.5	0.04
7	Twin turboprop	0.9	0.08
8	Jet trainer	0.7	0.06
9	Fighter aircraft	0.4	0.07
10	Fighter (with canard)	0.1	0.06
11	Bomber/military transport	1	0.08
12	Jet transport	1.1	0.09

Landing Gear Weight Factor

No.	Aircraft	K_{LG}
1	General aviation, home-built	0.48–0.62
2	Transport, cargo, airliner	0.28–0.35
3	Supersonic fighter	0.31–0.36
4	Remotely controlled model	0.35–0.52

Load Factor

No.	Aircraft	Maximum load factor (n_{max})
1	GA normal	2.5–3.8
2	GA utility	4.4
3	GA acrobatic	6
4	Home-built	2.5–5
5	Remote-controlled model	1.5–2
6	Transport	3–4
7	Supersonic fighter	7–10

Appendix E – Prometheus Performance Determination

In this appendix the Performance characteristics will be theoretically determined that were not measured/documented during the test flights of the Prometheus in the current gasoline-based propulsion system.

Available Performance Characteristics

The currently available Performance characteristics and the characteristics which directly affect the performance of the Prometheus are the following:

Characteristic	Value
Engine power	5.9 kW
Engine power	7.8 hp
Engine mass	2.880 kg
Propeller mass	0.250 kg
Muffler mass	0.700 kg
Fuel mass (full)	3.000 kg
Range	300 km
Endurance	3 h
Maximum speed	60 m/s
Cruise speed	42 m/s
C_{D_0}	0.02
e	0.8
Wing Area	1.085 m²
Take-off Weight	23.889 kg
Aspect Ratio Wing	9.44 [-]

Equivalent Electric Propulsion System

In this chapter the equivalent range for the Prometheus UAV will be determined if the Prometheus would have an electric propulsion system but with the same total mass as the current gasoline-based propulsion system. To determine the equivalent range for the electric system the following formulas shall be used:

Formula	Source	Formula #
$\dfrac{T}{W}^{FF}_{cruise} = q\,\dfrac{(C_{D_{min}})}{(W/S_{wing})} + \left(\dfrac{k}{q}\right)(W/S_{wing})$	[1]	(2-52)
$q = \dfrac{1}{2}\rho V^2$	[1]	(3-3)
$k = \dfrac{1}{\pi \cdot e \cdot AR_{wing}}$	[1]	(3-4)
$P/W = \dfrac{\dfrac{T}{W}^{FF} * V}{\eta_{prop}}$	[3]	(3-2)
$R_{max}^{Electric} = \dfrac{V_{cruise} \cdot W_{bat} \cdot E_{spec} \cdot \eta_{bat} \cdot f_{bat_{useful}}}{P_{motor} \cdot g} \cdot \dfrac{3600}{g}$	[8]	(0-1)
$W_{motor}^{FF} = \left((-0.922 * 10^{-5})(P_{max}^{VTOL})^2 + 0.196(P_{max}^{VTOL}) + 23.342\right) * g * 1000$	[3]	(2-39)
$W_{ESC} = \left((0.324 * 10^{-2})\left(\dfrac{P_{max}}{U}\right)^2 + 0.847\left(\dfrac{P_{max}}{U}\right) + 1.532\right) * g * 1000$	[3]	(2-40)
$W_{bat} = \left(W_{Engine} + W_{Fuel} + W_{Muffler}\right) - \left(W_{motor}^{FF} + W_{ESC}\right)$	[-]	(0-2)

Determine the $\left(\frac{T^{FF}}{W_{cruise}}\right)$ ratio from the efficiency and the energy equation for the fuel powered engine, using formula (3-3), (3-4) and (2-52).

$$q = \frac{1}{2}\rho V^2 = \frac{1}{2} \cdot 1.225 \cdot 42^2 = 1080.5 \ [kg/m^2]$$

$$k = \frac{1}{AR_{wing} \cdot \pi \cdot e} = \frac{1}{9.44 \cdot \pi \cdot 0.8} = 0.04215 \ [-]$$

$$\frac{T^{FF}}{W_{cruise}} = q\frac{(C_{D_{min}})}{(W/S_{wing})} + \left(\frac{k}{q}\right)(W/S_{wing}) = 1080.5\frac{(0.02)}{\left(\frac{23.889 \cdot 9.81}{1.085}\right)} + \left(\frac{0.04215}{1080.5}\right)\left(\frac{23.889 \cdot 9.81}{1.085}\right)$$

$$= 0.10848 \ [-]$$

Determine the theoretical power consumption at cruise, using formula (3-2). The propeller efficiency value is given by Gundlach [2] to be 0.8.

$$\frac{P}{W} = \frac{\frac{T^{FF}}{W} \cdot V}{\eta_{prop}} = \frac{0.10848 \cdot 42}{0.8} = 5.6952 \ [W/N]$$

$$P = \left(\frac{P}{W}\right) * W = (5.6952) \cdot (23.889 * 9.81) = 1334.6 \ [W]$$

Determine the weight of the electric motor and speed controller, using formulas (2-39) and (2-40):

$$W_{motor}^{FF} = \left((-0.922 * 10^{-5})(P_{max}^{FF})^2 + 0.196(P_{max}^{FF}) + 23.342\right) * g * 1000$$

$$= \left((-0.922 * 10^{-5})(5900)^2 + 0.196(5900) + 23.342\right) * \frac{9.81}{1000} = 8.425 \ N$$

$$W_{ESC} = \left((0.324 * 10^{-2})\left(\frac{5900}{22.2}\right)^2 + 0.847\left(\frac{5900}{22.2}\right) + 1.532\right) * \frac{9.81}{1000} = 4.468 \ N$$

Determine the weight of the battery for the case that the battery together with the electric motor and speed controller of the electric system will weigh the same as the original engine together with its fuel weight, using formula (0-2):

$$W_{bat} = \left(W_{Engine} + W_{Fuel} + W_{Muffler}\right) - (W_{motor}^{FF} + W_{ESC})$$

$$= \left((2.880 * 9.81) + (3.000 * 9.81) + (0.700 * 9.81)\right) - (8.425 + 4.468)$$

$$= 44.791 \ N$$

Determine the equivalent range for the Prometheus if it were electric-powered, using formula This formula was based on the formula (2-49).

$$R_{max}^{Electric} = \frac{V_{cruise} \cdot W_{bat} \cdot E_{spec} \cdot \eta_{bat} \cdot f_{bat_{useful}}}{P_{motor}} \cdot \frac{3600}{g} = \frac{42 \cdot 44.791 \cdot 140 \cdot 0.7 \cdot 0.9}{1334.6} \cdot \frac{3600}{9.81}$$

$$= 45624 \ m$$

Theoretical Maximum Rate-of-Climb

This chapter will determine what the theoretical maximum rate-of-climb is for the Prometheus in its current configuration. To determine the maximum rate-of-climb the following formulas shall be used:

Formula	Source	Formula #
$RoC_{max} = \left(\dfrac{T}{W}^{FF}_{cruise}\right) \cdot V_{RoC_{best}} - \dfrac{q \cdot C_{D_0}}{\left(\dfrac{W}{S}\right)} - \dfrac{k\left(\dfrac{W}{S}\right)}{q}$	[8] *(Based on)*	(0-3)
$k = \dfrac{1}{\pi \cdot e \cdot AR_{wing}}$	[1]	(3-4)
$q = \dfrac{1}{2} \cdot \rho \cdot V^2_{RoC_{best}}$	[8]	(0-4)
$V_{RoC_{best}} = \sqrt{\dfrac{2}{\rho} \cdot \left(\dfrac{W}{S_{wing}}\right) \cdot \sqrt{\dfrac{k}{3 \cdot C_{D_0}}}}$	[8]	(0-5)
$\dfrac{T}{W} = \dfrac{\left(\dfrac{P}{W}\right) \cdot \eta_{prop}}{V_{RoC_{best}}}$	[8] *(Based on)*	(0-6)

Determine the $\left(V_{RoC_{best}}\right)$ ratio from the efficiency, energy, and the simplified drag model equations, using formulas (3-4) and (0-5).

$$k = \frac{1}{AR_{wing} \cdot \pi \cdot e} = \frac{1}{9.44 \cdot \pi \cdot 0.8} = 0.04215 \, [-]$$

$$V_{RoC_{best}} = \sqrt{\frac{2}{\rho} \cdot \left(\frac{W}{S_{wing}}\right) \cdot \sqrt{\frac{k}{3 \cdot C_{D_0}}}} = \sqrt{\frac{2}{1.225} \cdot \left(\frac{23.889 \cdot 9.81}{1.085}\right) \cdot \sqrt{\frac{0.04215}{3 \cdot 0.02}}} = 17.19 \, [m/s]$$

Determine the thrust-to-weight ratio $\left(\frac{T}{W}\right)$ of the forward flight propulsion system from the dynamic pressure, and energy equations, using formulas (0-4) and (0-5). The propeller efficiency factor η_{prop} was derived from a 24 inch diameter, 12 inch pitch, 2-bladed propeller of APC [16]. The propeller efficiency, or figure of merit how APC calls it, was 0.52 at a rotation speed of 8000 rpm and an inflow speed of 17.19 m/s. The 8000 rpm is the rotational speed of the Prometheus engine at maximum power [22].

$$q = \frac{1}{2} \cdot \rho \cdot V^2_{RoC_{best}} = \frac{1}{2} \cdot 1.225 \cdot 17.19^2 = 180.99 \, [kg/m^2]$$

$$\frac{T}{W}^{FF}_{climb} = \frac{\left(\frac{P}{W}\right) \cdot \eta_{prop}}{V_{RoC_{best}}} = \frac{\left(\frac{5900}{23.889 \cdot 9.81}\right) \cdot 0.52}{17.19} = 0.7323 \, [-]$$

Determine the maximum rate-of-climb for the aircraft (RoC_{max}), using formula (0-5).

$$RoC_{max} = \left(\frac{T}{W}^{FF}_{cruise}\right) \cdot V_{RoC_{best}} - \frac{q \cdot C_{D_0}}{\left(\frac{W}{S}\right)} - \frac{k\left(\frac{W}{S}\right)}{q}$$

$$= (0.7323) \cdot 17.19 - \frac{180.99 \cdot 0.02}{\left(\frac{23.889}{1.085}\right)} - \frac{0.04215\left(\frac{23.889 * 9.81}{1.085}\right)}{180.99} = 13.03 \, [m/s]$$

Appendix F – Statement of Assumptions and Limitations

In this appendix a summary of all assumptions and limitations which were stated throughout the report in the methods implemented. These are the following:

- The initial mass estimation module functions with the assumption that the data on the existing UAV within the Janes database are similar in the characteristics of their end-use. To increase the accuracy of the initial mass estimation module more data on the desired classes of the UAV which the user wants to design.
- The power requirement module functions with the assumption that;
  - the minimum drag coefficient, does not significantly change throughout the mission phases,
  - the propeller efficiency does not significantly change during the mission phases,
  - the forward flight take-off power required must only accelerate the aircraft to its take-off speed,
  - the aircraft will not accelerate during the forward flight descent phase, thus the thrust(-to-weight) ratio during the descent phase does not become negative. *(due to a conversion of potential- to kinetic energy),*
  - the 3D lift coefficient for the lifting surfaces can accurately be estimated by utilizing the formula (3-8),
  - the Oswald efficiency factor can accurately be estimated by utilizing either formula (3-5) or (3-6),
  - the aircraft does not contain any high-lift devices that influence the maximum lift coefficient at any segment of the mission,
  - the weight of the aircraft does not change significantly during the mission,
  - the propeller/lifting rotor size for the vertical flight propulsion determined by the OTS lookup function is representable of the actual optimal propeller to be used.
  - The energy required to perform an aborted landing will not be considered in the sizing of the energy source
- The wing size and weight module functions with the assumption that;
  - the main wing has a strait, constant taper
  - the wing has a singular airfoil which is applied to the entire wing
  - the effects of dihedral do not have a significant influence on the performance of the wing
- The propulsion system size and weight module functions with the assumption that;
  - the propulsion system motors are not to exceed a maximum power predicted consumption of 12 kW per motor,
  - the propellers used for the aircraft have either 2, 3, or 4 blades,
  - the diameter of the forward flight propeller can be sized only depending on the number of blades and the amount of power that the propeller will receive from the motor.
- The energy source size and weight module functions with the assumption that;
  - the storage capacity of batteries is directly correlated with both the weight and volume of the battery,
  - no additional volume has been taken into account for subsystems that support the batteries,
  - the batteries utilized in the UAV can be shaped and sized as required, as a 'rubber battery'.

- The empennage and control surface size and weight modules function with the assumption that;
    - Both the horizontal- and the vertical stabilizers are constant-chord lifting surfaces. If the lifting surfaces of the aircraft are tapered rather than having a constant chord, place the Mean Geometric Chord of the lifting surfaces on the quarter chord line for the constant-chord lifting surface.
    - The tail length for both the horizontal- and the vertical stabilizers are equal.
    - The summed vertical stabilizer surface area of both stabilizers in the inverted U-tail configuration can be represented by the total surface area of the single vertical stabilizer of a conventional tail configuration.
    - By minimizing the weight of the tail, together with minimizing the lift the tail must produce during flight, a stable tail length value can be determined by the optimization method described in the empennage size and weight module
    - The rudder surface area and rudder chord are determined for both vertical stabilizers, not as one combined rudder surface. (this is to prevent any conflicts due to the twin-boom U-tail configuration)
- The landing gear size, placement, and weight module functions with the assumption that;
    - the extension and compression of the landing gear is assumed to be neglectable.
    - the centre of gravity of the aircraft is at the same height as the attachment points of the main landing gear, thus the centre of the wing thickness at the quarter chord, as shown in Figure 34.
    - no other structures on the UAV will have the risk of impacting the ground during ground operations and take-off rotation than the (end of the) tail, forward flight propeller, or the fuselage itself.
    - there is enough volume in the fuselage to have the nose landing gear collapse into.
    - the initial value for the take-off rotation angle (α_{To}) utilized in step 2, in the formula (3-23), is approximately equal to the $\alpha_{prop_{clearance}}$ which formula (3-24) determines.
    - the weight of the separate landing gear strut assemblies are equal to each other; thus, the nose gear weighs 1/3 the weight of the entire landing gear system, and in turn the main gear 2/3 the weight of the entire landing gear system.
- The weight and balance module functions with the assumption that;
    - the CG location of the forward flight motor and the propeller is at the base, or the location where the forward flight motor is mounted to the fuselage. Due to no applicable motor height-determining method available,
    - the CG location of the landing gear does not significantly change during flight in the case that the landing gear is able to retract.
- The fuselage size and weight module functions with the assumption that;
    - during the analysis for the optimal battery distribution, the fuselage weight, nor CG does not change in magnitude or location,
    - the weight of the fuselage can be determined by using an empirical formula derived from a conventional fuselage,
    - the relative error of the fuselage length will have a decreasing trend with an increasing number of iterations.